Dissection of TLR4-induced necroptosis using specific inhibitors of endocytosis and p38 MAPK

Ardeshir Ariana

A thesis submitted to the
Faculty of Graduate and Postdoctoral Studies
in partial fulfillment of the requirements for the
MSc degree in Microbiology and Immunology

Department of Biochemistry, Microbiology and Immunology
Faculty of Medicine
University of Ottawa

PREFACE

CONTRIBUTION OF COLLABORATORS

Dr. Zemin Yao's laboratory (University of Ottawa) provided all the reagents and plates used for preparing and mounting the cells for the confocal microscopy, and images were captured using a Zeiss 510 meta-confocal microscope.

APPROVALS

The experimental protocols used were approved by the University of Ottawa Animal Care Committee and include the protocols BMI1638 and BMI1639. A Biohazardous Materials Use Certificate was obtained from the University of Ottawa Office of Risk Management, Environmental Health and Safety.

ABSTRACT

Necroptosis is a pathway of inflammatory cell death that is associated with several pathologies and is induced by ligation of surface TLR or cytokine receptors in macrophages. Many signaling pathways depend on endocytosis, a process mediated by GTPases such as dynamin. We evaluated the role of dynamin-dependent endocytosis in the necroptosis of macrophages using various dynamin inhibitors. Using flow cytometry, we confirmed that during necrosome signaling, various dynamin inhibitors (e.g. Dyngo 4a and Dynasore) blocked the internalization of TLR4, which also resulted in the inhibition of cytokine production. Despite the similar impact of Dynasore and Dyngo 4a on TLR4 endocytosis and cytokine production, only Dyngo 4a prevented TLR4-induced necroptosis of macrophages. Further studies indicated that Dyngo 4a was a potent stimulator of the p38 MAPK pathway, and activation of this pathway by Dyngo 4a was responsible for the inhibition of necroptosis of macrophages following TLR4 signaling. Thus, these studies reveal the previously unknown role of the p38 MAPK pathway in regulating the activation of necrosome signaling.

ACKNOWLEDGMENTS

I would like to express my appreciation to the people who have supported and inspired me during my research.

First, I owe special thanks to my supervisor Dr. Subash Sad for the opportunity of working in his lab. Thank you for your very helpful guidance and excellent support throughout this project. Your encouragement has been a constant source of motivation over the last few years that I never forget it.

I would also like to express my gratitude to my thesis advisory committee members Dr. Marcelin Côté and Dr. Tommy Alain for their very helpful advice and contribution to this project. Thanks a lot, also, to my collaborators on the confocal imaging of the project, Dr. Zemin Yao and Mohsen Amiri for the opportunity to work together and for giving me insights into a cell biology mind.

I would also like to thank Dr. Marcelin Côté and Dr. Lisheng Wang for evaluating my thesis.

Furthermore, I want to thank all the current and former members of Dr. Sad's Lab for creating such a unique teamwork atmosphere. Special thanks to Mrs. Kim and Dr. Julie Joseph, for your unfailing support in teaching me lab techniques and very useful advice, to Norah AlTurki, for your patient guidance in teaching me lab techniques especially western blotting and cell culture, to Dikchha Rijal and Emmanuel S. Ametepe, for your generous help and encouragement. I also appreciate Andrew Wight, Stephanie Hajjar and David Cai for their precious comments on my thesis. Thank Aala Ali and, Saeedeh Al-Motaieri, Ph.D. students in Dr. Sewang Lee lab, and Tyler Renner, the Ph.D. student in Dr. Marc-André Langlois's lab for their generous help and encouragement. Working with all of you in this collaborative and inspiring environment was a great pleasure. Without your help, the fruitful scientific and sometimes not so scientific discussions as well as the good times we have shared, I would not have made it that far.

Last, but not least I owe my deepest thanks to my spouse and my children for their constant support and all my friends, near or far, for being always by my side.

TABLE OF CONTENTS

LIST OF ABBREVIATIONS

APAF-1	**Apoptotic Protease Activating Factor**
ARF6	**ADP (Adenosine diphosphate)-ribosylation factor 6**
ASK1	**Apoptosis signal-regulating kinase 1**
ATF2	**Activating transcription factor 2**
BAD	**Bcl-2-associated death promoter**
BAX	**Bcl-2-associated X protein**
BCL-2	**B-Cell Lymphoma Protein-2**
BCL-XL	**B-cell lymphoma-extra large**
BID	**BH3 (Bcl-2 homology 3) interacting-domain death agonist**
BMDM	**Bone Marrow Derived Macrophage**
CBA	**BD™ Cytometric Bead Array**
CCs	**clathrin-coated structures**
cFLIP1	**Cellular FLICE(caspase-8/a–h)-like inhibitory protein**
cIAP (1/2)	**Cellular Inhibitor of Apoptosis**
CLIC:GEEC	**Clathrin-independent carriers: GPI-AP enriched compartments**
GPI-AP	**Glycosylphosphotidylinositol-anchored protein**
CYLD	**Cylindromatosis**
DAMP	**Danger Associated Molecular Pattern**
DD	**Death Domain**
DED	**Death Effector Domain**
DISC	**Death-inducing signaling complex**
Dyn II	**Dynamin II**
EEA1	**Early endosome antigen 1**
EFA6B/D	**Exchange factor for ARF6**
ELISA	**Enzyme-linked Immunosorbent Assay**
ERK	**Extracellular signal–regulated kinase**
4HBD	**Four-helical bundle domain**
FADD	**Fas-associated protein with death domain**
FLIP	**FLICE-Like Inhibitory Protein**
4HBD	**Four-helical bundle domain**
GAS	**Gamma Activated Site**
GPCRs	**G Protein-Coupled Receptors**
GSK3β	**Glycogen synthase kinase 3 beta**
H2AX	**H2A histone family, member X**
HRP	**The enzyme horseradish peroxidase**
HSF1	**Heat shock transcription factor-1**
HSP90	**Heat shock protein 90**
IFN	**Interferon**
IFNAR 1	**Interferon α/β Receptor 1**
IFN-I	**Type I Interferon**
IkB	**Inhibitor of kappa B**
IKK	**Inhibitor of Nuclear Factor Kappa-B Kinase**
IL-10	**Interleukin 10**

IL-2RB	**Interleukin 2 receptor subunit beta**
IL-6	**Interleukin 6**
IRAK	**Interleukin-1 receptor-associated kinase**
IRF	**Interferon Regulatory Factor**
ISG	**Interferon Stimulated Gene**
ISGF3	**Interferon Stimulated Gene Factor 3**
ISRE	**Interferon-Stimulated Response Element**
JAK1	**Janus Kinase 1**
JNKs	**c-Jun N-terminal kinases**
KO	**Knockout**
LPS	**Lipopolysaccharide**
LT-βR	**Receptor for lymphotoxin-β**
LUBAC	**Linear ubiquitin chain assembly complex**
MAPKAPKs	**MAP Kinase Activated Protein Kinase**
MAPKs	**Mitogen-activated protein kinases**
M-CSF	**Macrophage Colony Stimulating Factor**
Mdivi-1	**selective inhibitor of Mitochondrial division**
MFI	**Mean fluorescence intensity**
MKKKs	**MAPK kinase kinases**
MKKs	**MAPK kinases**
MKs	**MAPKAPKs**
MLK3	**Mixed lineage kinase 3**
MLKL	**Mixed Lineage Kinase domain-Like Protein**
MLKs	**Mixed - Lineage Protein kinases**
MNKs	**MAPK-interacting kinases**
MSK1	**Mitogen- and stress-activated protein kinase-1**
mTNF	**Membrane TNF**
MTT	**3-(4,5-dimethylthiazol-2-yl)-2,5-diphenyltetrazolium bromide**
MyD88	**Myeloid Differentiation Primary Response Gene 88**
NEMO	**NFκB Essential Modulator**
NFκB	**Nuclear Factor Kappa-light-chain-enhancer of Activated B Cells**
p38 MAPK	**p38 Mitogen-Activated Protein Kinase**
p65 NFκB	**Subunit 65 of Nuclear factor kappa-light-chain-enhancer of activated B cells**
PAMP	**Pathogen Associated Molecular Pattern**
PBS	**Phosphate Buffered Saline**
PCD	**Programmed Cell Death**
PELI1	**Protein pellino homolog 1**
PI	**Propidium Iodide**
PIP	**Phosphatidylinositol Phosphate**
PIP5KIII	**Phosphatidylinositol-3-phosphate 5-kinase type III**
PKCε	**Protein kinase C epsilon type**
PM	**Plasma Membrane**
PolyI:C	**Polyinosinic-polycytidylic Acid**
PPM1b	**Protein phosphatase 1, beta isoform**
PRR	**Pattern Recognition Receptor**
R8	**RPMI with 8% Fetal Bovine Serum**
Rb1	**Retinoblastoma protein 1**

RCD	**Regulated cell death**
REL A/B	**Reticulo-endotheliosis viral oncogene homolog A/B**
RHIM	**Rip Homotypic Interaction Motif Domain**
RIPK1 (RIP1)	**Receptor Interacting Protein Kinase 1**
RIPK3 (RIP3)	**Receptor Interacting Protein Kinase 3**
RPM	**Revolutions per minute, a measure of the frequency of rotation**
RPMI	**Roswell Park Memorial Institute Medium**
RTK	**Receptor Tyrosine Kinases**
SM	**SMAC mimetic**
SMAC	**Secondary Mitochondrial Activator of Cell Death**
ST	***Salmonella enterica* serovar Typhimurium**
STAT	**Signal Transducers and Activators of Transcription**
sTNF	**Soluble TNF**
TAB1	**Transforming Growth Factor-Beta Activated Kinase 1 Binding protein 1**
TAD	**Tans-activation domain**
TAK1	**Transforming Growth Factor-Beta-Activated Kinase 1**
tBID	**Truncated BID**
TBK1	**Tank-Binding Kinase 1**
TBS	**Tris Buffered Saline**
TBST	**Tris Buffered Saline with Tween**
TGF	**Transforming Growth Factor**
TIRAP	**Toll-interleukin 1 Receptor Domain Containing Adaptor Protein**
TLR	**Toll Like Receptor**
TNF	**Tumor Necrosis Factor**
TNFR	**Tumor Necrosis Factor Receptor**
TRADD	**TNFR Associated Death Domain Protein**
TRAF2	**TNFR Associated Factor 2**
TRAIL	**TNF Related Apoptosis Inducing Ligand**
TRAM	**TRIF Related Adaptor Molecule**
TRIF	**TIR-domain Containing Adapter Inducing IFN-ß**
TYK2	**Tyrosine Kinase 2**
USF1	**Upstream Transcription Factor 1**
WT	**Wild-Type**
XIAP	**X-linked inhibitor of apoptosis protein**
zVAD	**Benzyloxycarbonyl-Val-Ala-Asp-fluoromethylketone Pan-caspase Inhibitor**

LIST OF FIGURES AND TABLES

LIST OF TABLES

1.0 INTRODUCTION

Cell death can occur as a result of pathophysiological conditions or the deprivation of growth factors, or it can be induced artificially. Host cell death by apoptosis plays an essential role in embryonic development and tissue homeostasis. The maintenance of an appropriate balance between cell death, cell proliferation and cell differentiation is necessary for adult tissue homeostasis throughout life (Fuchs and Steller, 2011). An active or regulated form of cell death relies on distinct molecular mechanisms that can not be reversed after their programming has ensued. Consequently, it can be genetically or pharmacologically manipulated (Linkermann and Green, 2014). The focus of this study is on necroptosis which, unlike apoptosis, is induced in the absence of caspase signaling and promotes inflammation. Necroptosis can occur in different types of cells in various organisms (Vanden Berghe et al., 2014; He and He, 2013). While necroptosis is considered to be a defense mechanism against pathogens, uncontrolled necroptosis promotes inflammatory pathologies such as sepsis, rheumatoid arthritis, multiple sclerosis and atherosclerosis (Ofengeim et al., 2015; Jouan-Lanhouet et al., 2014; Moore et al., 2013).

Macrophages are important effector cells of the innate immune system that play an important role in host defense and inflammation (Wynn and Vannella, 2016; Wynn et al., 2013). Phagocytosis of particulate matter or pathogens by macrophages enables them to sense danger signals efficiently, which leads to the secretion of inflammatory cytokines and chemokines that facilitate pathogen control. Phagocytosing pathogens enables macrophages to modulate intracellular signaling mechanisms, which impact the development and persistence of inflammatory response. In this regard, macrophages are the major targets of many virulent pathogens such as Ebola virus and HIV (Cobos-Jiménez et al., 2011).

Endocytosis, one of the most studied cellular processes, controls interactions of cells with the environment and many downstream cellular functions such as cell division, cell defense, and activation of signaling cascades. For many signaling pathways, receptor-mediated endocytosis is necessary for subsequent signal transduction (Sigismund et al., 2012; Scita and Di Fiore, 2010). Toll-like receptor (TLR) and cytokine receptor-signaling have been shown to be dependent on endocytosis of the receptor following ligation (Kagan et al., 2008; Schütze et al., 2008; Marchetti et al., 2006; Claudinon et al., 2009). While endocytosis plays an important role in TLR and cytokine signaling, the role of receptor endocytosis in necroptosis is not clear. This is particularly relevant since necroptosis signaling is induced by TLR and cytokine signaling. While there has been significant progress in the understanding of necroptotic pathways, the upstream signaling mechanism(s) that control the initiation of this important pathway of cell death are not clear. The intention of this study is to delineate key proteins involved in TLR4-mediated necroptosis of macrophages.

Chapter one will provide background on programmed cell death. It will explain about the interactions between apoptosis, necroptosis, and survival pathways, such as NF-κB and p38 MAPK. This chapter will also provide a brief background on endocytosis and its role in signal transduction and execution of regulated cell death.

1. 1. Programmed cell death

Currently, biochemical events in place of morphological manifestations are used to identify and classify different types of programmed cell death (PCD). In general, PCD is categorized into two major subtypes: caspase-dependent and caspase-independent (Fig. 1). Caspase-dependent cell death includes apoptosis and pyroptosis. Canonical apoptosis differs

from pyroptosis in terms of the type of caspases that are involved and the lack of production of pro-inflammatory cytokines. Pyroptosis, unlike apoptosis, involves activation of inflammatory caspases-1 and 11, which cleave pro-IL-1 cytokines such as IL-1b and IL-18, resulting in the activation and release of IL-1b and IL-18 (Linkermann and Green, 2014).

In contrast to pyroptosis, cell death by necroptosis occurs when caspase activation is inhibited. Interestingly, necroptosis and pyroptosis share a remarkable morphological event, which is the rupture of the cell membrane. This is in contrast to apoptosis where apoptotic blebs are formed during the terminal stages, and cell membranes do not rupture (Pasparakis and Vandenabeele, 2015).

Classical apoptosis is a non-inflammatory type of PCD, whereas pyroptosis and necroptosis are considered pathways of inflammatory cell death as their activation results in the release of various inflammatory molecules to the external milieu (Fig. 1). Apoptosis, which used to be considered the only form of PCD, is critical for many physiological processes. They include, but are not limited to, organ development, cell renewal, and lymphocyte selection (Elmore, 2007).

At the molecular level, it has been shown that apoptosis shares several sequential key steps with necroptosis (Pasparakis and Vandenabeele, 2015). What follows is a quick review of the mechanisms employed by apoptosis and necroptosis, including the formation of cytosolic complex II, apoptosome, ripoptosome, and necrosome. A brief comparison between apoptosis and necroptosis is also depicted in Table 1.

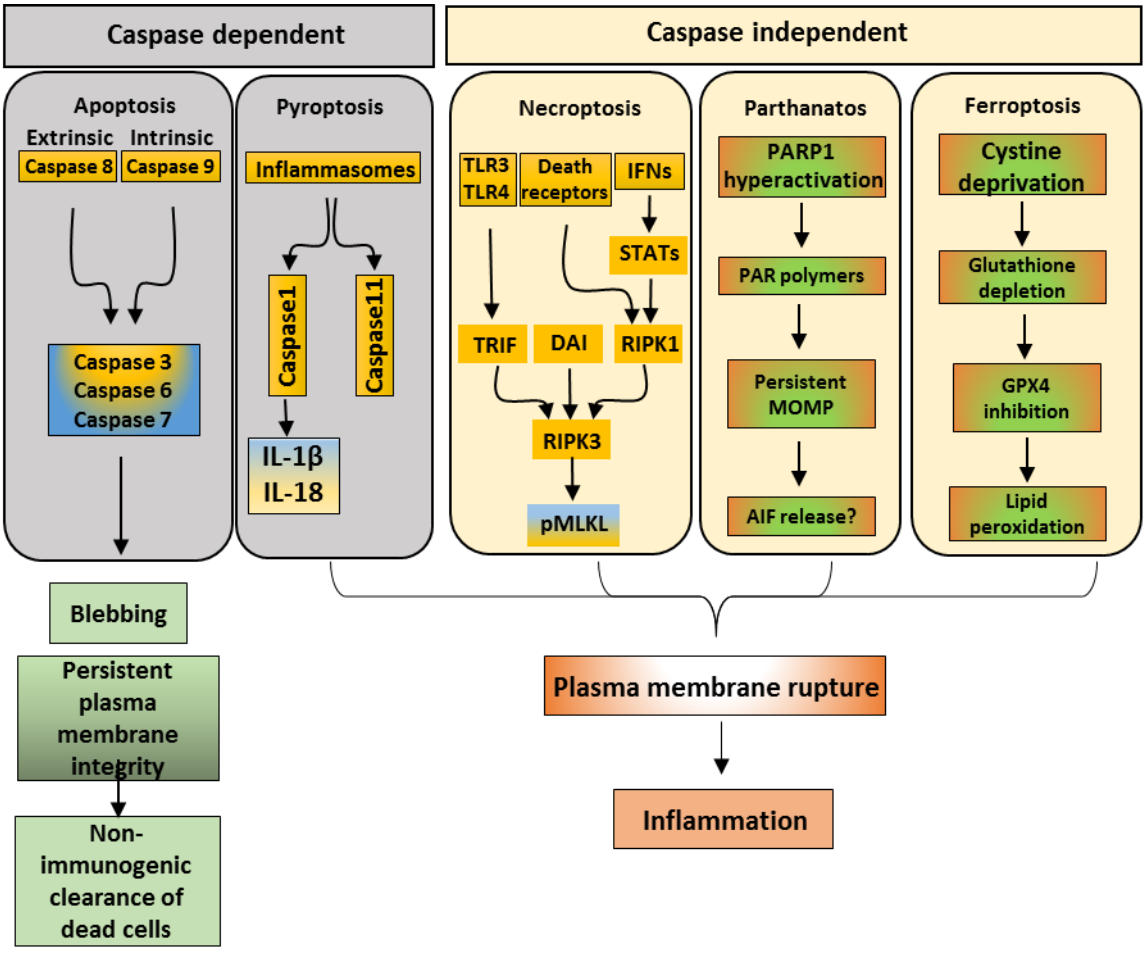
Caspase dependent
Caspase independent
Apoptosis
Extrinsic
Intrinsic
Caspase 8
Caspase 9
Caspase 3
Caspase 6
Caspase 7
Pyroptosis
Inflammasomes
Caspase1
Caspase11
IL-1β
IL-18
Necroptosis
TLR3
TLR4
Death receptors
IFNs
STATs
TRIF
DAI
RIPK1
RIPK3
pMLKL
Parthanatos
PARP1 hyperactivation
PAR polymers
Persistent MOMP
AIF release?
Ferroptosis
Cystine deprivation
Glutathione depletion
GPX4 inhibition
Lipid peroxidation
Blebbing
Persistent plasma membrane integrity
Non-immunogenic clearance of dead cells
Plasma membrane rupture
Inflammation

Figure 1. Classification of various types of regulated cell death. In this model, caspase dependency and immunogenic property are considered to differentiate various forms of regulated cell death.

1. 1. 1. Execution of apoptosis

Apoptosis can be triggered by a wide variety of stimuli. However, not all type of cells will necessarily die in response to the same stimulation. The most important hallmarks of apoptosis include a decreased cell size, condensed chromatin or pyknosis, dense cytoplasm and tightly packed organelles. In general, apoptotic pathways can be divided into the **extrinsic** or **intrinsic** pathways, depending on whether they involve mitochondrial signaling (Elmore, 2007; Fulda et al., 2010).

The **intrinsic** pathway of apoptosis involves but is not limited to, oxidative stress, DNA damage, hypoxia, radiation, and toxins. These stresses alter the inner mitochondrial membrane and result in the release of pro-apoptotic proteins such as cytochrome c, secondary mitochondria-derived activator of caspases (SMAC), and Bcl2-associated x protein (BAX) into the cytosol to induce intrinsic apoptotic signaling (Elmore, 2007). In the presence of dATP or ATP, cytochrome c binds to apoptotic protease activating factor 1 (APAF-1). This initiates heptamerization of APAF-1 that eventually makes an active complex called apoptosome. It is a cytosolic signaling platform that activates caspase-9 (Bratton and Salvesen, 2010). Activation of caspase-9 triggers a proteolytic cascade that, in turn, activates the effectors caspase-3, -6, and -7, which result in apoptosis (Bratton and Salvesen, 2010) (Fig. 2).

On the other hand, the **extrinsic** apoptotic pathway is induced through various transmembrane death receptors located on the cell surface of a target cell membrane. They include the tumor necrosis factor (TNF) receptor, TNF-related apoptosis-inducing ligand (TRAIL), and Fas receptor (CD95) (Schütze et al., 2008). The interaction of the ligand (i.e., FasL) on the membrane of cytolytic T cells with its receptor (i.e. Fas-R) located on the

surface of target cells leads to trimerization of the receptor. The clustering of the receptors' cytosolic death domains (DD) triggers an intracellular signaling cascade which begins with the recruitment of Fas-associated protein with death domain (FADD). The FADD's death-effector domain (DED) can interact with the DED of pro-caspase-8 or 10 to form a complex called death-inducing signaling complex (DISC). The DISC complex cleaves pro-caspases-8 or 10 and activates them, which in turn cleave and activate the execution pro-caspases such as caspase-3, -6, and -7. Activation of executive caspases, such as caspase-3 can trigger apoptosis (Fig. 2). Caspase-3 and -8 can also cleave pro-apoptotic BH3-Inteacting-domain Death (BID), agonist. Truncated BID (tBID) can then translocate to the mitochondria to inhibit anti-apoptotic Bcl-2 and Bcl-x proteins. Consequently, BAX and Bcl-2-associated death promoter (BAD) can be activated and release cytochrome c and SMAC, which in turn activates the intrinsic pathway of apoptosis. This shows how the extrinsic pathway can trigger the intrinsic pathway as well (Conrad et al., 2016) (Fig. 2).

1. 1. 2. Formation of cytosolic complexes

The soluble TNF (sTNF) and/or membrane TNF (mTNF) upon engagement with the TNF receptor 1 (TNFR1), result in a conformational change of the receptor. Homo-trimerization of the receptor facilitates the recruitment of the key proteins such as TNFR1-associated death domain proteins (TRADD) to the cytoplasmic tail of the receptor. Through TRADD, several other proteins are recruited to form complex I, a pro-survival complex (Brenner et al., 2015).

Complex I includes several E3 ubiquitin ligases such as TNF receptor-associated factor 2 (TRAF2) and cellular inhibitors of apoptosis (cIAP1 or cIAP2), in addition to receptor-interacting protein kinase 1 (RIPK1), and the linear ubiquitin chain assembly complex (LUBAC) which recruits transforming growth factor-β-activated kinase 1 (TAK1) - binding

protein (TAB) complex. TABs cause phosphorylation of inhibitor of kappa B (IkB) kinase 1 & 2 (IKK1, IKK2) and NF-κB essential modulator (NEMO) that ultimately lead to the activation of NF-κB. This complex can also activate mitogen-activated protein kinases (MAPKs)(Lu et al., 2006).

It has been shown that the K63-ubiquitination of RIPK1 promotes the maintenance of Complex I (Fig. 2) (Conrad et al., 2016). Activation of the deubiquitinase, CYLD or inhibition/degradation of cIAPs, TAK1, and NEMO can destabilize Complex I (Legarda et al., 2016; Schworer et al., 2014; Adhikari et al., 2007). Segregation of RIPK1 from Complex I results in the formation of Complex II including caspase-8 and FADD. When protein translation is inhibited by cycloheximide (CHX), Complex II**a** is assembled (Fig. 2), which includes TRADD, FADD, caspase-8 and $FLIP_L$ (catalytical activator of caspase-8). As explained before, the interaction of FADD and pro-caspase 8 leads to the activation of caspase-8 through an autoproteolytic cleavage process, which in turn activates pro-caspase -3 and -7 and results in apoptosis (Elmore, 2007).

When cIAP1/2 is degraded and X-linked inhibitor of apoptosis protein (XIAP) is inhibited by the treatment of cells with SMAC-mimetic, Complex II**b** is assembled, which consists of core components RIPK1, FADD and caspase-8, and is referred to as the ripoptosome. This complex causes RIPK1-dependent apoptosis (Fig. 2) (Schilling et al., 2014).

1. 1. 3. Execution of necroptosis

When the activity of caspase-8 is inhibited by inhibitors such as the cellular FLICE (caspase-8/a–h)-like inhibitory protein (cFLIP), this promotes the interaction of RIPK1 with RIPK3, which leads to the phosphorylation of the pseudokinase mixed-lineage kinase-like (MLKL). This complex is referred to as Complex II**c** or the necrosome (Fig. 2) (Chan et al., 2015).

As indicated above, necroptosis is induced in the absence of caspase activation and is considered to be a highly immunogenic form of cell death due to the release of immunogenic damage-associated molecular patterns (DAMPs) from the cell. A switch from Complex IIa or IIb to Complex IIc is a critical event that triggers sequential events leading to rapid permeabilization of the plasma membrane and committing to necroptosis. One critical step is heterodimerization of RIPK1-RIPK3 complex, which is formed through the interaction of their common domain, RIP homotypic interaction motif (RHIM) (de Almagro and Vucic, 2015). Auto- and trans-phosphorylation of RIPK1 and RIPK3 promote the interaction and dimerization of RIPK1-RIPK3 (Fig. 2). The next critical step is the oligomerization of RIPK3, which is a RHIM domain-dependent process. It has been shown that homodimerization of RIPK3 is enough to recruit and cause phosphorylation of MLKL. The phosphorylation of MLKL results in its oligomerization. The translocation of the MLKL trimers to the cell surface is the last critical step that compromises the integrity of the cell membrane (Fig. 2) (Galluzzi et al., 2014).

Currently, phosphorylation of MLKL is considered the terminal step in the induction of necroptosis. Dondelinger et al. (2014) demonstrated that the full four-helical bundle domain (4HBD) in the N-terminal region of MLKL is necessary and sufficient to trigger its

oligomerization and induce cell death. They also presented a model showing that MLKL can directly permeabilize plasma membrane and induce necroptosis.

Table 1. A comparison between apoptosis and necroptosis based on their various morphological and chemo-physiological characteristics.

Death modality	**Apoptosis**		**Necroptosis**
	Intrinsic	**Extrinsic**	
Morphology	Intact plasma membrane Blebbing of the plasma membrane Chromatin condensation (**pyknosis**) Nuclear fragmentation (**karyorrhexis**) Shedding of apoptotic bodies		Plasma membrane rupturing Cellular and organelle swelling (**oncosis**) Intact nuclei Mild chromatin condensation
Key regulatory proteins	BID, BAX/BAK Cytochrome c APAF-1 caspase-9	FADD caspase-8	RIPK1 (**inactive and active form**) RIPK3 (**active form**)
Death execution proteins	caspase-3, -6, -7	caspase-3, -6, -7	MLKL Ion channels (**Ca^{2+}, K^{+}, Mg^{2+}**)
Physiological function	Embryogenesis Homeostasis Immune cells regulation Pathogen defence		Embryogenesis Homeostasis Inflammation Neurodegeneration Thrombosis IR-injury
Synthetic inducer	Smac mimetics (e.g. Brinapan)		Combination of stimuli (**e.g. LPS, TNF, IFN-β, Poly I:C**) and **zVAD**
Synthetic inhibitor	zVAD-fmk (pan-caspase inhibitor) q-VD-Oph (pan-caspase inhibitor)		Necrostatin (**RIPK1 inhibitor**) GSK843, GSK872 (**RIPK3 inhibitor**) NSA, GW906742X (**MLKL inhibitor**)

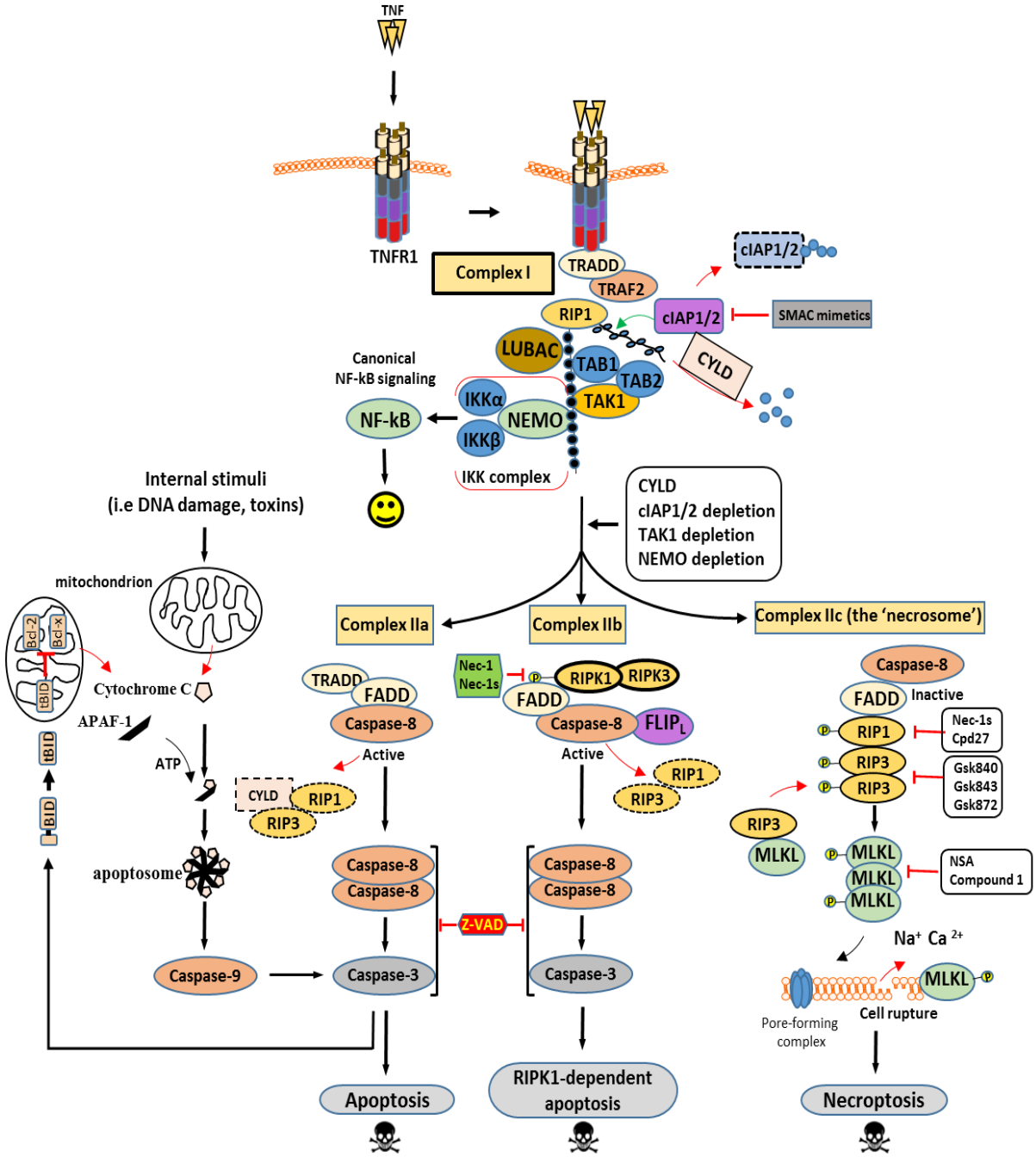
TNF
TNFR1
Complex I
TRADD
TRAF2
RIP1
cIAP1/2
SMAC mimetics
CYLD
LUBAC
TAB1
TAB2
TAK1
NEMO
IKKα
IKKβ
IKK complex
Canonical
NF-kB signaling
NF-kB
Internal stimuli
(i.e DNA damage, toxins)
CYLD
cIAP1/2 depletion
TAK1 depletion
NEMO depletion
mitochondrion
Bcl-2
Bcl-x
tBID
BID
Cytochrome C
APAF-1
ATP
apoptosome
Caspase-9
Complex IIa
Complex IIb
Complex IIc (the 'necrosome')
FADD
Caspase-8
Active
Nec-1
Nec-1s
RIPK1
RIPK3
FLIP$_L$
Caspase-3
Z-VAD
Inactive
Nec-1s
Cpd27
Gsk840
Gsk843
Gsk872
MLKL
NSA
Compound 1
Na+ Ca 2+
Pore-forming
complex
Cell rupture
Apoptosis
RIPK1-dependent
apoptosis
Necroptosis

Figure 2. Survival, apoptosis, and necroptosis pathways are alternative signaling events downstream of TNFR1 activation. Two complexes, Complex I (including TRAF2, cIAP1/2, RIPK1, and LUBAC) and Complex II (including FADD and caspase-8), play a critical role in determining the type of signal. While the main consequence of Complex I is inducing survival signals through the activation of NF-kB pathways and MAPKs cascades, Complex II is responsible for driving the cell death toward either extrinsic apoptosis or necroptosis. Extrinsic pathway of apoptosis can trigger the intrinsic pathway as well. The intrinsic pathway is characterized by permeabilization of the mitochondria and release of cytochrome c into the cytoplasm, which in turn, forms apoptosome that activates caspase 9. The interaction of FADD and pro-caspase-8 leads to the activation of caspase-8, which in turn activates pro-caspase-3 and -7 and results in apoptosis. When the activity of caspase-8 is inhibited by inhibitors such as cFLIP, the interaction of RIPK1 with RIPK3 is promoted. This interaction leads to the phosphorylation of MLKL to form Complex IIc or necrosome and results in necroptosis.

1.2. The Interactions between apoptosis, necroptosis, and survival pathways

A plethora of evidence indicates that there are mutual interactions among various proteins that participate in cell survival, cell death, and inflammation (Christofferson and Yuan, 2010; Dannappel et al., 2014; Galluzzi and Kroemer, 2008; Nikoletopoulou et al., 2013; Pasparakis and Vandenabeele, 2015; Vanden Berghe et al., 2015; Zhou and Yuan, 2014).

Engagement of TLR4 can result in pro-survival or pro-apoptotic signaling (Neal et al., 2012; Ruckdeschel et al., 2004; Tang et al., 2008). Ubiquitylation of RIPK1 is required for the activation of pro-survival pathways such as the NF-κB and MAPK pathways. Disassembly of the ubiquitin network of RIPK1 terminates pro-survival signaling and promotes pro-apoptotic or pro-necroptotic signaling (O'Donnell and Ting, 2012; O'Donnell et al., 2007). In addition, Ye et al. (2011) demonstrated that suppression of p38 MAPK and NF-κB augmented TNF-induced necroptosis and autophagy in L929 cells. Furthermore, McComb et. al. (2014) identified a predominant role of type I IFN (IFN-I) signaling in necroptosis of macrophages. They reported that macrophages derived from IFN-α receptor 1 (IFNAR1) knockout mice are highly resistant to necroptosis. IFN-I production is induced by TRIF pathway, which is recruited during TLR4 activation. In the absence of TRIF, there was a significant decrease in necroptosis of macrophages observed (McComb et. al., 2014).

Further studies of the pro-survival pathways (p38 MAPK and NF-κB) can help better describe their potential role in regulating necroptosis. This section will also elaborate on the role of IFNAR1 signaling and TRIF-dependent pathway, which is important in TLR4-driven necroptosis.

1. 2. 1. P38 MAPKs pathways

It has been shown that mammalian cells can activate four subfamilies of MAPKs including extracellular signal–regulated kinases (ERK 1/2, ERK5), c-Jun N-terminal kinases (JNKs), and p38 MAPK. MAPK signaling operates through a three-tiered MAPKKK–MAPKK–MAP kinase cascade (Fig. 3). Upon dual phosphorylation of tyrosine and threonine residues of a conserved Thr–Xaa–Tyr motif in the activation loop, the activation of MAPK cascades could be triggered. Activation of p38 MAPK plays a dual role in the context of programmed cell death. It can either promote cell survival or induce cell death through different pathways. The specific function of p38 MAPK depends on various factors including cell type, cell stimuli, and the type of p38 MAPK isoforms (Wagner and Nebreda, 2009).

The p38 MAPK subfamily can be divided based on the type of isoform, into two subclasses: p38 α/β and p38 γ/δ. The classification is based on three main aspects: First is the isoforms' sequence of amino acids (at least >70% identical amino acids). Second is the susceptibility of the isoforms to the low concentration of the inhibitors. For instance, p38α/β can be inhibited by SB203580 and SB202190; however, p38γ/δ are completely unaffected by these inhibitors, due to the prevention of inhibitor binding to the Thr106 in the ATP binding pocket. Third is the substrate selectivity of the isoforms. For example, p38α and p38β can phosphorylate MAPKAPK2 (MK2), MAPKAPK3 (MK3) better than p38γ and p38δ. This means that, despite the overlap of some substrates of p38 MAPK isoforms, there are some target proteins, which can be considered as isoform-specific substrates. The best examples are MK2 and MK3, which are good substrates of p38α and p38β, but not p38γ and p38δ isoforms (Fig. 3) (Cuenda and Rousseau, 2007).

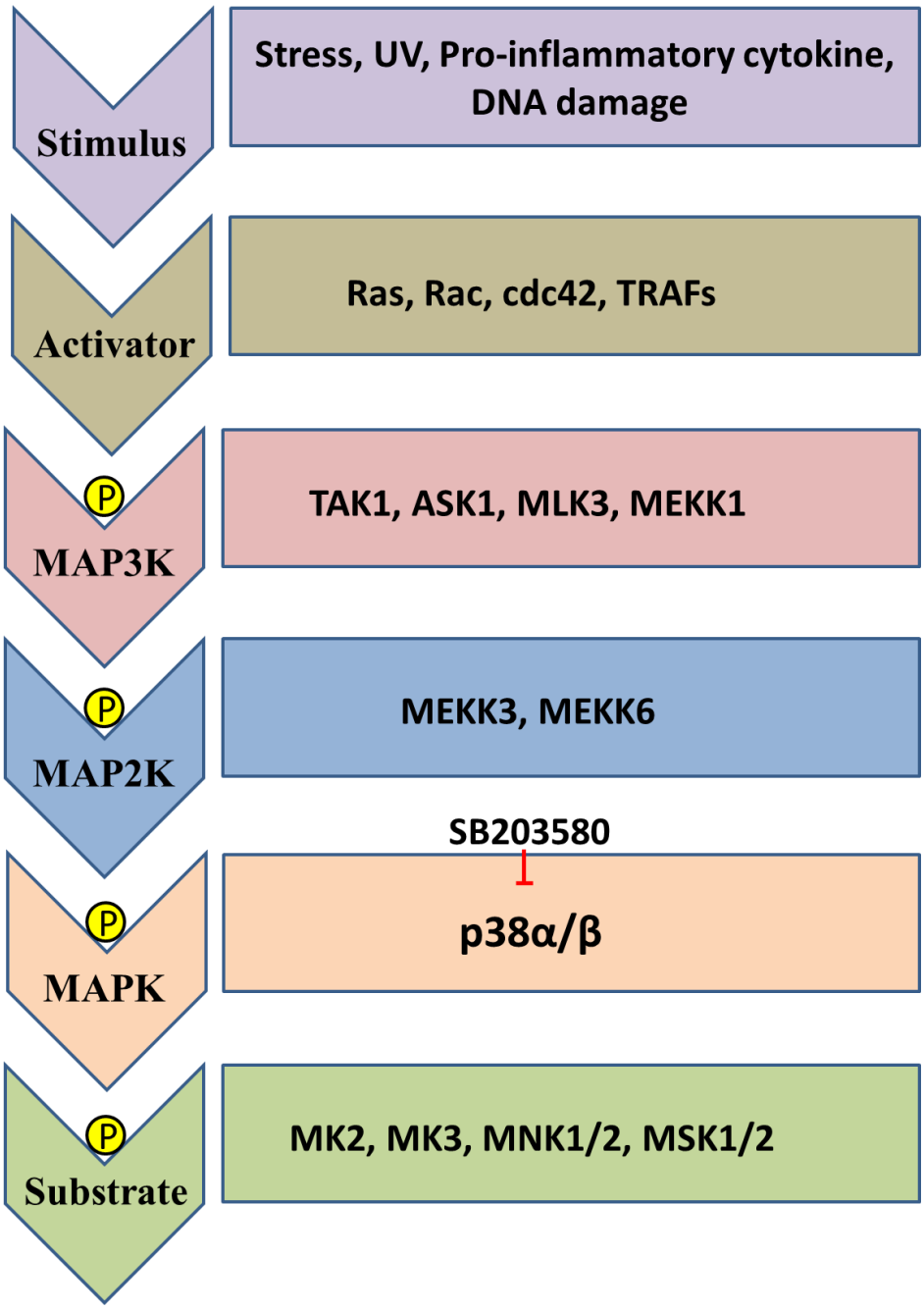
Stimulus
Stress, UV, Pro-inflammatory cytokine, DNA damage
Activator
Ras, Rac, cdc42, TRAFs
P
MAP3K
TAK1, ASK1, MLK3, MEKK1
P
MAP2K
MEKK3, MEKK6
SB203580
P
MAPK
p38α/β
P
Substrate
MK2, MK3, MNK1/2, MSK1/2

Figure 3. A schematic model of p38 MAPK signaling pathway. P38 MAPK can be activated throughout complex kinase cascades by a variety of stimuli such as stress and pro-inflammatory cytokine. Some cellular intermediates, such as GTPase or receptor adaptor proteins, transmit the upstream signal to the kinase cascades. Once activated, various isoforms of p38 MAPK either phosphorylate their cytoplasmic targets and transfer into the nucleus causing modulation of target transcription factors. P38 α/β are the major activators of MK2 and MK3; however, p38ϒ/δ usually does not activate these kinases. One of the other important differences between them is that p38α/β is inhibited by SB203580, one of the well-known inhibitors of p38, but this inhibitor does not have any impact on p38ϒ/δ.

The p38 MAPK isoforms are activated by various stimuli such as environmental stress and inflammatory cytokines. The canonical activation pathway of p38 MAPKs is through dual phosphorylation of the Thr-Gly-Tyr motif of the activation loop by MKK3 and MKK6. While MKK3 and MKK6 are highly selective MAPKK for p38 MAPKs, they do not activate other MAPKs like JNK or ERK1/2. Also, MKK6 and MKK3 (SKK3) are successively phosphorylated and activated by cell types- and stimulus-specific kinases (MKKK) that include, but are not limited to Mixed lineage kinase 3 (MLK3), Apoptosis signal-regulating kinase 1 (ASK1), and TAK1 (Fig. 3) (Cuenda and Rousseau, 2007).

It has also been shown that there are other possible activation mechanisms for MAPKs. One pathway, which is specific, is through binding of TAK1-binding protein 1 (TAB1) with p38α MAPK. Auto-phosphorylation is the major source of p38 MAPK activation following the interaction with TAB1. Another non-canonical pathway of p38 MAPK activation has been observed in T cells. In this alternative mechanism of activation, TCR-mediated stimulation activates proximal tyrosine kinases that result in the phosphorylation of p38α MAPK (Cuenda and Rousseau, 2007).

1. 2. 2. NF-kB pathway

NF-kB is a transcription factor that is available in many cell types and can be activated by TLR or cytokine signaling (Doyle and O'Neill, 2006; Legler et al., 2003). Once activated, it induces the transcription of various cytokines and chemokines that promote innate and adaptive immunity. NF-κB also promotes the transcription of various cell survival genes and has a suppressive impact on apoptosis (Khan et al., 2013). There are five proteins in the NF-kB family, which are divided into two classes. Class I consists of NF-κB1 and NF-κB2, which are large precursor proteins, p105 and p100 respectively, generate mature

subunits, p50 and p52, after processing. Class II includes Rel A, Rel B, and c-Rel which have transactivation domains (TAD) in their C-terminal and generate the mature NF-kB subunit p65.

The canonical (classical) pathway of NF-kB activation can be initiated by cytokine receptor (e.g., TNFR1 or IL-1R) or pattern-recognition receptor (e.g., TLR4) engagement. Receptor engagement binds TRADD to the interacting receptor, which in turn, result in the assembly of other critical proteins such as FADD, TRAF2, and RIPK1 (Oeckinghaus et al., 2011).

The activation of IKK complex is the result of RIPK1-dependent TAK1 activation (Morioka et al., 2014; Takaesu et al., 2003). In this critical step, TAK1 phosphorylates (activates) IKKβ and is negatively regulated by some phosphatases such as beta isoform of magnesium-dependent protein phosphatase 1 (PPM1b) (Chen et al., 2015; Wang et al., 2016a). Activation of IKKα/β, in turn, phosphorylates IkB, the inhibitory proteins of NF-κB dimers. The phosphorylation of IkB results in its ubiquitination and ultimately proteasome-mediated degradation (Scheidereit, 2006). This releases the bound NF-κB dimers, which then relocate into the nucleus and act as transcription factors for many genes such as pro-inflammatory cytokines (Fig. 4 A) (Oeckinghaus et al., 2011). In contrast, the non-canonical (alternative) pathway is induced by NIK-mediated IKKα homodimer activation which leads to IKKα-induced p100-Rel B complex phosphorylation (activation). The partial processing of p100 generates the transcriptionally active p52-Rel B complexes, which enter the nucleus and activate the expression of various target genes (Fig. 4 B) (Sun, 2010; Oeckinghaus et al., 2011).

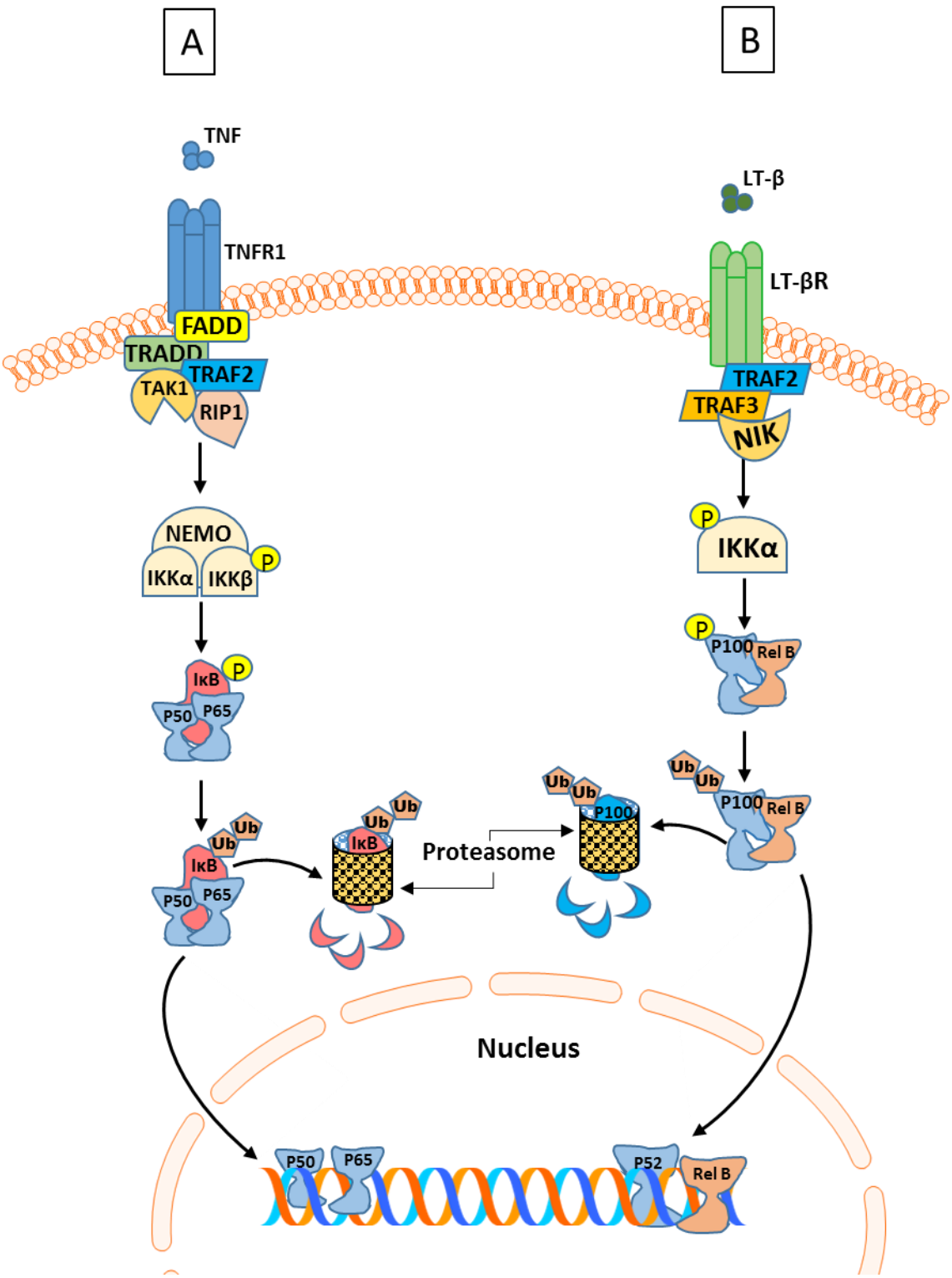
A
B
TNF
TNFR1
FADD
TRADD
TRAF2
TAK1
RIP1
NEMO
IKKα
IKKβ
P
IκB
P50
P65
Ub
Proteasome
LT-β
LT-βR
TRAF2
TRAF3
NIK
IKKα
P100
Rel B
Nucleus
P52

Figure 4. The canonical and non-canonical pathways of NF-kB activation. The canonical pathway (**A**) can be induced by various stimuli such as TNF. Stimulation of TNFR1 leads to the recruitment of TRADD, which provides an assembly platform for other key proteins such as FADD and TRAF2. RIP1 is associated with TRAF2 that phosphorylates (activates) IKKβ, which in an NEMO-dependent manner, phosphorylates IkB, the inhibitor of NF-kB dimers under resting conditions. Phosphorylation of IkB results in its ubiquitination and ultimately proteasome-mediated degradation which thus releases the bound NF-κB dimers to translocate to the nucleus. In contrast, the noncanonical pathway (**B**), induced by certain TNF family cytokines, such as lymphotoxin-β (LT-β) and is mediated by IKKα-induced phosphorylation of p100 associated with Rel B, which results in partial processing of p100 to generate p52-Rel B, a transcriptionally active complex. The activation of IKKα and phosphorylation of p100 is an NIK-dependent process, which is regulated by TRAF3, TRAF2 and LT-βR, receptor for lymphotoxin-β.

1. 2. 3. IFNAR1 signaling promotes necroptosis

Recent studies have changed the notion that IFN-I signaling and necroptosis are nonrelated events, and unveiled the important role of IFNAR1 signaling in necroptosis. An investigation conducted by Robinson et al. (2012) on macrophages infected with *Salmonella enterica* serovar Typhimurium (ST) revealed that IFN-I signaling promotes necroptosis of macrophages infected with ST. More specifically, McComb et al. (2014) reported that macrophages derived from IFNAR1 knockout mice are highly resistant to necroptosis. Stimulating cells with LPS, polyinosinic-polycytidylic acid (poly I:C), TNF, or IFN-β in combination with zVAD, a pan-caspase inhibitor, McComb et. al. (2014) identified a predominant role of IFN-I signaling in necroptosis of macrophages. Their results also demonstrated that IFN-β–induced necroptosis of macrophages operates through IFN-stimulated gene factor 3 (ISGF3) signaling, which is a trimeric transcriptional complex composed of STAT1, STAT2, and IRF9. Furthermore, the authors showed that an IFNAR1/RIPK3-induced necroptosis resulted in potent inflammatory pathology *in vivo*. Brault et al.(2016) demonstrated that TNF production is a downstream event of IFN-I signaling and is required to trigger necroptosis. Additionally, it was discovered that IFN-I is essential to induce TNF-mediated auto-necroptosis of macrophages and showed its role in priming the cells to express key proteins such as TNFR2 and MLKL (Legarda et al., 2016). Although Legarda et al. (2016) added important pieces to the puzzle of necroptosis, the mechanistic relationship among TNF production, TNFR1 and R2, and IFN-I signaling in necroptosis remains unclear.

1. 2. 4. TRIF-dependent pathway promotes TLR4-driven necroptosis

Various studies have confirmed that engagement of TLR4 by lipopolysaccharide (LPS) can promote necroptosis in primary macrophages (He et al., 2011; Legarda et al., 2016; Linkermann and Green, 2014; McComb et al., 2014; Robinson et al., 2012; Vandenabeele et al., 2010). Upon TLR4 detection of LPS, a specific pathogen-derived ligand, the receptor signaling cascade is initiated by binding of the adaptor protein MyD88 adaptor-like (Mal) to the cytoplasmic tail of the receptor. This leads to the recruitment of adaptor protein MyD88 and activation of the MyD88 dependent signaling pathway. Then, the MyD88 associates with interleukin-1 receptor-associated kinase 4 and 1 (IRAK4 and IRAK1) and TNF-R-associated factor 6 (TRAF6) at the plasma membrane. TRAF6 activates the cellular inhibitor of apoptosis protein 1 and 2 (cIAP1 and cIAP2), which act as E3 ligases and induce ubiquitylation of many important proteins such as RIPK1 and TRAF3. Ubiquitylation of RIPK1 is required for the maintenance of Complex I, which in turn promotes the recruitment of NF-κB essential modulator (NEMO) and TGFβ-activated kinase 1 (TAK1) complexes. As explained before, activation of TAK1 and IKK complex can activate survival pathways, NF-κB and MAPKs cascades (Fig. 5) (Morioka et al., 2014; Brenner et al., 2015).

Stimulation of TLR4 can recruit another adaptor protein, TIR-domain-containing adapter-inducing interferon-β (TRIF), which is associated with TLR4 via the TRIF-related adaptor molecule (TRAM). Following receptor activation, the TRIF signaling is initiated in a delayed manner, which is preceded by the MyD88-dependent signaling. TRIF then recruits TRAF6 and RIPK1, which leads to the activation of NF-κB and MAPK cascade like that happens when MyD88 is activated (Fig. 5) (Wertz and Dixit, 2010). Interestingly, necroptosis of macrophages has been shown to be quite attenuated in the absence of TRIF signaling (McComb et al., 2014; Linkermann and Green, 2014; He et al., 2011). Since it has

been shown that the relocation of TLR4 into endosomes facilitates the TRIF signaling pathway (Wang et al., 2012), it is conceivable that endocytosis of the receptor may be required for necroptosis (Fig. 5).

Activation of the TRIF pathway, unlike MyD88 pathway, activates a unique signaling program that involves activation of the transcription factor IRF3. The activation of IRF3 is initiated with the recruitment of TRAF3. The next step is the formation of a non-canonical IKK complex including TANK-IKKε-TBK1, which in turn phosphorylates IRF3 at the serine/threonine site, resulting in its homodimerization. Overall, the transcriptional activity of IRF3 via binding to the promoter and enhancer region of IFN-I genes induces the production of IFN-Is, which mediates protection against viral infections (Wang et al., 2016b). McComb et al. (2014) observed a partial but significant rescue from necroptosis in mouse macrophages lacking IRF3.

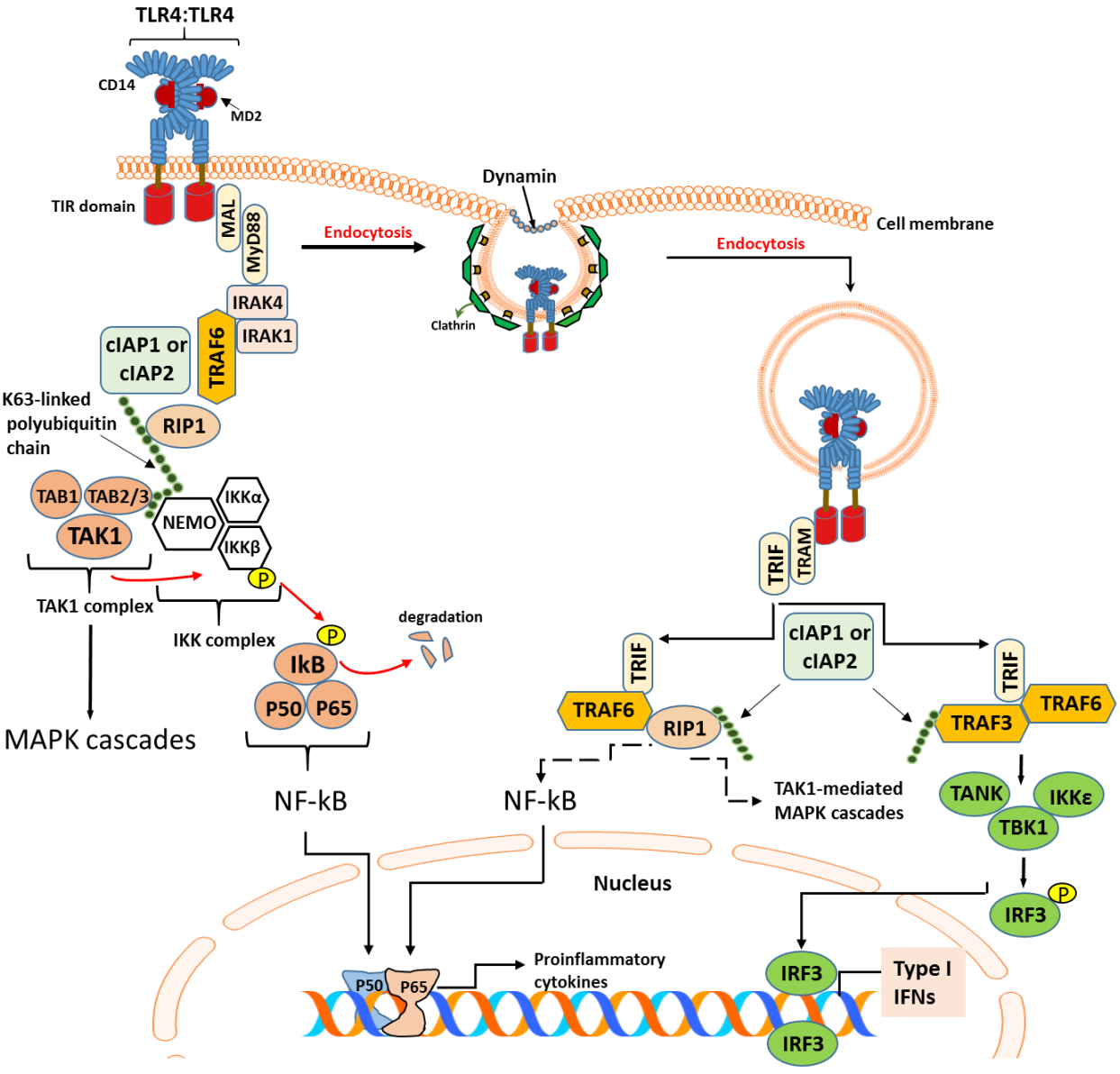
TLR4:TLR4
CD14
MD2
TIR domain
MAL
MyD88
IRAK4
IRAK1
TRAF6
cIAP1 or cIAP2
K63-linked polyubiquitin chain
RIP1
TAB1
TAB2/3
TAK1
NEMO
IKKα
IKKβ
P
TAK1 complex
IKK complex
degradation
IkB
P50
P65
MAPK cascades
NF-kB
Endocytosis
Dynamin
Clathrin
Cell membrane
Endocytosis
TRIF
TRAM
cIAP1 or cIAP2
TRIF
TRAF6
RIP1
TRIF
TRAF3
TRAF6
NF-kB
TAK1-mediated MAPK cascades
TANK
IKKε
TBK1
IRF3
P
Nucleus
P50
P65
Proinflammatory cytokines
IRF3
IRF3
Type I IFNs

Figure 5. Activation of the TRIF-dependent pathway, but not the MyD88-dependent pathway, is an endocytosis-dependent event. TLR4 manages two subsets of signaling: TIRAP/MyD88-dependent and TRAM/TRIF-dependent. The MyD88-dependent pathway is an early but transient pathway and is mainly responsible for MAPK cascades and NF-κB signaling, while the TRIF-dependent pathway is a late but constitutive signaling pathway and is an activator of IRF3 and IFN-Is production. TRIF-dependent, unlike MyD88-dependent, pathway is an endocytosis-dependent pathway which appears to be a dynamin-dependent endocytosis.

1. 3. Endocytosis

Endocytosis is one of the most studied cellular processes. It controls many cellular functions such as cell division, cell defense, and activation of signaling cascades. For many signaling pathways, receptor-mediated endocytosis is necessary for subsequent signal transduction (Scita and Di Fiore, 2010).

Section 1.3 will discuss the classification of endocytosis. The section also examines both dynamin-independent and -dependent endocytosis. Finally, section 1.3 considers how endocytosis is related to the execution of regulated cell death.

1. 3. 1. Classification

Blouin and Lamaze (2014) have suggested a classification model that is based on the cellular proteins involved in endocytosis events. Accordingly, endocytosis can be divided into two major pathways that are dynamin-dependent and dynamin -independent (Fig. 6) (Blouin and Lamaze, 2013). Although this way of classification is very helpful in discriminating between different types of endocytosis, there are some cases that do not completely fit this model. For instance, It has been shown that the activation of ARF6 can be dependent on GTP hydrolysis activity of dynamin II (Fig. 7) (Okada et al., 2015). Thus, while ARF6-dependent endocytosis is categorized in the dynamin-independent group, it could also be considered as dynamin-dependent endocytosis.

1. 3. 2. Dynamin-dependent endocytosis

Dynamin-dependent endocytic pathways are well-known mechanisms responsible for packaging and internalizing a wide variety of transmembrane receptors and their ligands (Marchetti et al., 2006; Scita and Di Fiore, 2010). These pathways are dependent on

dynamin, a large GTPase protein. Oligomerization of dynamin, around the neck of nascent endocytic compartments, completes the vesicle (endosome) formation from the plasma membrane by constricting and/or stretching the neck of invaginated cell membranes. All three isoforms of dynamin (I–III) are expressed by mammalian cells. While dynamin II is globally expressed in all tissues, dynamin I is mostly expressed in neuronal or neurosecretory cells and dynamin III is found in neurons, testis, and megakaryocytes (Reems et al., 2008). As already mentioned, dynamin has been implicated in other endocytic pathways, such as in ARF6-dependent endocytosis (Fig. 6, 7).

Another important function of dynamin is the reorganizing of F-actin filaments in cytoskeletal-based events such as phagocytosis and endosome trafficking in the cell (Ferguson and De Camilli, 2012) (Fig. 7). Coating proteins such as clathrin, caveolin, and IL2Rβ play a major role in the formation of vesicles. While these proteins contribute to dynamin-dependent endocytosis, they are also found in the other types of dynamin-independent endocytosis (Blouin and Lamaze, 2013).

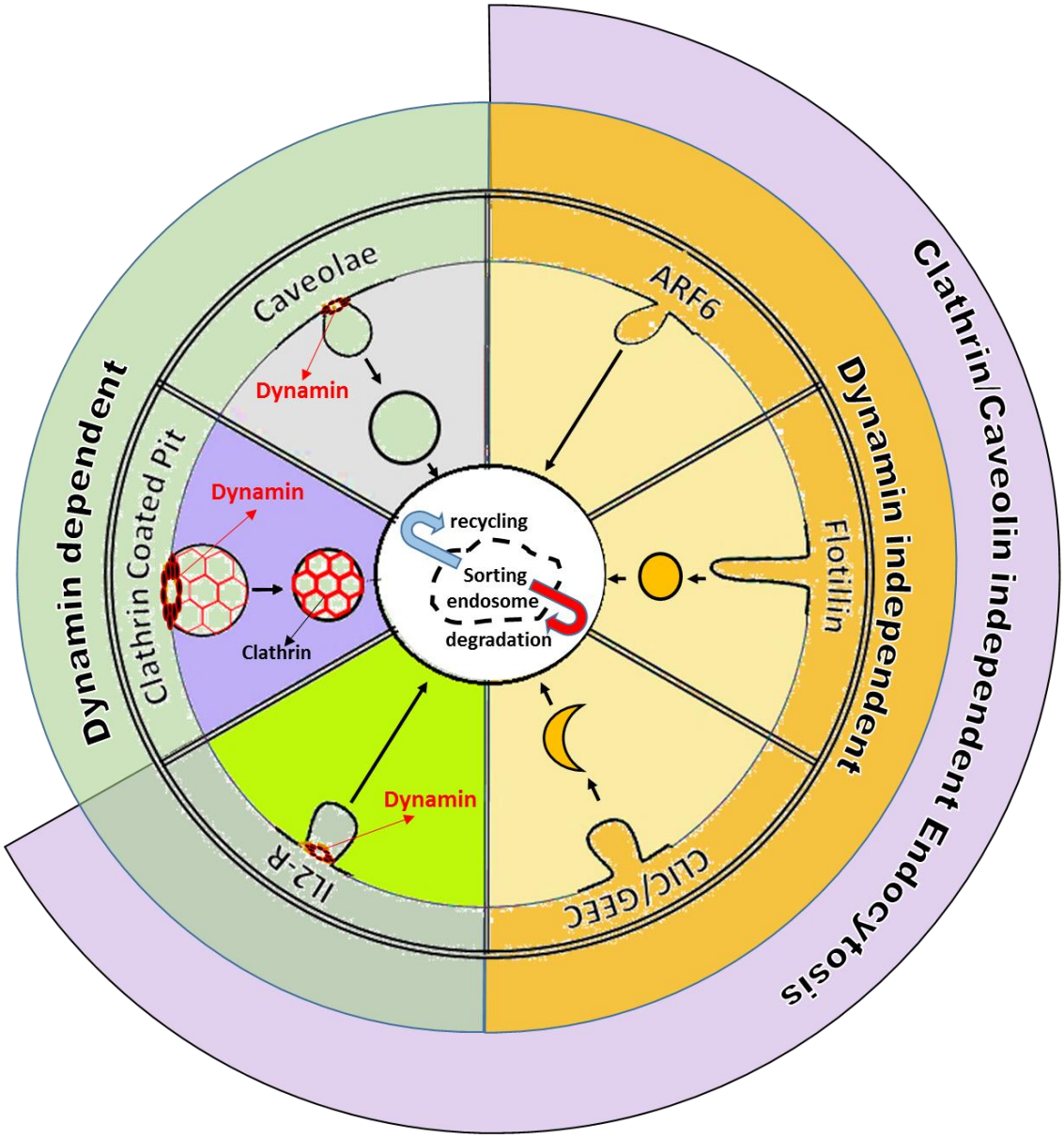
Clathrin/Caveolin independent Endocytosis
Dynamin dependent
Dynamin independent
Caveolae
Dynamin
Clathrin Coated Pit
Dynamin
Clathrin
IL2-R
Dynamin
ARF6
Flotillin
CLIC/GEEC
recycling
Sorting
endosome
degradation

Figure 6. Putative types of endocytosis. Various molecules (such as proteins) can enter the cell via clathrin and clathrin-independent endocytic pathways. Dynamin, as a large GTPase, is also required for the detachment of endocytic vesicles in many endocytosis events. Accordingly, classification of endocytosis can benefit from this fact to be divided into two major groups, dynamin-dependent, and dynamin-independent endocytosis. However, it is a controversial ranking, as in few cases, activation of ARF6 is not independent of dynamin. The IL2R pathway is the only clathrin and caveolae-independent pathway and requires dynamin for endocytosis process.

.

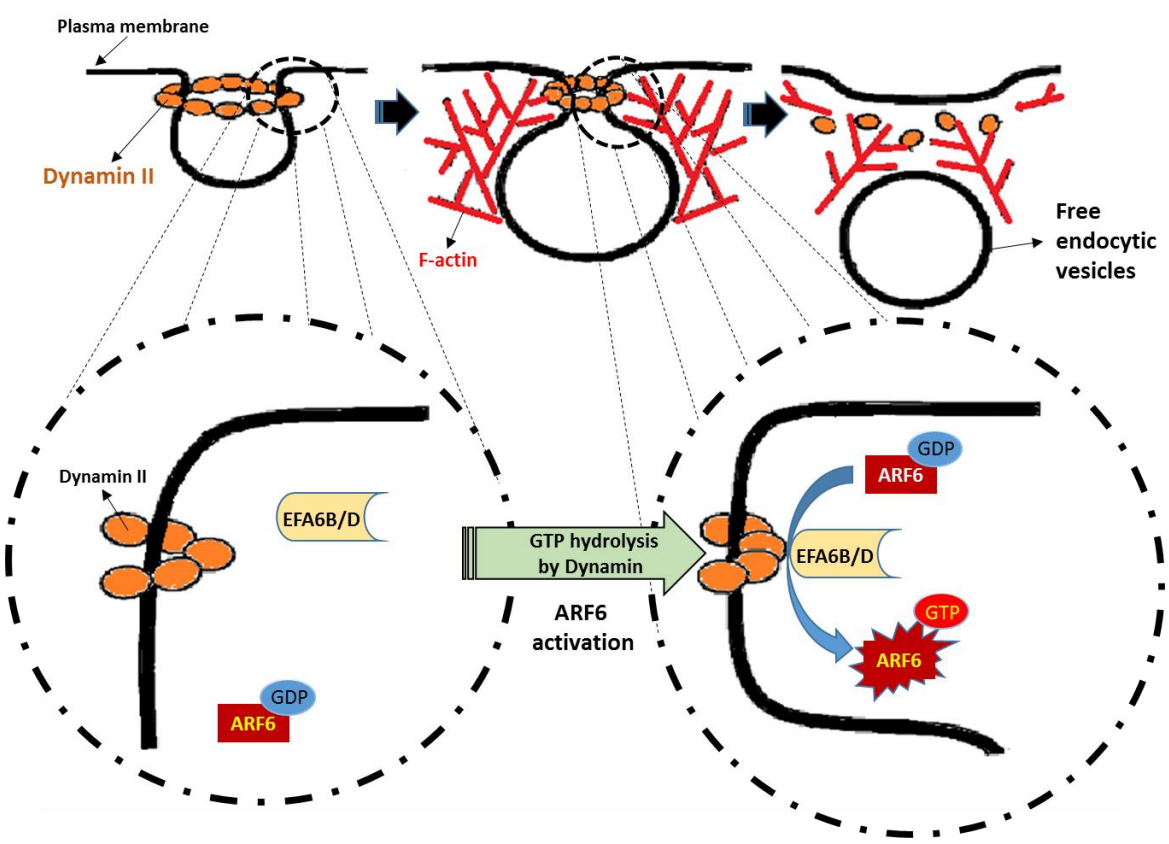
Plasma membrane
Dynamin II
F-actin
Free
endocytic
vesicles
Dynamin II
EFA6B/D
GDP
ARF6
GTP hydrolysis
by Dynamin
ARF6
activation
GDP
ARF6
EFA6B/D
GTP
ARF6

Figure 7. **The proposed model for the dynamin-dependent mechanism of ARF6 activation in a clathrin-mediated endocytosis**. ARF6-specific guanine nucleotide exchange factors (GEFs), EFA6B and EFA6D, interact with dynamin II to activate ARF6.

1. 3. 3. Dynamin-independent endocytosis

ARF6, clathrin-independent carriers/GPI-Enriched Endocytic Compartments (CLIC/GEEC), and Flotillin are major proteins that promote endocytosis and are classified as the "Dynamin-independent endocytosis" pathway (Fig. 6). ARF6 is a small GTPase and a member of the ARF family. ARF6 is essential to a wide range of cellular events such as clathrin-dependent and -independent endocytosis, exocytosis, phagocytosis, macropinocytosis, as well as remodeling of the actin cytoskeleton in membrane ruffle and pseudopodia formation. Considering the important role of ARF6-dependent endocytosis in both MyD88- and TRIF-dependent pathways of TLR4 signaling, ARF6 could be an important target protein to regulate TLR4-driven signaling (Van Acker et al., 2014; Wan et al., 2010).

As mentioned before, clathrin and caveolin are important coating proteins involved in many endocytosis events. However, there are clathrin and caveolin-independent endocytosis. For example, CLICs/GEECs are clathrin-independent endocytic pathways that are mediated by the uncoated tubulovesicular primary carriers which are directly derived from the plasma membrane and mature into tubular early endocytic compartments (Lundmark et al., 2008). These types of endocytic mechanisms, favor other types of GTPase proteins such as cell division control protein 42 (CDC42) (Sabharanjak et al., 2012). Chloride intracellular channel 4 (CLIC4) is a well-studied protein within CLIC family which is abundantly expressed in macrophages and is a positive regulator of LPS-induced TRIF/IRF3 signaling. (He et al. 2011).

Researchers have suggested that Flotillins are involved in many cellular processes such as receptor signaling, phagocytosis, endocytosis, and regulation of actin cytoskeleton. Flotillins, also named reggies, are evolutionarily highly conserved proteins that serve as scaffolding proteins in lipid rafts. Thus, they are generally considered as marker

proteins of lipid microdomains (Zhao et al., 2011). Two homologous members, Flotillin-1 and Flotillin-2, have been identified for this family. While Flotillin-2 has a wide range of distribution, Flotillin-1 seems to be limited to mammalian cells (Zhao et al., 2011). Wei et al. (2013) found that Flotillin-2 can play a crucial role in cellular homeostasis and cell survival by protecting lung epithelial cells against Fas-induced apoptosis and impeding the pro-apoptotic effect of caveolin-1.

1. 3. 4. Endocytosis and receptor signaling

Cell surface receptors enable the cell to identify and react to signals from the outer environment. Various ligand-induced signals can emerge from the receptors located on the cell membrane or relocated into the endosome (Irannejad et al., 2015). These signals can cause distinct biological responses, ranging from proliferation and differentiation to cell death (Miaczynska and Stenmark, 2008).

Stimulation of a cell surface receptor initiates a cascade of signals from the plasma membrane. However, upon engagement, many receptors usually relocate to the endosomal compartment. It is a diverse, profound, and dynamic tubulovesicular system that reaches out all through the cytoplasm (Doherty and McMahon, 2009).

Trafficking of a ligand-receptor complex inside this system modulates cell signaling. This modulation can happen either by signal termination through degradation of receptors in lysosomes and proteasomes, or via recycling of the receptor and reusing it on the cell surface, where it can be restimulated by extracellular ligands. Thus, endocytic bodies can be important sites for the cell signaling pathways (Barbieri et al., 2016).

Emerging findings have revealed that endocytosis can modulate cell signaling by merging and integrating various cascades on the surface of endosomes (Samaj et al., 2004;

Watanabe et al., 2014). These studies indicate that endocytosis is required for downstream signaling of various receptors such as Receptor Tyrosine Kinases (RTKs), G Protein-Coupled Receptors (GPCRs), and TLRs (Goh and Sorkin, 2013; McKay and Morrison, 2007; Zastrow and Hanyaloglu, 2008). This suggests that endosome formation acts as a platform for a full signaling spectrum of many receptors. It can also emphasize the critical role of receptor internalization, which selectively transmits the signals either towards cell death or survival pathways (Schütze and Schneider-Brachert, 2009; Schütze et al., 2008). For instance, the clathrin-dependent endocytosis of IFNAR1 is essential for activating of the downstream proteins such as STAT1 and STAT2 (Marchetti et al., 2006). Moreover, it has been shown that dynamin-dependent internalization of TLR4 can promote late TRAM/TRIF pathway, which is responsible for IRF3-mediated type I interferon induction (Kagan et al., 2008). In contrast, the TIRAP-MyD88, which is an early signaling pathway, initiates at the cell surface membrane; thus, it is not affected (Fig. 5). On the other hand, while the TRIF pathway depends on endocytosis, the type of ligand can play a critical role in inducing simultaneous internalization of TLR4. Rajaiah et al. (2014) used a TLR4/MD2 agonistic antibody (UT12) and a synthetic small-molecule TLR4 ligand (1Z105) to stimulate the receptor endocytosis and found, unlike LPS-induced TLR4 endocytosis, the 1Z105- induced TLR4 endocytosis and TRIF-signaling pathway are dissociable events.

Although the internalization of many receptors is assumed to be essential for the associated signal transduction, there are some cases where the endocytosis of a receptor is not required for its downstream signals. The endocytosis of IFN-gamma receptors is a typical example (Marchetti et al., 2006).

1. 3. 5. Endocytosis and execution of regulated cell death

TNF is a highly pleiotropic cytokine and ligand of the receptors TNFR1 and TNFR2, the receptors located on the cell surface. TNF-α induces intracellular signal transduction and has the potential to elicit cell death (apoptosis). Recent findings indicate a role for the receptor trafficking and involvement of endocytosis in the transmission of signals that lead either to apoptosis or cell survival (Schütze et al., 2008). By blocking the formation of clathrin-coated endosomes, Schütze et al. (2008) showed that TNFR1 internalization is required for the receptor signaling-induced apoptosis. TNFR1 is internalized rapidly, within minutes of TNF signaling, leading to the assembly of the DISC complex (TRADD, FADD, and caspase-8) and cell death by apoptosis (Schneider-Brachert et al., 2004). Thus, the endocytosis of TNFR1 and CD95 (Fas L) might be a prerequisite for the efficient recruitment of DISC proteins to induce the extrinsic pathway of apoptosis (Fig. 8). It has also been demonstrated that targeting Dynamin 2 by Dynasore can inhibit cardiomyocyte apoptosis following oxidative stress (Gao et al., 2016).

Collectively, studies have shown that dynamin-dependent endocytosis is required for apoptosis. Despite extensive studies on apoptosis, the impact of dynamin and endocytosis on other regulated cell death pathways, such as necroptosis in macrophages, is not clear.

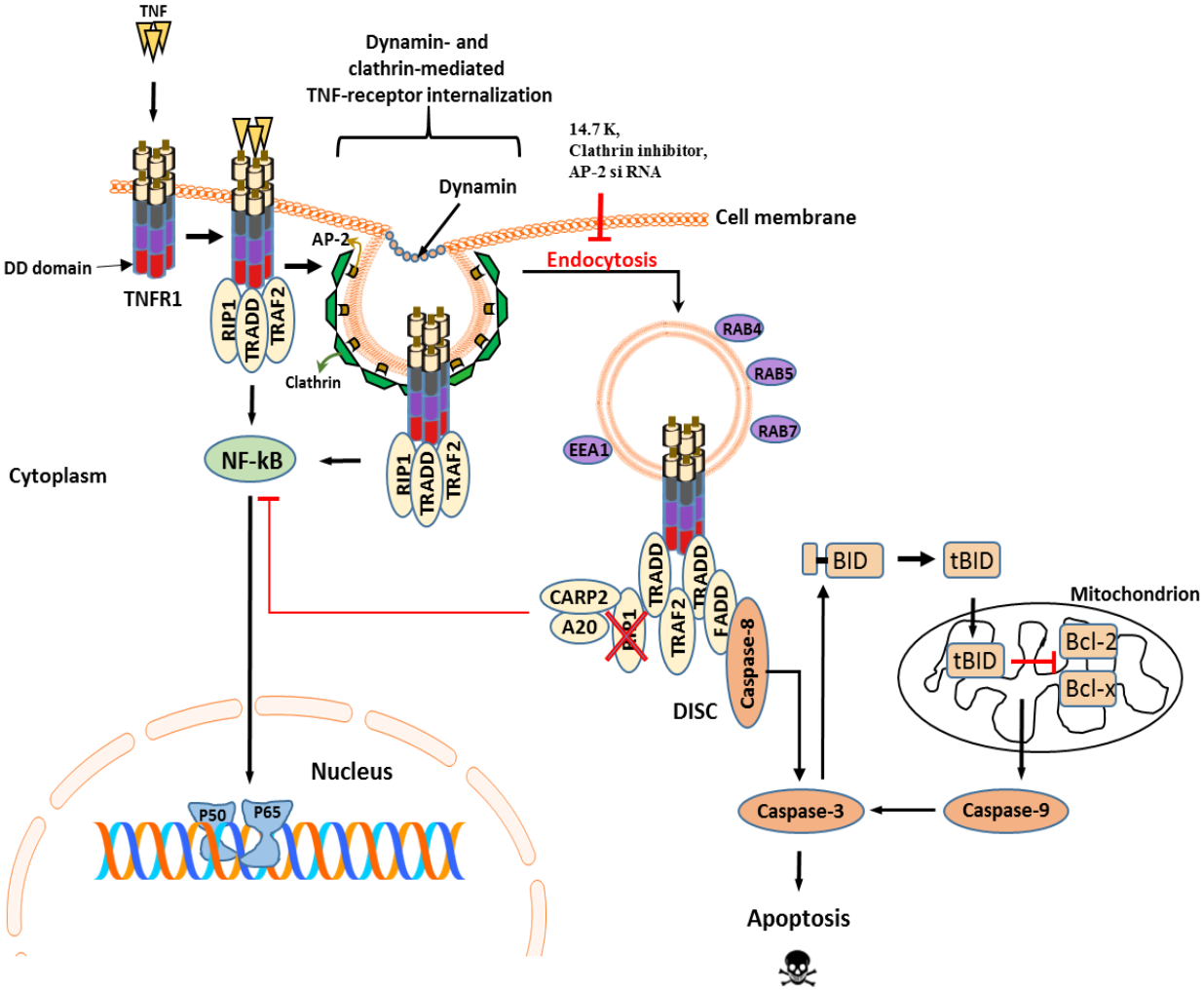
TNF
Dynamin- and
clathrin-mediated
TNF-receptor internalization
14.7 K,
Clathrin inhibitor,
AP-2 si RNA
Dynamin
Cell membrane
AP-2
DD domain
TNFR1
RIP1
TRADD
TRAF2
Endocytosis
Clathrin
RAB4
RAB5
RAB7
EEA1
Cytoplasm
NF-kB
RIP1
TRADD
TRAF2
CARP2
A20
RIP1
TRADD
TRAF2
TRADD
FADD
Caspase-8
DISC
BID
tBID
Mitochondrion
tBID
Bcl-2
Bcl-x
Nucleus
P50
P65
Caspase-3
Caspase-9
Apoptosis

Figure 8. TNFR1-induced apoptosis requires endocytosis of the receptor. Activation of the cell surface TNFR1 receptor triggers a cascade of signaling events, including the death domain (DD)-dependent recruitment and assembly of the death-inducing signaling complex (DISC), that culminate in cellular apoptosis. Recruitment of DISC components to the activated receptor predominantly occurs when the receptor has internalized and moved into an endosomal compartment. Inhibition of the receptor internalization impairs DISC formation and apoptosis. 14.7K: is a potent anti-immune protein encoded by the E3 region of adenoviruses; AP-2: is an adaptor complex in clathrin-mediated endocytosis. EEA1, is an early endosome marker that regulates fusion between primary endocytic vesicles and sorting endosomes; RAB proteins are small GTPase proteins, which have roles in regulatory recycling.

2.0 HYPOTHESIS and STATEMENT OF OBJECTIVES

While there has been significant progress in the understanding of necroptotic pathways, the upstream signaling mechanisms that lead to cell death by necroptosis are not clear. This study will delineate the role of key proteins involved in TLR4-mediated necroptosis of macrophages. Since receptor internalization plays a key role in cytokine signaling, we hypothesize that TLR4 endocytosis is essential for necroptosis signaling in macrophages.

This thesis aims to:

1: Evaluate the impact of dynamin inhibitors on TLR4-induced necroptosis:

- Impact on cell viability (MTT assay, Fluorescent microscopy)
- Impact on cytokine expression (ELISA, CBA)
- Impact on the activation of various kinases involved in necrosome signaling (Western blotting)

2: Evaluate the impact of dynamin inhibitors on TLR-4 internalization in macrophages:

- Impact on the localization of receptor and/or key proteins involved in necroptosis (Flow Cytometry and confocal microscopy)
- Impact on the interaction of upstream and downstream proteins involved in survival and necrosome signaling (Western blotting)

3: Evaluate the impact of p38 MAPK and downstream MAPKAPK2 (MK2) pathways on TLR4-induced necroptosis:

- Impact on cell viability (MTT assay)
- Impact on the activation of various kinases involved in necrosome signaling (Western blotting)

3.0 MATERIAL AND METHODS

3.1. Animals

All mice (table 2.) were housed under the specific pathogen-free condition and maintained in accordance with CCAC guidelines at the University of Ottawa Animal facility. Protocols and procedures were approved and monitored by the University of Ottawa Animal Care Committee and Ethics Board. All mice were age and sex-matched for experiments. Unless stated otherwise, all knockout mice were on a C57BL/6 genetic background.

3. 2. Generation of bone marrow derived macrophages

To grow murine bone marrow derived macrophages, the following lab protocol was used: **1**- Coating CO2-euthanized mice thoroughly by 70% ethanol. **2**- Removing fur surrounding the fore and hind legs prior to limb excision by Scissors and tweezers. **3**- Removing muscles and tissue carefully from bones using scissors, tweezers, and gauze soaked in 70% ethanol and placing in RPMI + 8% FBS + 55 μM 1000X β- mercaptoethanol (2ME) + 50 ng/ml gentamycin. **4**- Flushing bones through a 100 nm cell strainer with R8+gentamycin by using a small gauge needle to harvest pluripotent hematopoietic stem cells. **5**- Counting the number of cells by taking 10 μl aliquot while remaining cells were centrifuged at 1600 RPM for 8 minutes. **6**- Coating 50 mm plastic Petri dishes with macrophage colony stimulating factor (M-CSF) at 5 ng/ml. To prevent macrophages from clumping in culture, M-CSF was spread evenly over the bottom of the Petri dish using an L spreader. **7**- Re-suspending the cell pellet in R8 + gentamycin and approximately $15x10^{6}$ cells were added to each Petri dish. **8**- Adding R8 + gentamycin to petri dishes for a final volume of 10 ml. **9**- Incubating petri dishes at 37°C for 6 days to allow macrophage

differentiation to occur. The purity of macrophages was confirmed by flow cytometry (CD11b+/F4/80+).

Table 2. Mouse strains used for experiments.

Mouse Strain	Source	Other Information
TNFAR1/2 -/-	Jackson Laboratories	Stock #003243
IFNAR1 -/-	A kind gift from Dr. Kaja Murali-Krishna (Emory University, USA)	Mice were backcrossed to C57BL/6 for 14 generations as described by Kolumam et *al.* (2005) from mice generated as described by Müller et *al.* (1994)
TRIF -/-	Jackson Laboratories	Stock #005037
MYD88 -/-	Jackson Laboratories	Stock #009088
STAT1 -/-	Taconic	129S6 genetic background Generated as described by Meraz et *al.* (1996)
IRF9 -/-	Bones provided by Dr. Karen Mossman (McMaster University, Canada)	Generated as described by Kimura et *al.* (1996)
RIPK3 -/-	A kind gift from Dr. Vishva Dixit (Genentech, USA)	Generated as described by Newton et *al.* (2004)
C57BL/6	Jackson Laboratories	Stock #000664

Table 3. Inhibitors and agonists used for experiments.

Inhibitor/Agonist	Source	Notes	Concentrations
Z-VAD-FMK	ApexBio (Cat. # A1902)	Pan-caspase inhibitor	10-100 μM
Poly I:C	Sigma-Aldrich (Cat. # P1530)	dsRNA mimetic used to stimulate TLR3	0.5-20 μg/ml
Necrostatin-1 (Nec-1)	Sigma-Aldrich (Cat. # 9037)	Inhibitor of RIPK1 kinase activity	5 -30 μM
Ultra-pure LPS from E. coli 055:B5	Sigma-Aldrich (Cat. # L4524)	Cell wall component of gram-negative bacteria used to stimulate TLR4	1-100 ng/ml

Gsk 843	Glixx (Cat # GLXC-03989)	Inhibitor of RIPK3 kinase activity	5μM
Genistein	Sigma-Aldrich (Cat. # G6649)	inhibitor of caveolin-mediated endocytosis	10-100 μM
Dingo 4a	Selleckchem (Cat. # S7163)	potent inhibitor of dynamin	10-60μM
Mdivi 1	Tocris Bioscience (Cat. # 3982)	inhibitor of Dnm1- and Drp1-mediated mitochondrial division	50 μM
Dynasore	Tocris Bioscience (Cat. # 2897)	Inhibitor of dynamin	10-300 μM
Dynole	Tocris Bioscience (Cat. # 4222)	Inhibitor of dynamin	1-50 μM
Dynamin inhibitor V34-2	Calbiochem (Cat. # 324414)	Inhibitor of dynamin	75-2400ηM
Z-IETD-FMK	ApexBio (Cat. #B3232)	Inhibitor of caspase-8	10-100 μM
Filipin complex from Streptomyces filipinens	Sigma-Aldrich (Cat. # F9765)	Inhibitor of caveolae and caveolae-like structures	1 μg/mL
OcTMAB	Abcam biochemicals (Cat. # ab120467)	Inhibitor of dynamin	1-10 μM
MiTMAB	Abcam biochemicals (Cat. # ab120466)	Inhibitor of dynamin	1-10 μM
Pro-Myristic acid	Abcam biochemicals (Cat. # ab120476)	a MiTMAB and OcTMAB negative control	1-25 μM
SB203580	Cell signaling (Cat. #5633)	Inhibitor of p38MAPK	10-50 μM
LY2228820	Selleckchem (Cat. # S1494)	P38 MAPK inhibitor	4 μM
PF 3644022	Selleckchem (Cat. # 4279)	MAPKAPK2 (MK2) inhibitor	5 μM

Table 4. **Primary and secondary antibodies used for western blot analysis.**

Antibody	Source	Dilution Used
Mouse anti-RIPK1	BD (Cat # 610459)	1:1000 in Milk
Rabbit anti-RIPK3	ProSci Inc. (Cat # 2283)	1:1000 in Milk
Mouse Anti-β-actin	BD (Cat # 612656)	1:1000 in Milk/or BSA
Rabbit Anti-cIAP1/2	Cyclex (Cat # CY-P1041)	1:1000 in Milk
Mouse Anti-alpha-tubulin	Santa cruz (Cat # Sc-5286)	1:1000 in Milk
Rat-Anti MLKL clone 3H1	Cedarlane (Cat # MABC604)	1:1000 in BSA
Rabbit anti-p38 MAPK	Cell signaling (Cat #8690)	1:1000 in BSA
Rabbit anti-Phospho-p38 MAPK	Cell signaling (Cat #4511)	1:1000 in BSA
Rabbit anti NF-κB p65	Cell signaling (Cat # 8242)	1:1000 in BSA
Rabbit anti Phospho-NF-κB p65	Cell signaling (Cat # 3033)	1:1000 in BSA
Rabbit anti-pSTAT1 (Ser727)	Cell signaling (Cat #9177)	1:1000 in BSA
Rabbit anti-pSTAT1 (Tyr701)	Cell signaling (Cat #9167)	1:1000 in BSA
Rabbit anti-STAT1	Cell Signaling (Cat# 9172)	1:1000 in BSA
Mouse anti-FADD monoclonal antibody (1F7)	ENZO (Cat # ADI-AAM-212-E)	1:1000 in Milk
Goat anti-Rabbit IgG (H+L) HRP	Bio RAD (Cat #170-6515)	1:5000
Goat anti-Rat IgG (H+L) HRP	Millipore (Cat #AP183)	1:5000
Goat anti-Mouse IgG (H+L) HRP	Santa Cruz (Cat # Sc 2031)	1:5000
Rabbit anti- IRF3	Cell Signaling (Cat# 4302)	1:1000 in BSA
Rabbit anti-Phospho IRF3	Cell Signaling (Cat# 4947)	1:1000 in BSA
Rat Anti-caspase-8	ENZO (Cat # 1G12)	1:1000 in Milk
Rabbit anti-MK2	Cell signaling (Cat #3042)	1:1000 in BSA
Rabbit anti-Phospho-MK2	Cell signaling (Cat #3007)	1:1000 in BSA

3. 3. In vitro inhibitor assays

Various small molecule inhibitors and agonists as listed in Table -3 were used to treat the cells. According to the literature, among three different classes of dynamin inhibitors, the most effective ones were selected to test.

The first reported dynamin inhibitors are long chain ammonium salts, of which the most potent are Myristyl trimethyl ammonium bromide (MiTMAB) and octadecyltrimethyl ammonium bromide (OcTMAB) were chosen as the most potent inhibitors in this class (Hill et al., 2004). The inhibition of dynamin activity by MiTMABs via interfering with the binding of the PH-domain to phospholipids, results in blocking dynamin recruitment to the membrane (Quan et al., 2007).“Dynasore” group is the second class of dynamin inhibitors. Dynasore was identified based on the screening of 16,000 small molecules. It is a potent inhibitor of dynamin I, dynamin II and dynamin related protein 1 (Drp-1). A non-competitive interfering with the GTPase activity of dynamins is considered as its mode of action (Macia et al., 2006). To avoid some disadvantages of Dynasore such as binding stoichiometrically to detergents used for in vitro drug screening, more potent reagents than Dynasore termed the “Dyngo analogues” have been developed (Mccluskey et al., 2013) . Among them, Dyngo 4a is considered as the most effective compound. The third group of dynamin inhibitors, the Dynole series have been invented to non-competitively inhibit dynamin GTPase activity and dynole 34-2 (2-cyano-3-(1-(2-(dimethylamino)-ethyl)-1*H*-indol-3-yl)-*N*-octylacrylamide) is the most potent member of this group (Hill et al., 2009). Furthermore, Mdivi-1 is a selective inhibitor of Drp-1, with no impact on dynamin proteins.

Techniques varied for each experiment. Thus, details are provided in the text. In general, one day before treatment, BMDMs were seeded at $7x10^4$ or $2.5\ x10^5$ cells/well in a 96-well or 24-well flat bottom tissue culture plate (Falcon), respectively. After treatment

with appropriate concentrations of inhibitors and agonists, cells were usually left for 24 hours before assessing viability.

Table 5. Description of biological activity with the related chemical structure of dynamin inhibitors used in this study.

Dynamin Inhibitors	Description*	Chemical structure
Dynasore	A cell-permeable semicarbazone compound that inhibits the GTPase activity of dynamin1/2 (IC_{50} ~15 µM) and Drp1, while exhibiting no significant effect against two other small GTPases, MxA and Cdc42. Dynasore inhibits endocytosis through blockage of dynamin at the late invagination stage. Inhibition of lipid raft fusion through impact on actin filaments is an off target of Dynasore.	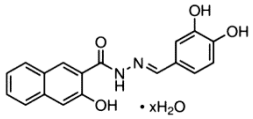
Dyngo-4a	A potent dynamin inhibitor with IC50 of 0.38 µM, 1.1 µM, and 2.3 µM for DynI (brain), DynI (rec), and DynII (rec), respectively. Inhibition of lipid raft fusion through impact on actin filaments is an off target of Dyngo 4a.	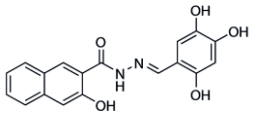
Dynole	Dynamin I inhibitor (IC_{50} = 1.3 µM). Inhibits receptor-mediated endocytosis (RME) (IC_{50} = 5.0 µM).	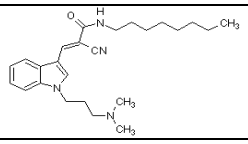
Mdivi-1	Selective inhibitor of Dnm1 GTPase (IC_{50} = 1 - 10 µM); attenuates Dnm1- and Drp1-mediated mitochondrial division. Inhibits mitochondrial outer membrane permeabilization (MOMP) and attenuates apoptosis.	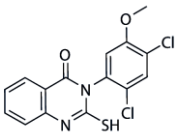
MiTMAB	Cell-permeable dynamin I and dynamin II inhibitor (IC_{50} values are 3.1 and 8.4 µM for inhibition of dynamin I and dynamin II GTPase, respectively). Targets the pleckstrin homology (PH) (lipid binding) domain. Competitive with phospholipid and non-competitive with GTP. Inhibits receptor-mediated and synaptic vesicle endocytosis (IC_{50} values are 19.9 and 2.2 µM, respectively). Inhibits cancer cell growth.	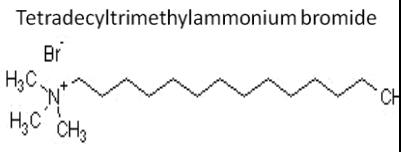
OcTMAB	Cell-permeable dynamin I and dynamin II inhibitor (IC_{50} values are 1.9 and 4.4 µM for inhibition of dynamin I and II GTPase, respectively). Targets the pleckstrin homology (PH) (lipid binding) domain. Competitive with phospholipid and non-competitive with GTP. Inhibits receptor-mediated endocytosis (IC_{50} = 6.7 µM). Inhibits cancer cell growth.	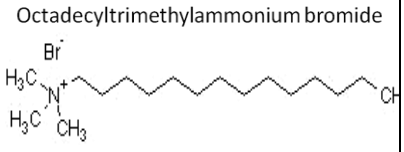

* The information has been provided by companies' websites.

3. 4. Cell viability test (MTT assay)

3-(4, 5-dimethylthiazol-2-yl)-2,5-diphenyltetrazolium bromide (MTT) was used to measure cell viability. After collecting cell supernatant, 100µl/well of MTT reagent (0.5 mg/ml in R8) was added into the 96-well plate and incubated at 37°C for two hours. Cells were lysed by adding 5mM HCl in isopropyl alcohol and vigorously mixed to solubilize the MTT crystals. Optical density values were obtained by measuring absorption at 570 nm with a reference wavelength of 650 nm on a Molecular Devices Emax plate reader. SoftMax Pro and Graphpad Prism 6 were used to analyze the data. Unless otherwise stated, the data were normalized to the corresponding stimulated control in the absence of zVAD (i.e. LPS+zVAD treated cells were normalized to LPS treated cells while TNF+zVAD treated cells were normalized to TNF). Statistical analysis was performed using GraphPad Prism 6 (La Jolla, CA, USA). Unpaired Student's t test was used to confirm the statistical significance of differences between results. All error bars shown represent standard error of the mean (S.E.M.).

3. 5. Western blotting

BMDM cells were seeded in a 24-well plate, at 2.5-3x10^5cells/well after 6 days in culture with M-CSF as described previously. The cells were treated with inhibitors and/or stimulants at different time points (time course) in the following day. After finishing the time course, cells were washed with cold PBS and immediately put on ice.The cells were lysed using 1% SDS lysis buffer with 1% β-mercaptoethanol and transferred to 1.5 mL Eppendorf tubes. Samples were boiled at 96°C in a hot plate to minimize protein degradation and frozen at -20°C for future use. Standard protocol for western blot analysis was followed. Lysates were run on a 1.5 mm 15-well 8%, 10% or 15% polyacrylamide gel depending on the size of

the proteins of interest. Gels were typically loaded with 25 µl of lysate and run at 135 V for one hour and 16 minutes. A PVDF membrane was soaked with 100% methanol for minutes before the transfer step. The transfer was run at 100 V for an hour. An ice pack was added to the transfer cassette to prevent overheating. Once transferred, the membrane was blocked with 5% skim milk in Tris Buffered Saline Solution (TBS – 0.5M Tris, 1.5 NaCl pH 7) with 0.5% Tween- 20 (TBST) or 5% bovine serum albumin (BSA) depending on the manufacturer's protocol for one hour at room temperature on the shaker. Primary antibodies diluted in appropriate blocking buffer (5% milk or BSA), added to the membrane in a sealed plastic pouch and incubated overnight on the shaker at 4°C. Antibodies and corresponding dilutions used are listed in Table 4. Diluted primary antibody was kept for few months by adding 0.2% sodium azide to diluted antibodies in milk or BSA. Membranes were then washed with TBST five times at five-minute intervals before adding secondary antibody diluted in the appropriate blocking buffer (5% milk or BSA) for 45 min to one hour. Secondary antibody was discarded and membranes were washed again as previously mentioned. Membranes were visualized using either luminol ELC substrate (Thermo Scientific #32106) or the highly sensitive West Femto ECL substrate (Thermo Scientific #34095) depending on the level of protein expression. A photosensitive film (Sigma-Aldrich, Carestream Heath 785019) was used to examine protein expression. Results were quantified using Image-J software to perform the densitometric analysis.

3. 6. Flow cytometry

Cells were stained using the antibodies listed in table 4 in phosphate buffered saline (PBS) with 1% bovine serum albumin (BSA) at a concentration of 0.5-1µL/ million cells.

Samples were acquired on a CyAN-ADP (Beckman Coulter) or Fortessa (BD Biosciences) and analyzed using Kaluza (Beckman Coulter) and/or Flow-Jo (FlowJo, LLC).

3. 7. IFN-β production

Using the L929 cell line (obtained from Dr. Bruce Beutler, USA), the expression of IFN-β was assessed with a cloned luciferase reporter gene under the regulation of an ISRE-containing promoter. A frozen stock of ISRE-L929 cells was revived in 10% FBS + 2ME +Dulbecco's Modified Eagle's Medium (DMEM) and incubated at 37°C for several days to allow cells to proliferate. ISRE-L929 cells were seeded at $5x10^4$cells/well and incubated at 37°C with 40 µl of samples (culture supernatants) for 4 hours. Cells were rinsed with PBS and then lysed with 25µl/well of 1X lysis buffer supplied in the luciferase assay system kit (Promega, E1500). After adding 100 µl of luciferase assay reagent to each well containing lysed cells, luminescence was measured using a Molecular Devices Emax plate reader. Data were analyzed using SoftMax Pro and Graphpad Prism 6.

3. 8. Cytokine and chemokine quantification

100µl of supernatants was collected from each well and analyzed to measure cytokines and chemokines using cytokine bead array (CBA) kits (BD Bioscience) or Enzyme-linked immunosorbent assays (ELISAs). Murine IL-10 (BD Biosciences, 555252), TNF (BD Biosciences, 560478), IL-6 (BD Biosciences, 555240), and IL-12 (BD Biosciences, 555256) were measured using ELISA and CBA while MIP-1a was measured using CBA. For ELISA, plates were coated with capture antibody at 4°C overnight. The following day sealed plate was aspirated and washed 3 times with washing buffer (PBST-0.5% tween). Next, the plate

was blocked with 100 µL/well of assay diluent for 1 hour and incubated with the supernatants and standard for two hours. Detecting antibodies and streptavidin-HRP were added and incubated for another one hour. For the IL-6 plate only, detection antibody and Steptavidin-HRP were added separately. HRP substrate was added, and the reaction stopped by adding stop solution ($2NH_2SO4$) according to the reactivity of the standards in each plate. The absorbance was measured at 450 nm – 570 nm on a Molecular Devices Emax plate reader. Data were collected and analyzed using SoftMax Pro and Graphpad Prism 6.

3. 9. Immunofluorescence

Differentiated BMDMs were treated with various reagents as described in the text for 24 hours, then stained with Hoëchst (2.5µg/mL; Invitrogen 33342) and propidium iodide (PI) (1:10 dilution; BD Pharmingen, 550825) in RPMI lacking phenol for 25-30 minutes to distinguish live and dead cells. Hoëchst can stain both dead and live cells in blue color. However, PI is able to stain the nucleus of only dead cells in red color. Consequently, live cells are detectable by their blue color and dead cells by their pink (Blue +Red) color. A Zeiss AxioObserver D1 microscope and the AxioVision Rel. 4.8 program were used to capture and analyze images. The Lumenera Infinity Analyze program was used to quantitate the rate of cell death.

3. 10. Confocal microscopy

Day-6 to 8 BMDMs were seeded on 6-well glass bottom dishes (Ibidi GmbH) for overnight in RPMI supplemented with 10% FBS. The cells were fixed with 4% paraformaldehyde for 15 min at room temperature and, after two washes with phosphate-buffered saline (PBS), permeabilized with 0.05% saponin for 30 min. After incubation with

the appropriate primary antibody against TLR4 (ab22048- mouse monoclonal) for 1 h at room temperature, the cells were washed twice with PBS and incubated with the compatible secondary antibody (goat anti-mouse) for an overnight in 4 ºC. Cells were also stained with PE conjugated antibody against EEA1. Nuclei were stained with DAPI. Next day, after two washes with PBS and drying, mountain medium (Ibidi GmbH) was added to the cells and were imaged using a Zeiss 510 meta confocal microscopes. Images were captured using 60X.1.4 objective and numerical aperture with a proper laser according to the secondary antibodies specificity.

4.0 RESULTS

4. 1. Requirements for TLR4-induced necroptosis of mouse BMDMs

4. 1. 1. TLR-4 or cytokine receptor engagement and caspase inhibition are required for the induction of necroptosis in macrophages

To study the upstream events involved in necroptotic signaling in bone marrow-derived macrophages (BMDMs) from wild-type (WT) C57BL/6J mice, cells were treated with various stimuli *in vitro* for 6 or 24 hours. A colorimetric assay using 3-(4,5-dimethylthiazol-2-yl)-2,5-diphenyltetrazolium bromide (MTT) was used to assess cell viability. Live cells, unlike dead cells, are able to reduce MTT (yellow) into formazan crystals which, if treated with isopropanol solution, form a purple color resulting in higher optical density (OD) values. Treatment of BMDMs generated, as described in "Material and Methods", with lipopolysaccharide (LPS) not only did not cause cell death, but also resulted in noticeably higher OD values (Fig. 9 A) indicating higher metabolic activity in these cells. Furthermore, treating macrophages with zVAD alone, a pan-caspase inhibitor, did not have any impact on cell viability (Fig. 9 A). BMDMs, however, died by necroptosis when cells were treated with LPS, TNF or IFN-β in combination with zVAD. Cell death was inhibited by treatment with necrostatin-1, a RIPK1 inhibitor (Fig. 9 A, C-D), or Gsk, a RIPK3 inhibitor (Fig. 9 A), indicating that the mode of cell death was necroptosis.

These results indicate that cytokine-receptor, TLR4 signaling or caspase inhibition alone does not induce necroptosis, and that cytokine-receptor or TLR4 signaling in conjunction with caspase inhibition is required for the induction of necroptosis in murine macrophages.

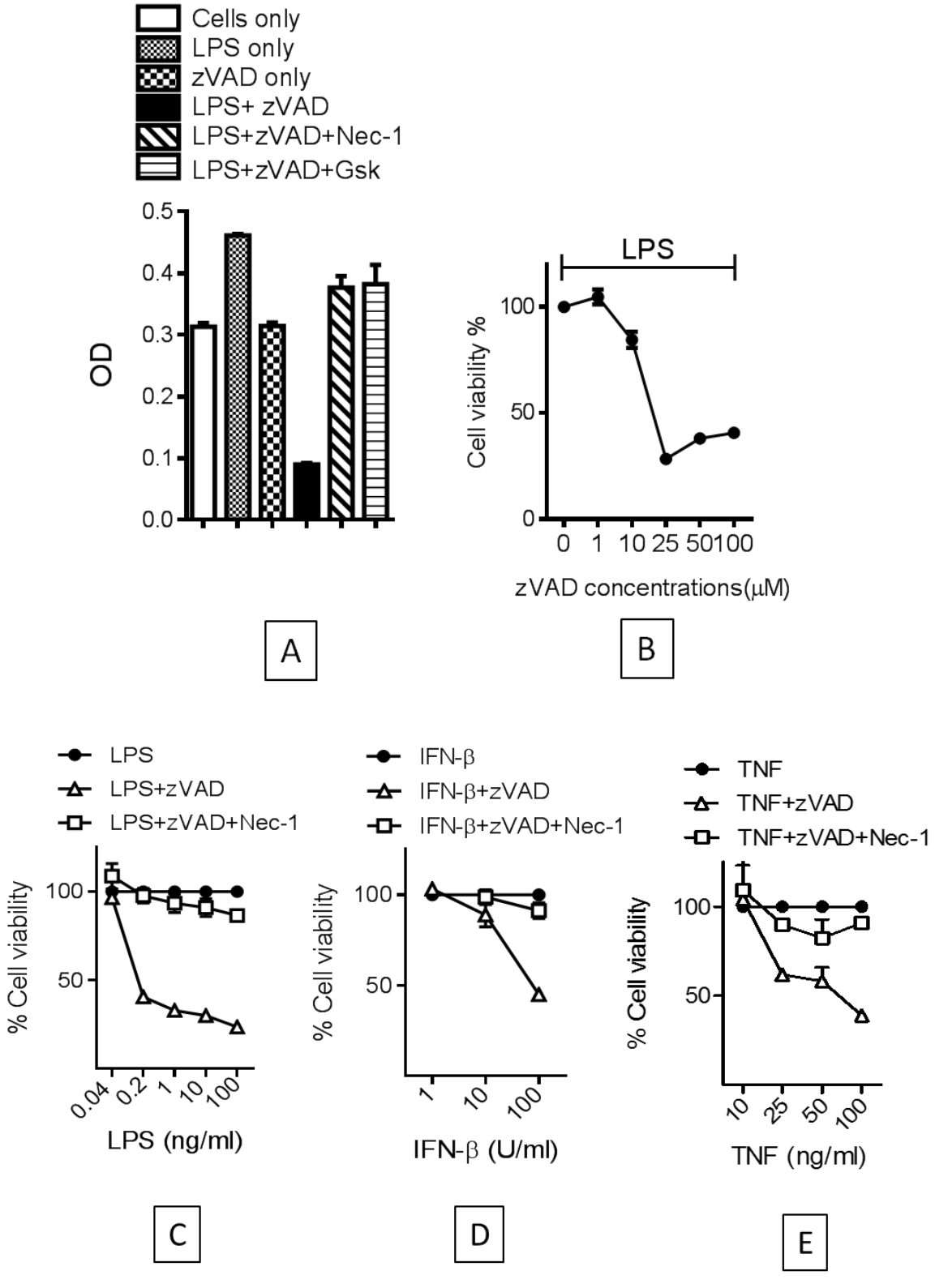
Cells only
LPS only
zVAD only
LPS+ zVAD
LPS+zVAD+Nec-1
LPS+zVAD+Gsk
OD
0.5
0.4
0.3
0.2
0.1
0.0
LPS
Cell viability %
100
50
0
0 1 10 25 50100
zVAD concentrations(μM)
A
B
LPS
LPS+zVAD
LPS+zVAD+Nec-1
% Cell viability
100
50
0.04 0.2 1 10 100
LPS (ng/ml)
IFN-β
IFN-β+zVAD
IFN-β+zVAD+Nec-1
% Cell viability
100
50
1 10 100
IFN-β (U/ml)
TNF
TNF+zVAD
TNF+zVAD+Nec-1
% Cell viability
100
50
10 25 50 100
TNF (ng/ml)
C
D
E

Figure 9. Concurrent inhibition of caspase activity and engagement of TLR4 or cytokine receptor (IFNAR1 or TNFRs) promote necroptosis of macrophages. OD values or cell viability percentage of BMDMs from WT C57BL/6 were measured by MTT assay after treating with various stimuli and inhibitors in 96-well plates for 24 hours. Treatments include LPS (100ng/mL) ± zVAD (50μM) ± Nec-1(30μM) or Gsk (5μM) (A); LPS (100ng/mL) + various concentrations of zVAD (0-100μM) (B); various concentration of LPS (0.04 -100ng/mL) ± zVAD (50μM) ± Nec-1(30μM) (C), or various concentration of IFN-β (1-100U/mL) ± zVAD (50μM) ± Nec-1(30μM) (D), or various concentration of TNF (10-100ng/mL) ± zVAD (50μM) ± Nec-1(30μM) (E). Data are representative of at least three independent experiments.

4. 1. 2. LPS- and IFN-β-induced necroptosis follow different time kinetics

The treatment of WT BMDMs with a combination of LPS and zVAD caused cell death after three hours. The rate of death increased over time, reaching more than 75% at the 24-hour point. The mechanism of cell death was necroptosis as the cells were rescued by Nec-1 (Fig. 10 A). While the treatment of cells with IFN-β and zVAD resulted in necroptosis, the time kinetics of cell death was significantly slower (Fig. 10 B).

4. 1. 3. Necroptosis signaling reaches a point of no return shortly after stimulation

Murine macrophages from WT mice were treated with a combination of TLR4 ligand (LPS 100 ng/mL) and the pan-caspase inhibitor (zVAD 50μM) to induce necroptosis. Necrostatin-1 (Nec-1 30 μM), which inhibits necroptosis, was added at various time intervals over the course of nine hours (0, 1, 3, 6, 9) to determine the specific time period during which it would be required to inhibit necroptosis. Results indicated that the addition of Nec-1 one hour post treatment with LPS+zVAD inhibited necroptosis, but the addition of Nec-1 three hours post treatment failed to rescue from necroptosis. This indicates that necroptosis signaling in the case of LPS+zVAD treatment reaches a point of no return within the first few hours (Fig. 11 A).

While the treatment of cells with IFN-β + zVAD resulted in necroptosis, the point of no return was achieved at a much later time (Fig. 11 B), which was commensurate with the delayed time kinetics of necroptosis previously observed with IFN-β+zVAD (Fig. 10 B). According to a report previously published by our lab (McComb et al., 2014), IFNAR1 plays a critical role in LPS-induced necroptosis and it had been assumed that IFN-β would act through an autocrine mechanism. Therefore, a series of experiments were conducted to clarify the role of IFN-β and IFNAR1 signaling in TLR4-mediated necroptosis.

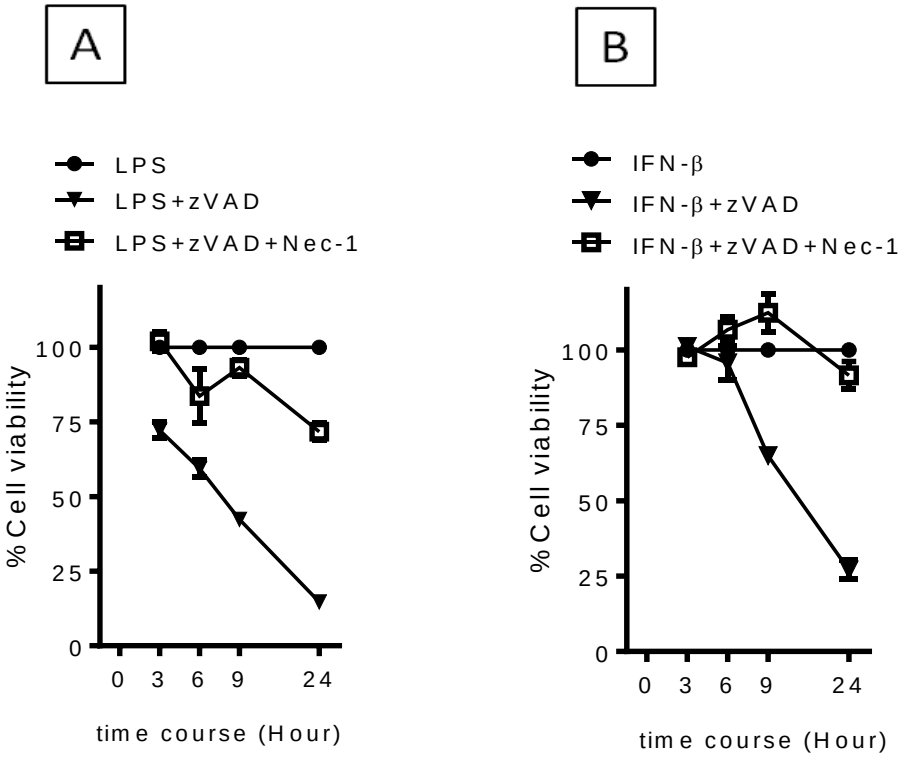
A
LPS
LPS+zVAD
LPS+zVAD+Nec-1
% Cell viability
100
75
50
25
0
0 3 6 9 24
time course (Hour)
B
IFN-β
IFN-β+zVAD
IFN-β+zVAD+Nec-1
% Cell viability
100
75
50
25
0
0 3 6 9 24
time course (Hour)

Figure 10. Different time kinetics of necroptosis induced by LPS- or IFN-β signaling in macrophages. BMDMs from WT macrophages were stimulated with LPS (A)(100ng/mL) or IFN-β (1000U/mL) (B) ± zVAD (50μM) ± Nec-1 (46μM) in 96-well plates. Cell viability, for five interval post stimulations during 24 hours, was measured by MTT assay. Percent survival was calculated relative to the cells stimulated with LPS only. Data are representative of at least three independent experiments performed in triplicate.

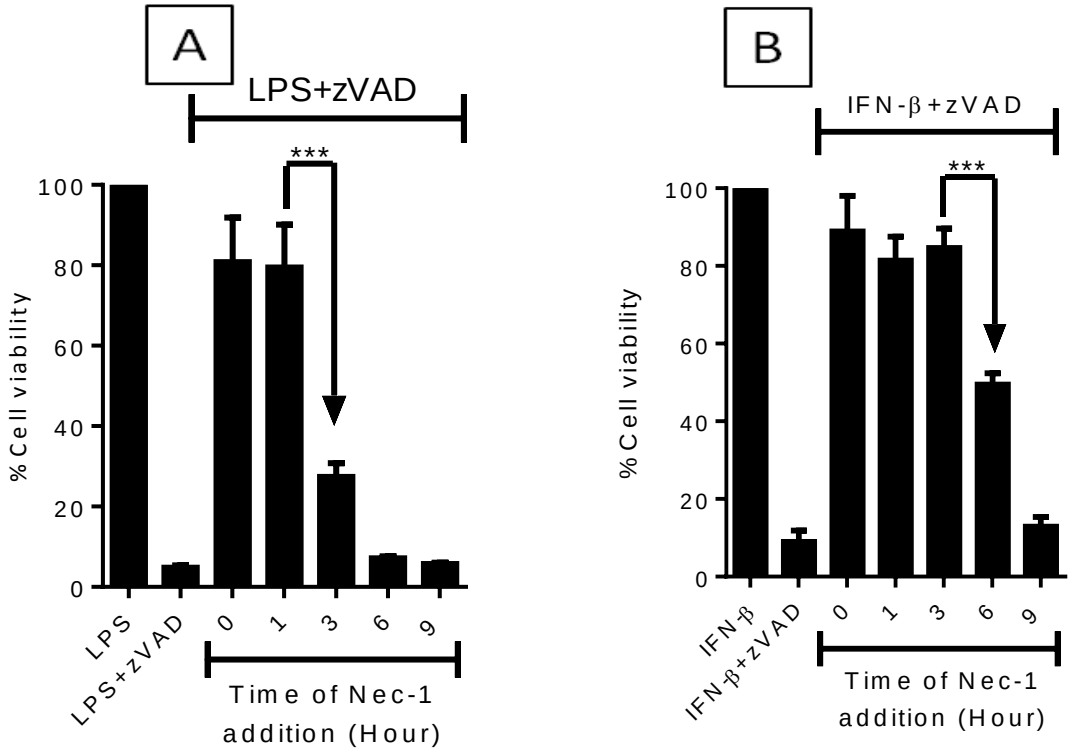
A
LPS+zVAD
***
100
80
60
40
20
0
% Cell viability
LPS
LPS+zVAD
0
1
3
6
9
Time of Nec-1
addition (Hour)
B
IFN-β+zVAD
***
100
80
60
40
20
0
% Cell viability
IFN-β
IFN-β+zVAD
0
1
3
6
9
Time of Nec-1
addition (Hour)

Figure 11. **Critical time point for rescuing BMDMs from LPS- or IFN-β-induced necroptosis.** Treatment of BMDMs from WT with LPS (100 ng/mL) (A) or IFN-β (1000 U/mL) (B) ± zVAD (50μM) ± Nec-1 (30μM) in 96-well plates after certain period (0. to 9 hours) to evaluate the range of *in vitro* critical time for rescuing macrophages against necroptosis. Cell viability during 24 hours was measured by MTT assay, for five intervals (0-9 hours) post treatment with Nec-1 (30μM), an inhibitor of necroptosis. Percent survival was calculated relative to the cells stimulated with LPS or IFN-β only. Data are representative of at least three independent experiments performed in triplicate. Black arrows show the ending point of this time for each set of treatment.

4. 1. 4. LPS-induced necroptosis is significantly dependent on IFNAR1 signaling

Macrophages deficient in IFNAR1 displayed potent protection against necroptosis induced by LPS+zVAD (Fig. 12 A). Since IFNAR1 signaling operates through the ISGF3 complex that is composed of STAT1, STAT2, and IRF9 (McComb et al., 2014), the impact of these signaling molecules in LPS-induced necroptosis was tested. STAT1- and IRF9-deficient macrophages displayed significant protection against necroptosis induced by LPS+zVAD (Fig. 12 B). Although the impact of TNFR1/2 on necroptosis was not clear (Fig. 12 C), TRIF deficient macrophages showed significant resistance to cell death in a six or 24-hour cell death assay (Fig.13). This indicates that the TRIF pathway has a noticeable role in promoting necroptosis of macrophages, and IFNAR1 signaling is the dominant pathway responsible for the induction of necroptosis in macrophages.

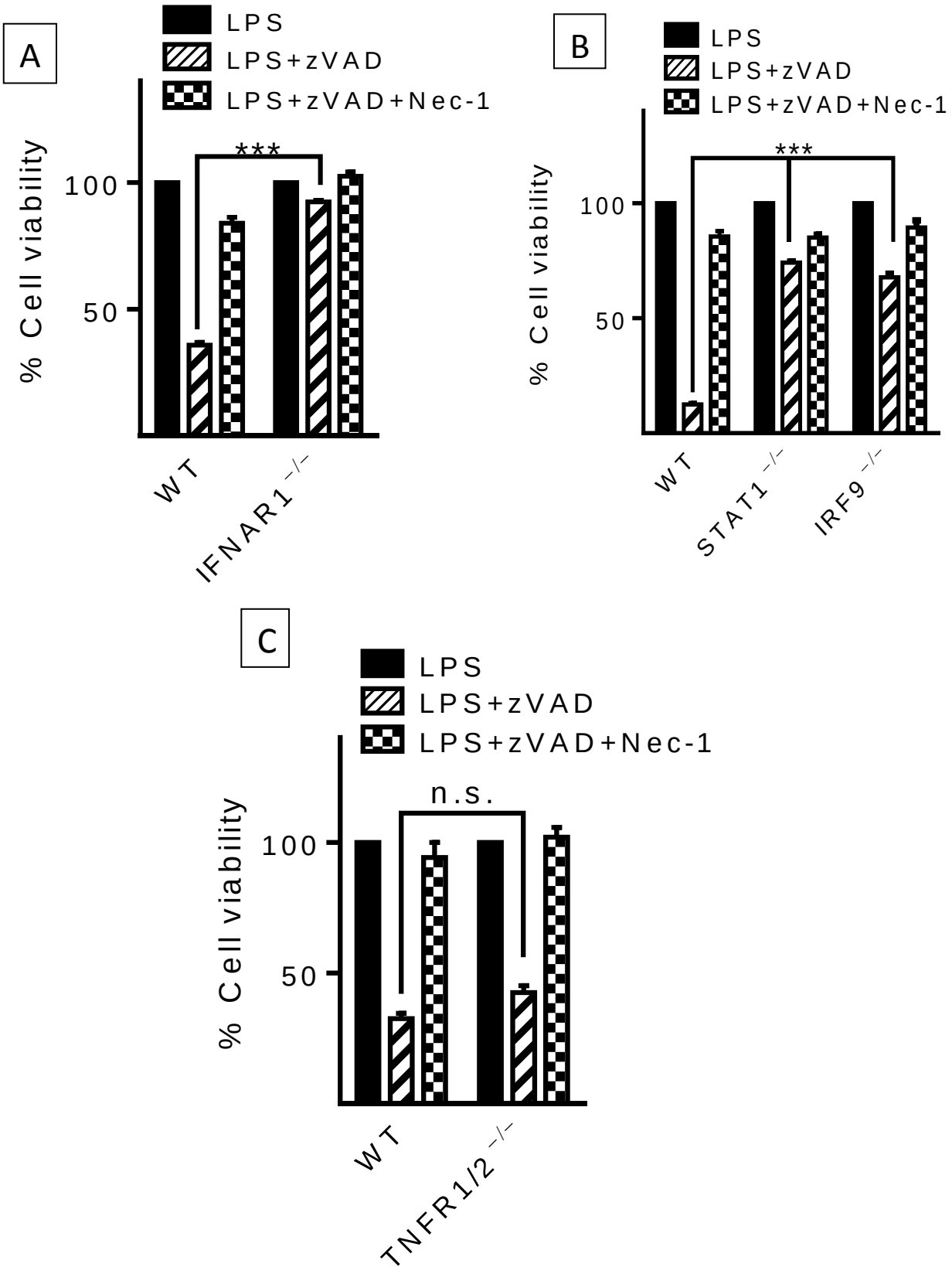
A
LPS
LPS+zVAD
LPS+zVAD+Nec-1
% Cell viability
100
50
***
WT
IFNAR1 −/−
B
LPS
LPS+zVAD
LPS+zVAD+Nec-1
% Cell viability
100
50
***
WT
STAT1 −/−
IRF9 −/−
C
LPS
LPS+zVAD
LPS+zVAD+Nec-1
% Cell viability
100
50
n.s.
WT
TNFR1/2 −/−

Figure 12. **IFNAR1 signaling, not TNFR1/2 signaling, promotes necroptosis in macrophages.** Cell viability during 24 hours was measured by MTT assay after treatment BMDMs from WT, IFNAR1, IFNAR1 downstream (STAT1, and IRF9) (A-B), and TNFR1/2 knockout mice (C), with LPS (100ng/mL) ± zVAD (50μM) ± Nec-1 (30μM) in 96-well plates. Data are representative of at least three independent experiments performed in triplicate. Data was normalized based on the LPS data. *** $P < 0.001$.

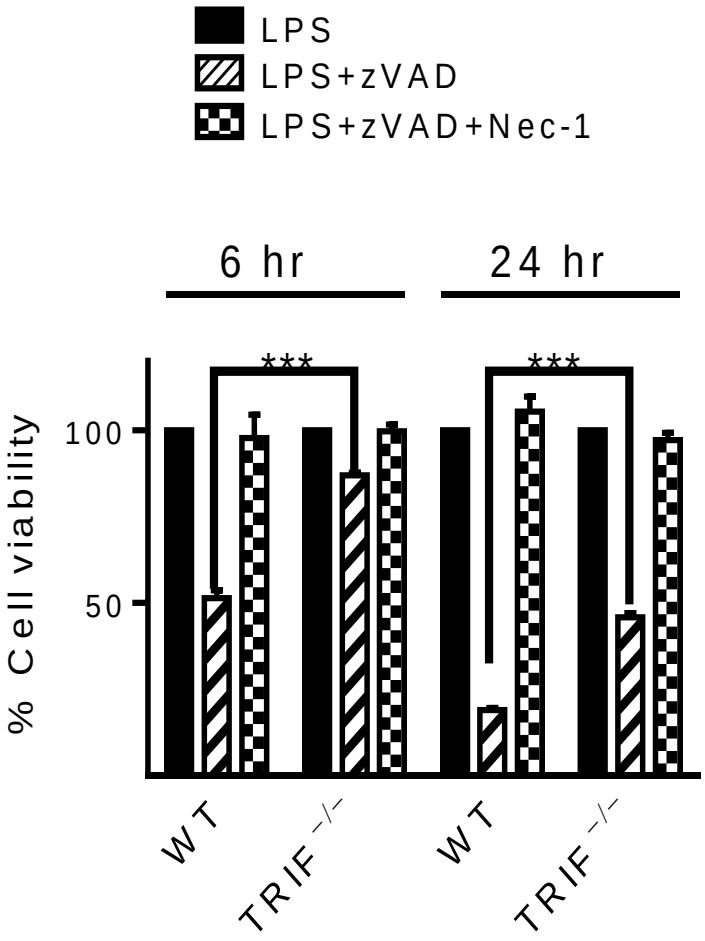
LPS
LPS+zVAD
LPS+zVAD+Nec-1
6 hr
24 hr
***
***
% Cell viability
100
50
WT
TRIF−/−
WT
TRIF−/−

Figure 13. **TRIF signaling significantly expedites the induction of necroptosis following TLR-4 engagement.** Cell viability for 6 or 24 hours was measured by MTT assay after treatment of BMDMs from WT, or TRIF deficient mice treated with LPS (100ng/mL) ± zVAD (50μM) ± Nec-1 (30μM) in 96-well plates. Data are representative of at least three independent experiments performed in triplicate. Data was normalized based on the LPS data. *** $P < 0.001$.

4. 1. 5. LPS-induced necroptosis is independent of autocrine IFN-β secretion in WT BMDMs

Having confirmed the critical role of IFNAR1 signaling in necroptosis, we determined whether the secretion of IFN-I during TLR4 signaling is required to induce necroptosis of macrophages. A neutralizing antibody against the IFNAR1 was used to block the ability of secreted IFN-I to bind IFNAR1. Blocking the IFNAR1on the cells treated with LPS+zVAD did not prevent necroptosis (Fig. 14). When necroptosis was induced by treating cells with IFN-β+zVAD, blocking IFNAR1 with an antibody resulted in cell survival (Fig. 14). The previous report suggests that IFN-I is secreted and acts through an autocrine mechanism to induce necroptosis (McComb et al., 2014). However, our data clearly demonstrated that autocrine IFN-I secretion during LPS stimulation was not required for the induction of necroptosis. Taken together, these results indicate that while IFNAR1 signaling is required for necroptosis following TLR4 signaling, this does not appear to involve the secretion of IFN-I.

4. 2. Dynamin-dependent endocytosis is dispensable for necroptosis of macrophages

4. 2. 1. Dynamin promotes internalization of TLR4 following LPS/zVAD treatment

To investigate the early events in necroptosis of macrophages following TLR signaling, the fate of cell surface TLR4 following LPS treatment of macrophages was evaluated. Using various dynamin inhibitors, such as Dynasore, many researchers have shown that TLR4 internalization is a dynamin-dependent process (Kagan et al., 2008; Rajaiah et al., 2015). Therefore, we were interested in understanding whether the inhibition of dynamin could prevent TLR4 internalization following LPS+zVAD treatment. More specifically, we wanted to address the impact of dynamin in necroptosis.

WT BMDMs were pre-treated for 30 minutes with various dynamin inhibitors such as Dynasore, Dyngo 4a, and Dynole, or were left without pre-treatment (control) prior to the addition of LPS+zVAD. The expression of TLR4 on the cell surface of macrophages was measured by the mean fluorescence intensity (MFI) of TLR4. The MFI level of the cells pre-treated with dynamin inhibitors was significantly higher than the cells that had been treated with only LPS+zVAD. The results confirmed that TLR4 internalization was blocked by all three dynamin inhibitors indicating that the type of endocytosis of TLR4 is dynamin-dependent (Fig. 15 A-C). Furthermore, we used confocal microscopy to visualize the impact of dynamin inhibitors on TLR4 internalization following LPS+zVAD treatment.

Cells were stained with appropriate antibody against TLR4 and EEA1 (as described in the "Material and Methods"). Nuclei were stained with DAPI (blue). As expected, confocal microscopy showed that Dyngo 4a, a dynamin inhibitor, significantly blocked TLR4 endocytosis. Further analysis of the images showed a detectable co-localization of TLR4 with EEA1 in the cells that had not been treated with the dynamin inhibitor (Fig. 16, A). Interestingly, co-localization of TLR4 and EEA1 was not detected in the cells pre-treated with Dyngo 4a (Fig. 16, B). Cells treated with the dynamin inhibitor, Dyngo 4a, did not show any co-localization of TLR4 and EEA1. Collectively, these results confirm that dynamin plays a crucial role in the internalization of TLR4 to the endosomal compartment.

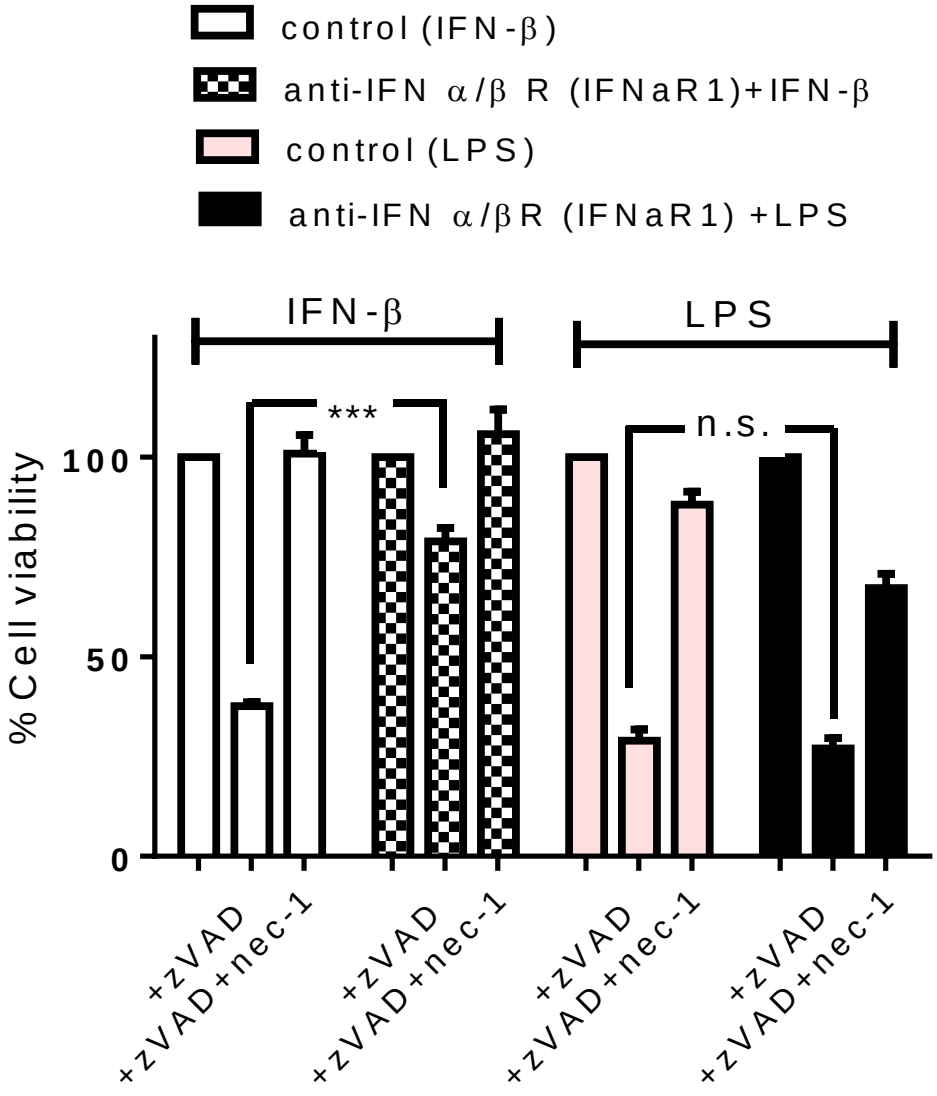
control (IFN-β)
anti-IFN α/β R (IFNaR1)+IFN-β
control (LPS)
anti-IFN α/βR (IFNaR1) +LPS
IFN-β
LPS
***
n.s.
% Cell viability
100
50
0
+zVAD
+zVAD+nec-1
+zVAD
+zVAD+nec-1
+zVAD
+zVAD+nec-1
+zVAD
+zVAD+nec-1

Figure 14. Autocrine IFN-I is not required for LPS-induced necroptosis of macrophages. Cell viability during 24 hours was measured by MTT assay after treatment the control and pre-treated BMDMs with anti-IFN-I receptor (10µg/mL) before treating the cells with IFN-β (1000U/mL) ± zVAD (50µM) ± Nec-1 (30µM) or LPS (100ng/mL) ± zVAD (50µM) ± Nec-1 (30µM) in 96-well plates. Graphs show the percentage of viable cells ± SEM relative to cells treated with the corresponding stimuli in the absence of zVAD. Data are representative of at least three independent experiments with triplicate each. ***P < 0.001.

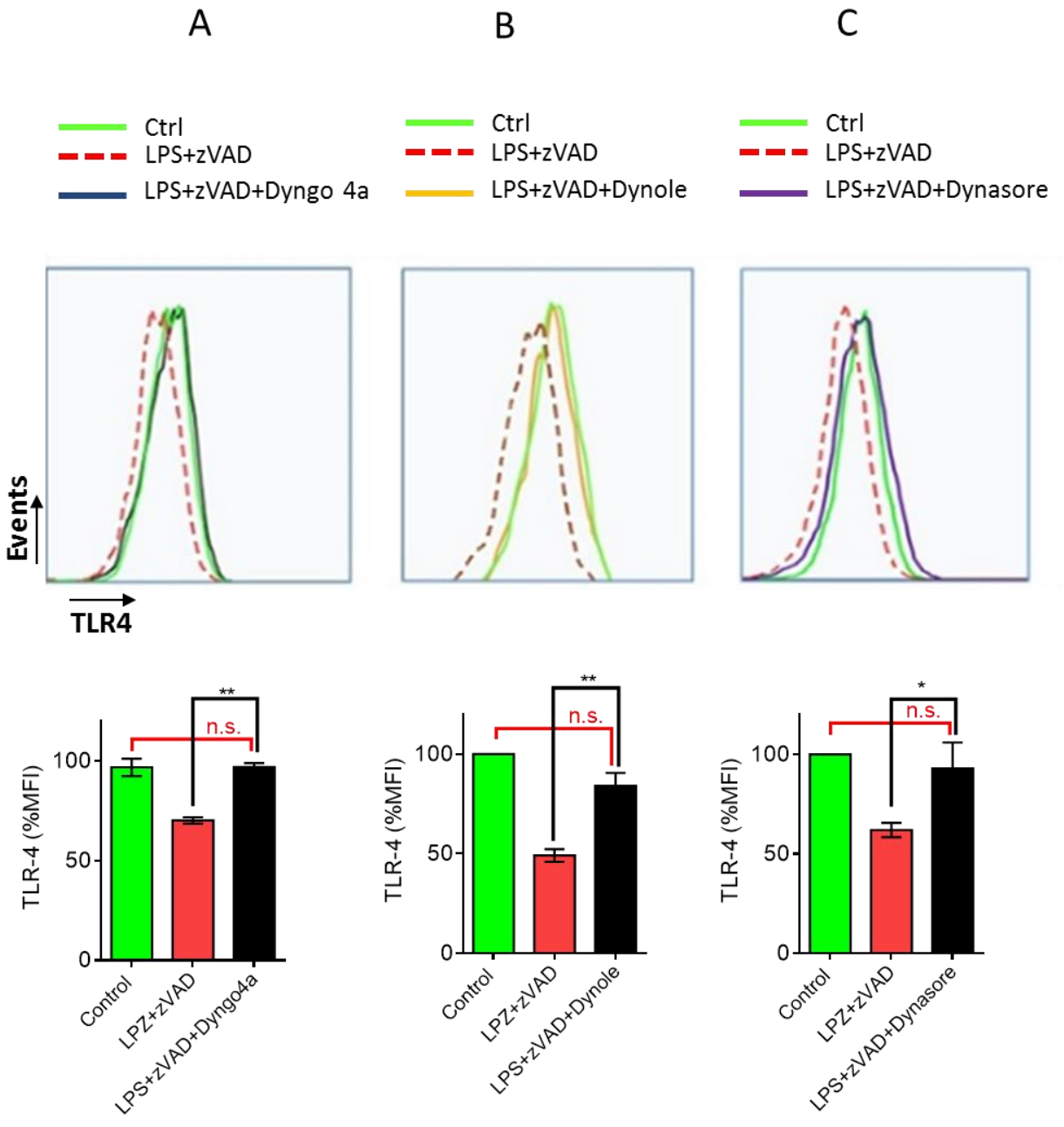
A
B
C
Ctrl
LPS+zVAD
LPS+zVAD+Dyngo 4a
Ctrl
LPS+zVAD
LPS+zVAD+Dynole
Ctrl
LPS+zVAD
LPS+zVAD+Dynasore
Events
TLR4
TLR-4 (%MFI)
100
50
0
**
n.s.
Control
LPZ+zVAD
LPS+zVAD+Dyngo4a
TLR-4 (%MFI)
100
50
0
**
n.s.
Control
LPZ+zVAD
LPS+zVAD+Dynole
TLR-4 (%MFI)
100
50
0
*
n.s.
Control
LPZ+zVAD
LPS+zVAD+Dynasore

Figure 15. Dynamin inhibitors prevent internalization of TLR4 following LPS+zVAD treatment. Surface expression of TLR4 on non-treated and pre-treated BMDMs from with Dynasore (80µM) (A), Dynole (10µM) (B) or Dyngo4a (50µM) (C) was compared to control (only cells) 1.5 hours after treatment with LPS (100ng/mL) +zVAD (50µM). the expression of TLR4 was measured. Results were obtained using flow cytometry and are shown in histograms (up) or in bar graphs (down) by the percentage of mean fluorescence intensity (%MFI) relative to control. Statistical comparison of the data (student t-test) is shown by asterisks (*). *$p < 0.5$; **$P < 0.05$.

LPS+zVAD

A

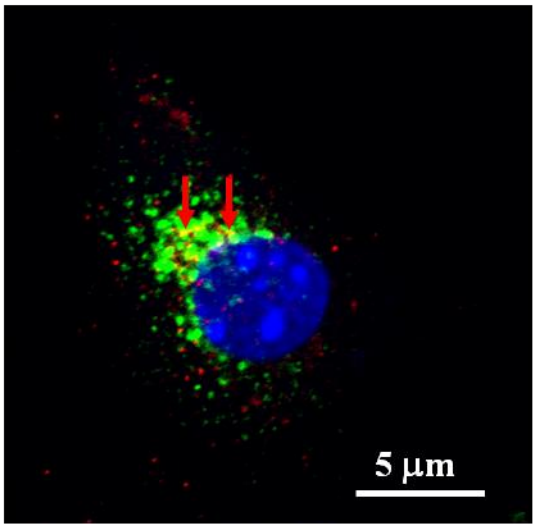

B

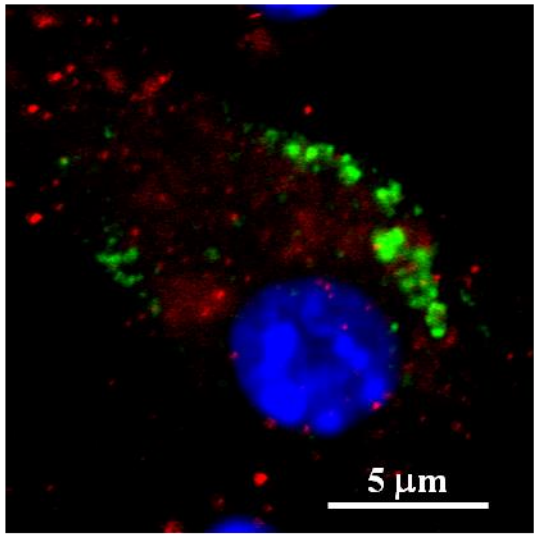

LPS+zVAD+Dyngo4a

NUCLEUS, EEA1, TLR4

Figure 16. Confocal microscopy images revealed Dyngo 4a can significantly block TLR4 internalization during necrosome signaling. BMDMs were treated with LPS (100 ng/mL) + zVAD (50 μM) ± Dyngo4a (50 μM) in six-well glass bottom dishes for 1.5 hours. Cells were examined by confocal microscopy after immunofluorescence staining with anti-TLR4 (green) for the receptor, anti-EEA1 (red) for the early endosome, and DAPI (Blue) for the nucleus. Yellow color indicates colocalization of TLR4 and EEA1 (red arrows in A). Results are representative of 3 separate experiments. Bars are equal to 5μm.

4. 2. 2. Dyngo 4a, in contrast to other dynamin inhibitors, inhibits LPS-induced necroptosis

Having observed that various dynamin inhibitors blocked TLR4 internalization (Fig. 15, 16) and activation of IRF3 (which is dependent on the endocytosis of TRIF), we assumed that these inhibitors could potentially inhibit TLR4-induced necroptosis of macrophages (Fig. 17). To evaluate this, primary mouse macrophages were treated with LPS+zVAD after pretreatment with or without various dynamin inhibitors, such as Dynasore, Dyngo 4a, Dynole and Mdivi-I. Surprisingly, only those cells that had been pre-treated with Dyngo 4a survived (Fig. 18). Dynasore, which has been used extensively to block TLR4 internalization (Kagan et al., 2008; Rajaiah et al., 2015) failed to prevent necroptosis. These results were further corroborated by immunofluorescence microscopy following the staining of cells with propidium iodide (PI) and Hoechst. Internalization of PI is indicative of cell necrosis. Dynasore failed to inhibit cell death by necroptosis whereas Dyngo 4a displayed a strong ability to prevent necroptosis (Fig. 19).

The discrepancy between Dynasore and Dyngo 4a in rescuing cells from necroptosis was further explored by inducing TLR3 signaling with poly-I:C (pI:C). In contrast to LPS, which engages TLR4 on the cell surface, pI:C engages TLR3, which is mainly confined to the endosomal compartment (Tsai et al., 2015). Dyngo 4a rescued the cells from necroptosis induced by LPS as well as pI:C, whereas Dynasore failed to do so (Fig. 20 A, B). Since TLR3 is confined mainly to the endocytic compartment, these results raised the question if Dyngo 4a inhibits necroptosis in a dynamin-dependent or -independent manner.

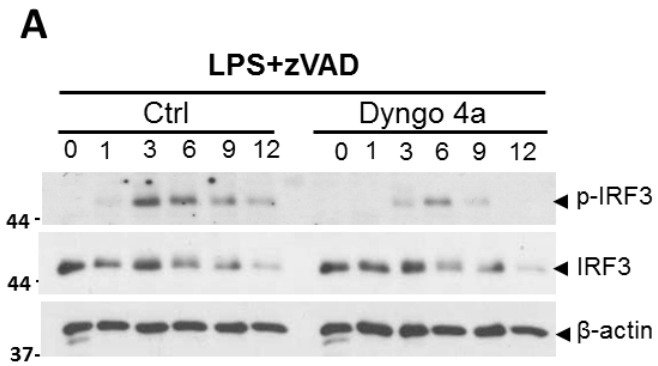
A
LPS+zVAD
Ctrl
Dyngo 4a
0 1 3 6 9 12 0 1 3 6 9 12
44
44
37
p-IRF3
IRF3
β-actin

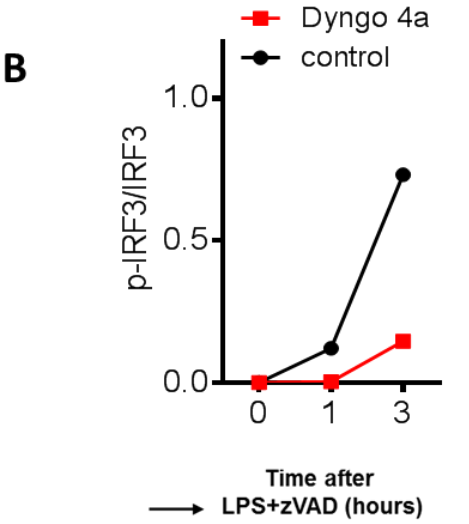
B
Dyngo 4a
control
p-IRF3/IRF3
1.0
0.5
0.0
0
1
3
Time after
LPS+zVAD (hours)

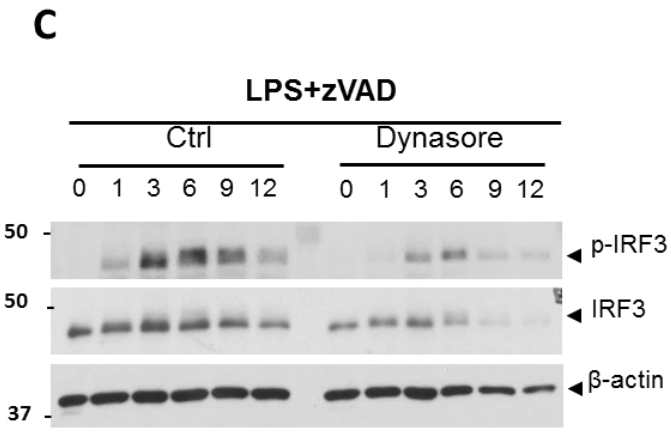
C
LPS+zVAD
Ctrl
Dynasore
0 1 3 6 9 12 0 1 3 6 9 12
50
50
37
p-IRF3
IRF3
β-actin

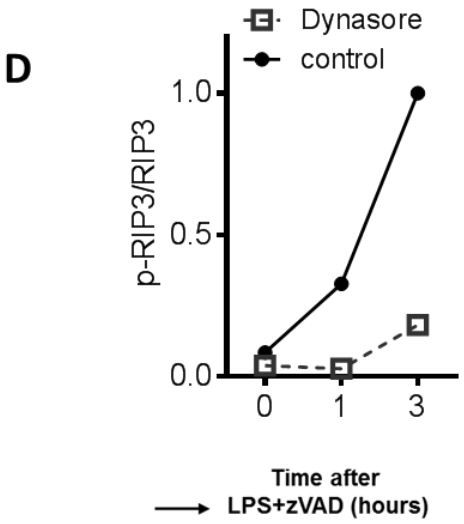
D
Dynasore
control
p-RIP3/RIP3
1.0
0.5
0.0
0
1
3
Time after
LPS+zVAD (hours)

Figure 17. Dynamin inhibitors, Dyngo 4a and Dynasore, down-regulate activation of IRF3, a TRIF-dependent key protein. Immunoblot and densitometric analysis of IRF3, modulated by Dyngo 4a (A-B) and Dynasore (C-D) following TLR4 driven necroptosis. BMDMs from WT mice were grown in vitro and treated with LPS (100ng/mL) + zVAD (50uM) ± Dyngo 4a (50µM) /or Dynasore (80µM) in 24-well plates for six-time intervals (0-12 hours) as indicated. Samples were lysed with SDS buffer and were then examined for phosphorylated IRF3 and total unphosphorylated part by western blotting. The p-IRF3/IRF3 ratio was calculated by densitometric analysis (B and D), which is shown for the first three-hour post activation. Data are representative of at least two independent experiments.

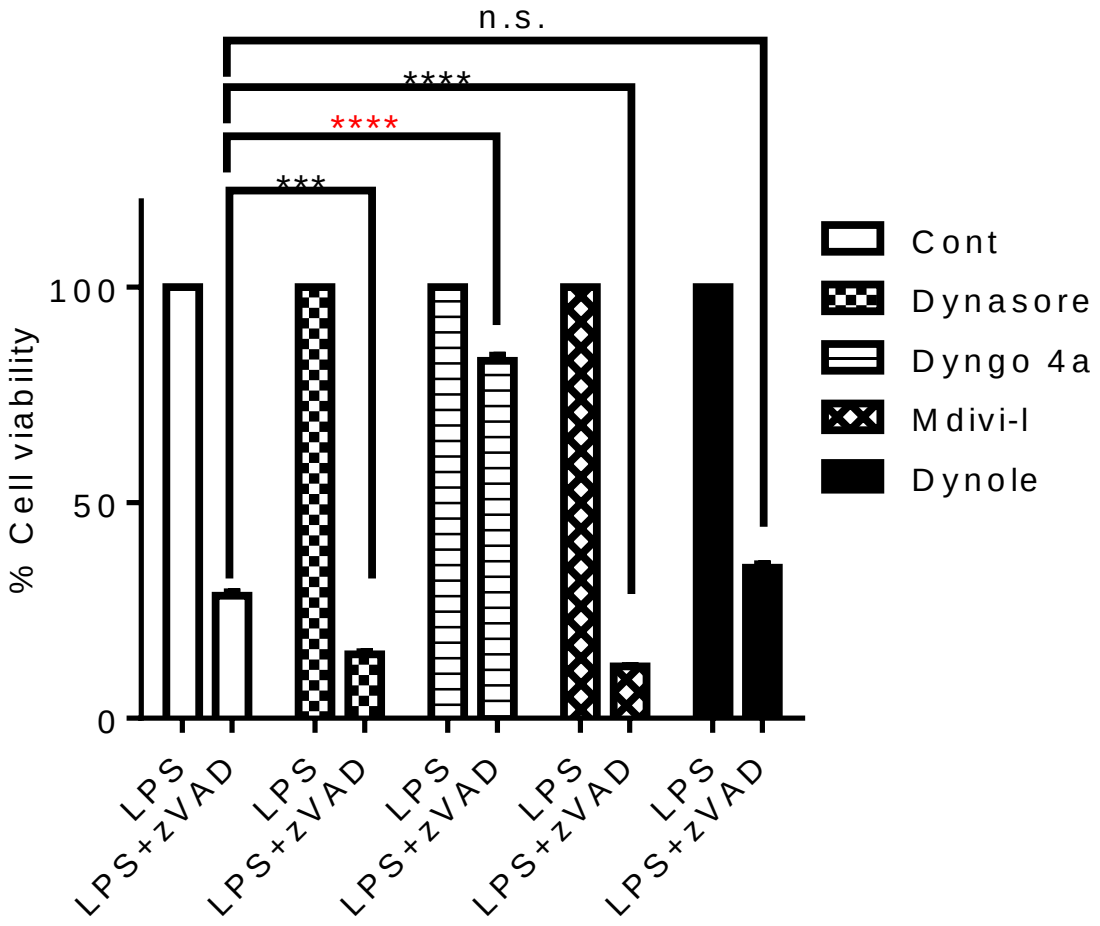
n.s.
****
****
***
% Cell viability
100
50
0
LPS
LPS+zVAD
LPS
LPS+zVAD
LPS
LPS+zVAD
LPS
LPS+zVAD
LPS
LPS+zVAD
Cont
Dynasore
Dyngo 4a
Mdivi-l
Dynole

Figure 18. Dyngo 4a, unlike other dynamin inhibitors, significantly prevented macrophages necroptosis following TLR4 signaling. BMDMs from WT were pre-treated with various dynamin or dynamin-like inhibitors such as Mdivi-1(10μM), Dynole (10μM), Dyngo 4a (40μM), and Dynasore (80μM) for 30min, determines the fate of the BMDM cells after treating with LPS (100 ng/mL) ± zVAD (50μM) in 96-well plates. Graphs show the percentage of viable cells ± SEM relative to control (treated with LPS alone). Statistic comparison of the data (t-test) is shown by asterisks (*). ***P < 0.001; ****P < 0.0001. Data are representative of at least three independent experiments performed in triplicate.

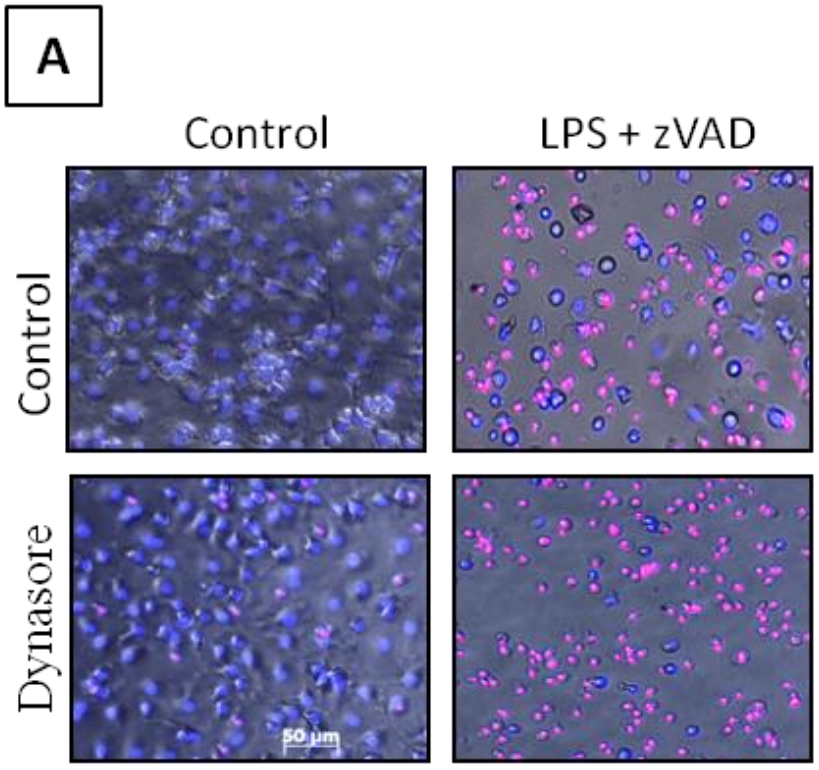
A
Control
LPS + zVAD
Control
Dynasore
50 µm

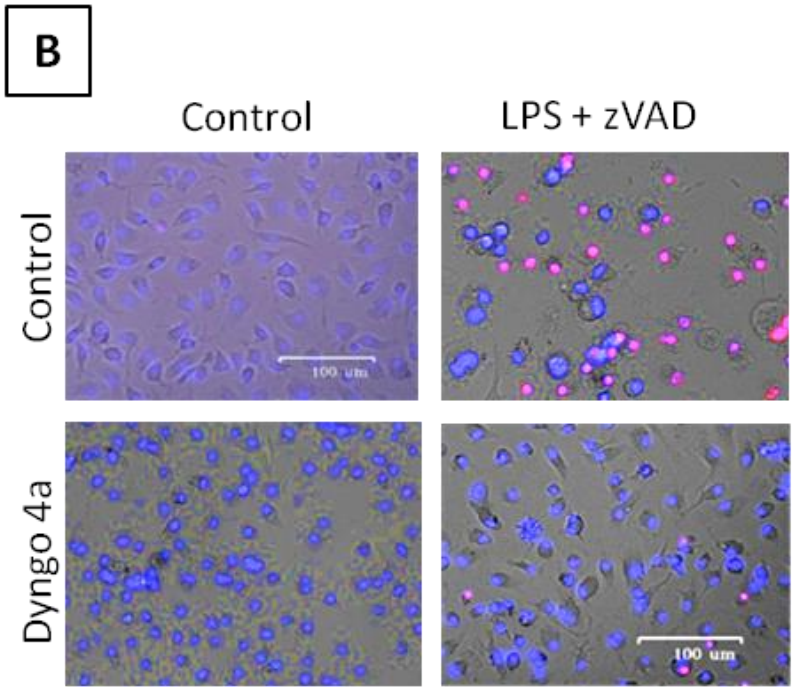
B
Control
LPS + zVAD
Control
Dyngo 4a
100 um
100 um

Figure 19. Dyngo 4a, but not Dynasore, inhibits TLR4-driven necroptosis of macrophages. BMDMs from WT were pre-treated with Dyngo 4a (50μM) or Dynasore (80μM) for 30 minutes. The cells were post-treated by LPS (100ng/mL) with or without zVAD (50 μM) in 24-well plates, and were examined for the cell viability using Hoechst (Hoechst: blue for dead and live cells) and propidium iodide (PI:red for only dead cells) co-staining. Spots in pink color indicate dead cells while blue spots are live cells.

A

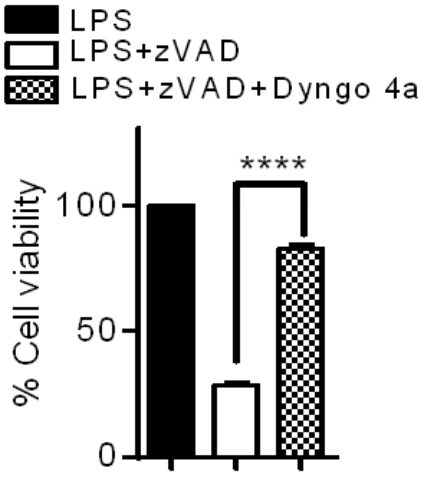
LPS
LPS+zVAD
LPS+zVAD+Dyngo 4a
% Cell viability
100
50
0
****

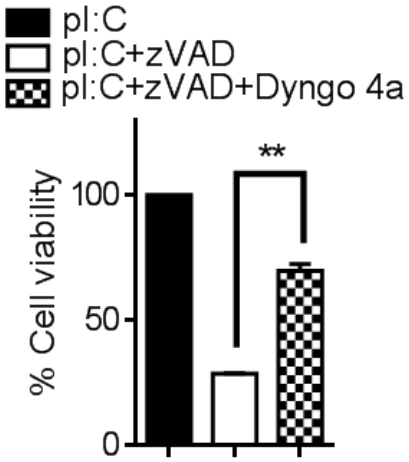
pI:C
pI:C+zVAD
pI:C+zVAD+Dyngo 4a
% Cell viability
100
50
0
**

B

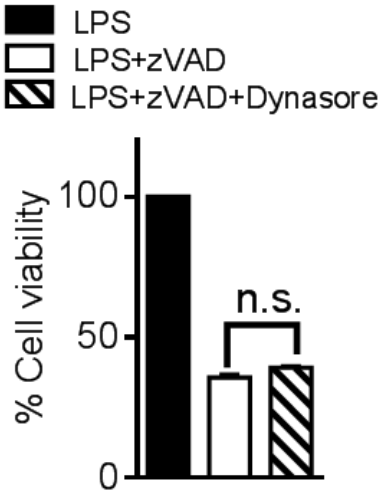
LPS
LPS+zVAD
LPS+zVAD+Dynasore
% Cell viability
100
50
0
n.s.

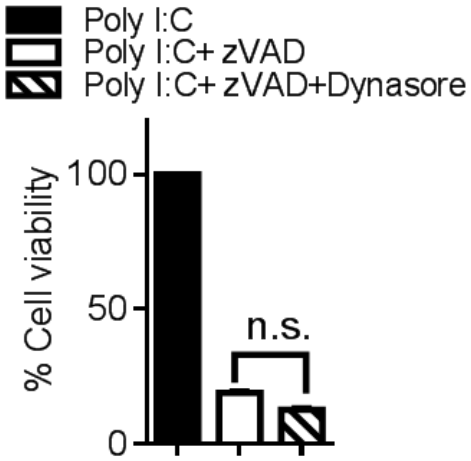
Poly I:C
Poly I:C+ zVAD
Poly I:C+ zVAD+Dynasore
% Cell viability
100
50
0
n.s.

Figure 20. Dyngo 4a, unlike Dynasore, inhibited TLR3-induced and TLR4-induced necroptosis. BMDMs from WT mice (C57BL/6) were pre-treated with Dyngo 4a (50µM) (A) or Dynasore (80µM) (B) or left with no pre-treatment for 30 minutes and then treated with LPS (100ng/mL), or Poly I:C (20µg/mL) with or without zVAD (50 µM) in 96-well plates. After 24 hours of incubation, the cell viability was measured by MTT assay. Graphs show the percentage of viable cells ± SEM relative to control (treated with LPS alone). All experiments were done at least in triplicates. ** $P < 0.01$; ****$P < 0.0001$.

4. 2. 3. Inhibition of dynamin-dependent endocytosis reduces cytokine production by macrophages

Researchers have shown previously that the blockage of TLR4 internalization by dynamin inhibitors results in suppression of cytokine production (Kagan et al., 2008; Latvala et al., 2014). We thus determined whether Dynasore, which inhibited TLR4 internalization but failed to rescue from necroptosis, inhibited cytokine production by macrophages following necroptosis signaling. Macrophages were treated with LPS+zVAD for six hours in the presence or absence of Dyngo 4a (Fig. 21 A) or Dynasore (Fig. 21 B). Cytokine production was measured in the supernatants by enzyme-linked immunosorbent assay (ELISA) or cytometry bead array (CBA). Both Dyngo 4a and Dynasore substantially reduced cytokine secretion in macrophages during necroptosis signaling (Fig. 21 A, B). These results revealed that receptor internalization is an important event in cytokine secretion.

4. 2. 4. The impact of dynamin inhibitors on necroptosis signaling in macrophages following TLR4 engagement

Necroptosis of cells is induced by the activation (phosphorylation) of RIPK1, which, upon phosphorylation, associates with RIPK3, FADD, and caspase-8. This leads to the phosphorylation of RIPK3 and its association with, and phosphorylation of, the pseudokinase MLKL (Galluzzi et al., 2014; Rodriguez et al., 2016). Because of phosphorylation, MLKL is trimerized, which then results in translocation of MLKL to the cell surface. Through mechanisms that are not clear, relocalization of MLKL to the cell membrane increases membrane permeability to various ions, resulting in cell rupture and necroptosis.

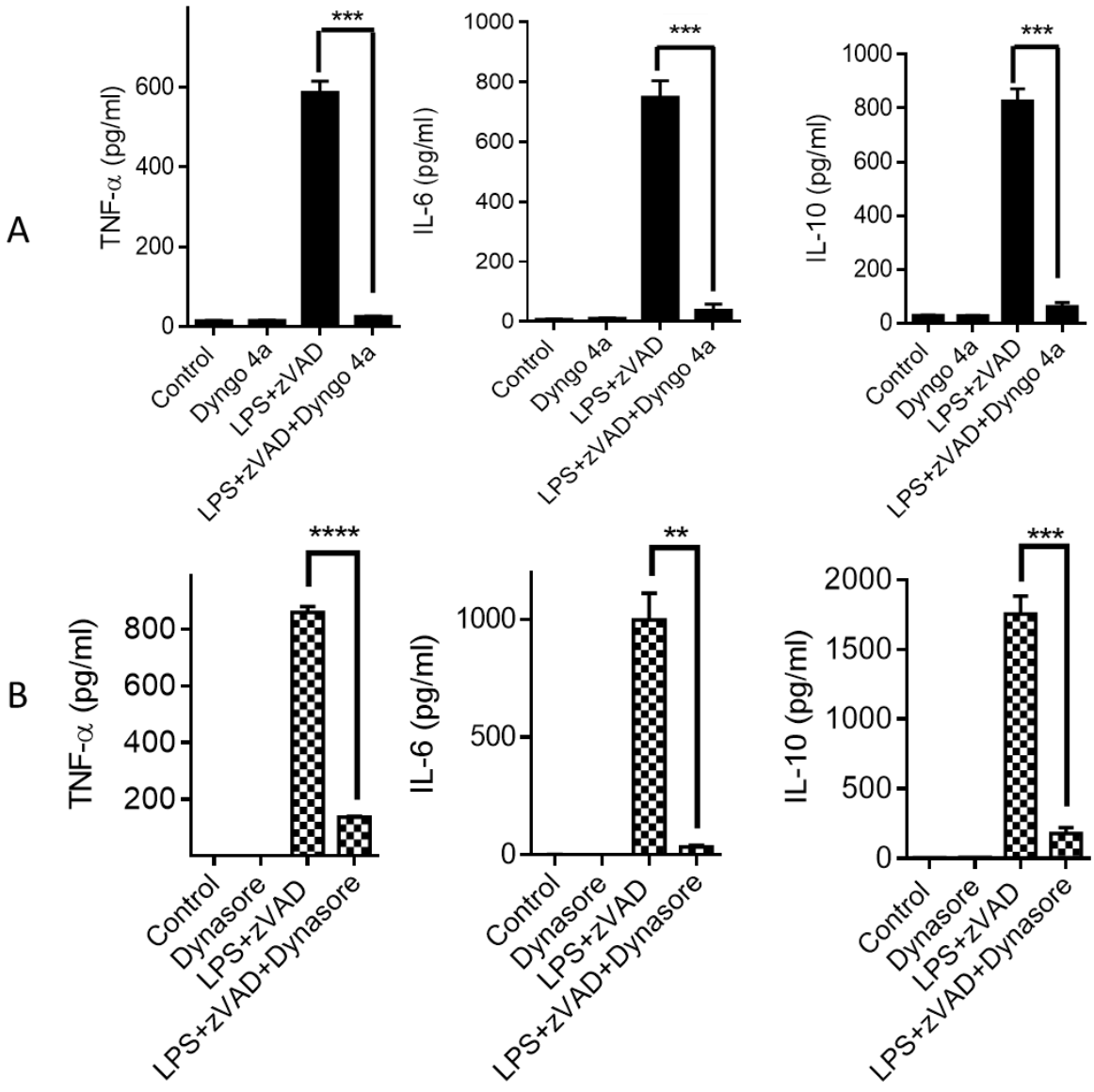
A
TNF-α (pg/ml)
0
200
400
600
***
Control
Dyngo 4a
LPS+zVAD
LPS+zVAD+Dyngo 4a
IL-6 (pg/ml)
0
200
400
600
800
1000
***
Control
Dyngo 4a
LPS+zVAD
LPS+zVAD+Dyngo 4a
IL-10 (pg/ml)
0
200
400
600
800
1000
***
Control
Dyngo 4a
LPS+zVAD
LPS+zVAD+Dyngo 4a
B
TNF-α (pg/ml)
200
400
600
800
****
Control
Dynasore
LPS+zVAD
LPS+zVAD+Dynasore
IL-6 (pg/ml)
0
500
1000
**
Control
Dynasore
LPS+zVAD
LPS+zVAD+Dynasore
IL-10 (pg/ml)
0
500
1000
1500
2000
***
Control
Dynasore
LPS+zVAD
LPS+zVAD+Dynasore

Figure 21. Dyngo 4a and Dynasore are able to inhibit cytokine expression during TLR4-induced necrosome signaling. Pro- and Anti- inflammatory cytokines in supernatants were collected after six hours. BMDMs from WT stimulated 30 min. with/without dynamin inhibitors (Dyngo 4a, A; Dynasore, B) and post-treated with/without LPS (100ng/mL) + zVAD (50μM). Graphs show cytokine concentrations measured by ELISA or CBA. Data are representative of at least two independent experiments. **P < 0.1; ***P < 0.01; ****P < 0.001.

To evaluate the impact of dynamin on necrosome signaling, we stimulated the cells with LPS+zVAD in the presence or absence of Dyngo 4a or Dynasore and measured the changes in various cell signaling molecules using western blotting. Both Dyngo 4a and Dynasore were used since they both inhibited TLR4 internalization and cytokine expression; however, only Dyngo 4a inhibited necroptosis. Cell extracts were collected at various time intervals following LPS+zVAD treatment, and phosphorylation of key proteins involved in necroptosis signaling was evaluated by western blotting (Fig. 22 A-C). Densitometric analysis of western blots was carried out to quantify the change in activation of signaling proteins. Since the commitment of cells to undergo necroptosis occurs early during TLR4 signaling, densitometric analysis was performed only during the first three-hour post activation (Fig. 22 A-C). Interestingly, Dyngo 4a enhanced phosphorylation of RIPK1 while Dynasore had no impact on it (Fig. 22 A).

It has been previously reported that the upper band of RIPK1 is the phosphorylated form of RIPK1 (McComb et al., 2012, 2014; Robinson et al., 2012). The phosphorylation of RIPK1 is an early event that occurs during necrosome signaling following TLR4 signaling, even in the absence of zVAD (McComb et al., 2014). Our results indicated that the TLR4 signaling driving RIPK1 activation proceeds even when dynamin signaling is blocked (Fig. 22 A). When the phosphorylation of the downstream kinase RIPK3 was evaluated, both Dyngo 4a and Dynasore induced potent inhibition of RIPK3 phosphorylation, although Dyngo 4a appeared to induce stronger inhibition of RIPK3 phosphorylation (Fig. 22 B). These results indicate that dynamin signaling impacts the phosphorylation of RIPK3, but not RIPK1. When the phosphorylation of the further downstream pseudokinase MLKL (the terminal step in necroptosis) was evaluated, Dyngo 4a inhibited the phosphorylation of MLKL whereas Dynasore had no impact (Fig. 22 C).

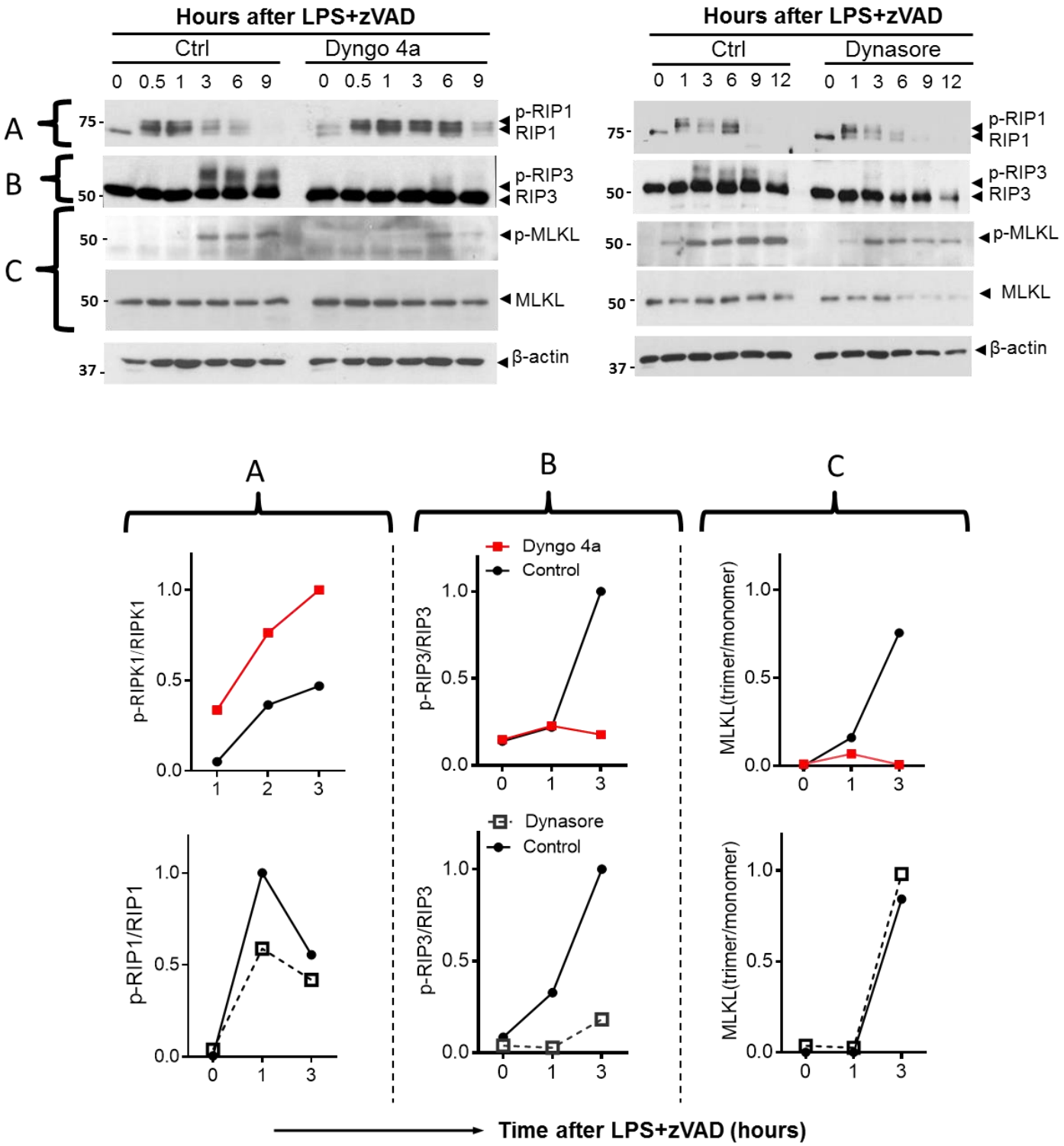
Hours after LPS+zVAD
Ctrl
Dyngo 4a
0 0.5 1 3 6 9
Hours after LPS+zVAD
Ctrl
Dynasore
0 1 3 6 9 12
A
B
C
75
50
50
50
37
p-RIP1
RIP1
p-RIP3
RIP3
p-MLKL
MLKL
β-actin
p-RIPK1/RIPK1
p-RIP1/RIP1
p-RIP3/RIP3
MLKL(trimer/monomer)
Dyngo 4a
Control
Dynasore
Control
Time after LPS+zVAD (hours)

Figure 22. **Immunoblot and densitometric analysis of necrosome proteins modulated by Dyngo 4a and Dynasore following TLR4-driven necroptosis.** BMDMs from WT mice were pre-treated with or without Dyngo 4a (50µM) or Dynasore (80µM) for 30 minutes and post-treated with LPS (100ng/mL)+ zVAD (50uM) in 24-well plates for varying time intervals (hour) as indicated. Samples were lysed with SDS buffer and the cell lysates were then examined for the key proteins involved in necrosome, such as RIPK1 (A), RIPK3 (B), and MLKL (C) by western blots. Densitometric analysis of each protein is shown only for the first three-hour post activation. Western blot data are representative of three independent experiments

This differential impact of Dyngo 4a versus Dynasore on the phosphorylation of MLKL correlates with the impact these two inhibitors have on cell death.

To delve further into the mechanism behind the unique suppressive effect of Dyngo 4a on necroptosis, we measured the activation of various signaling proteins such as p38 MAPK, p65 NF-kB and STAT1 following necrosome signaling. Western blot analysis showed that neither inhibitor appeared to have any impact on the activation (phosphorylation) of p65 NF-kB and STAT1 (Tyr 701) following necrosome signaling (23, 24 A & B). Interestingly, unlike the cells pretreated with Dynasore, the cells pretreated with Dyngo 4a showed a marked initial activation (phosphorylation) of p38 MAPK and STAT1 (Ser 727) (Fig. 23, C and D). Densitometric analysis of western blots was carried out to evaluate the impact of the dynamin inhibitors on p38 MAPK and STAT1 (Ser 727) (Fig. 24 C). These results indicate that Dyngo 4a, in contrast to Dynasore, inhibits the phosphorylation of MLKL and induces early phosphorylation of p38 MAPK (Fig. 24 D).

4. 2. 5. Dyngo 4a inhibits necroptosis of macrophages following cytokine receptor engagement

After observing that Dyngo 4a efficiently inhibited the necroptosis of macrophages following TLR signaling, we evaluated whether Dyngo 4a also inhibits the necroptosis of macrophages induced by cytokine receptor signaling. We treated cells with IFN-β or TNF in the absence or presence of the pan-caspase inhibitor zVAD. Where appropriate, Nec-1 was used to determine the mechanism of cell death in a group of cells that had been pre-treated with Dyngo 4a, as described previously. Cell viability was measured by MTT assay at 24-hour post-treatment. Dyngo 4a rescued the cells from necroptosis induced by IFN-β+zVAD or TNF+zVAD (Fig. 25 A-B).

We evaluated whether Dyngo 4a also inhibits the activation of various known signaling proteins following IFN-β/zVAD treatment (Fig. 25 C-D). Cells were extracted at varying time intervals (over the course of nine hours), and the activation of proteins was evaluated by western blotting. The results showed that the phosphorylation of RIPK3 and consequently the phosphorylation of MLKL (and trimerization) were inhibited in the cells treated with Dyngo 4a (Fig. 25 C 1-3). As with the results of the LPS+zVAD experiment, Dyngo 4a did not inhibit RIPK1 phosphorylation. Although inhibition of dynamin was previously shown to inhibit IFNAR1 endocytosis (Marchetti et al., 2006), our results demonstrated that the prevention of IFNAR1 endocytosis by Dyngo 4a does not appear to inhibit the activation of RIPK1 as the downstream of IFNAR1. Furthermore, while the cells pretreated with Dyngo 4a showed no significant impact on p65 NF-kB and STAT1 (Tyr 701) (Fig. 25 D 4-5), a marked preliminary activation (phosphorylation) of p38 MAPK and STAT1 (Ser 727) was detected (Fig. 25 D 6-7). Taken together, these results demonstrate that treatment with Dyngo 4a and IFN-β+zVAD induces early phosphorylation of p38 MAPK and inhibits the phosphorylation of MLKL, similar to what was observed when cells were treated with Dyngo 4a and LPS+zVAD.

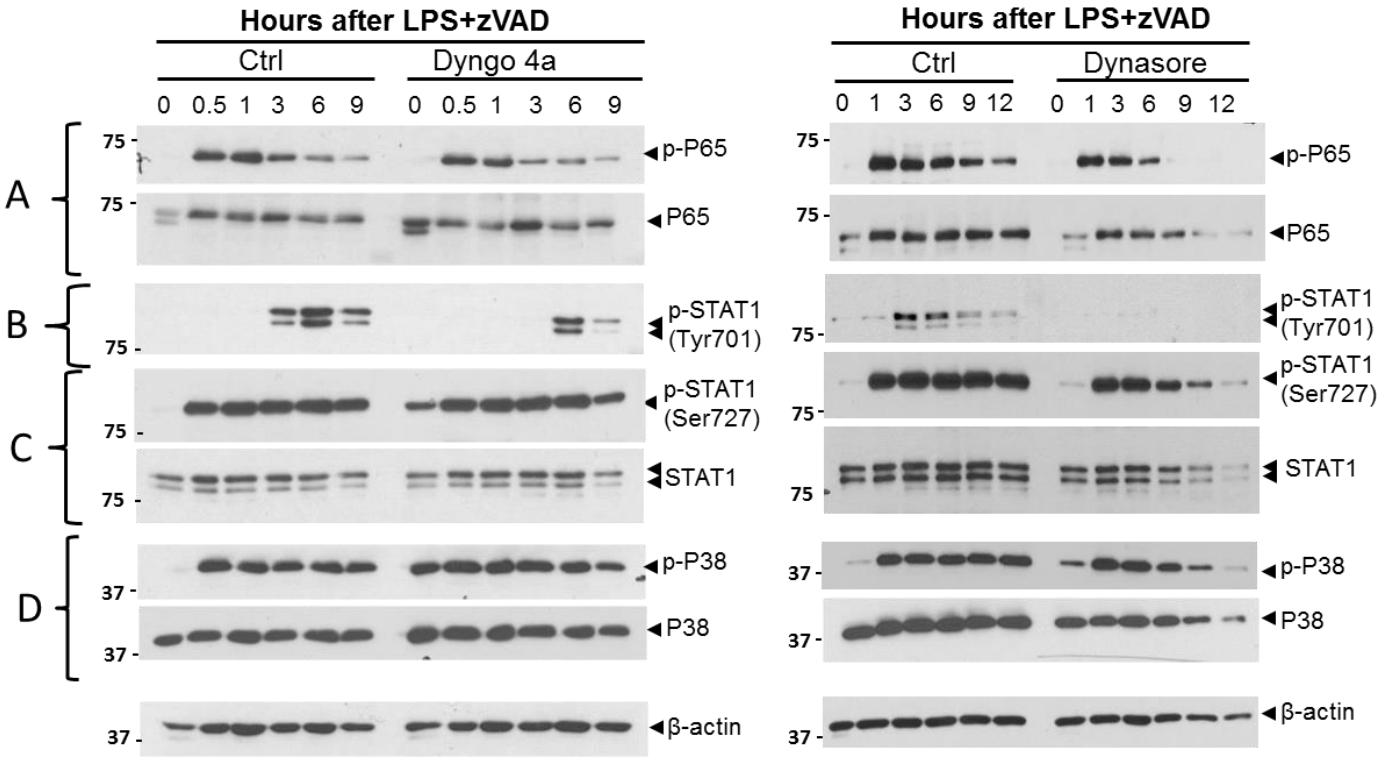
Hours after LPS+zVAD
Ctrl
Dyngo 4a
0 0.5 1 3 6 9 0 0.5 1 3 6 9
A
B
C
D
75
75
75
75
37
37
37
p-P65
P65
p-STAT1 (Tyr701)
p-STAT1 (Ser727)
STAT1
p-P38
P38
β-actin
Hours after LPS+zVAD
Ctrl
Dynasore
0 1 3 6 9 12 0 1 3 6 9 12
75
75
75
75
37
37
37
p-P65
P65
p-STAT1 (Tyr701)
p-STAT1 (Ser727)
STAT1
p-P38
P38
β-actin

Figure 23. **Immunoblot analysis of necrosome-associated proteins modulated by Dyngo 4a and Dynasore following TLR4-driven necroptosis.** BMDMs from WT mice treated with LPS (100ng/mL)+ zVAD (50uM) ± Dyngo 4a (50µM) or Dynasore (80µM) in 24-well plates for varying time intervals (hour) as indicated. Samples were lysed with SDS buffer and the cell lysates were then examined for the key proteins potentially associated with necroptosis signaling such as p65 NF-kB, STAT1, and p38 MAPK by western blotting. The data are representative of three independent experiments.

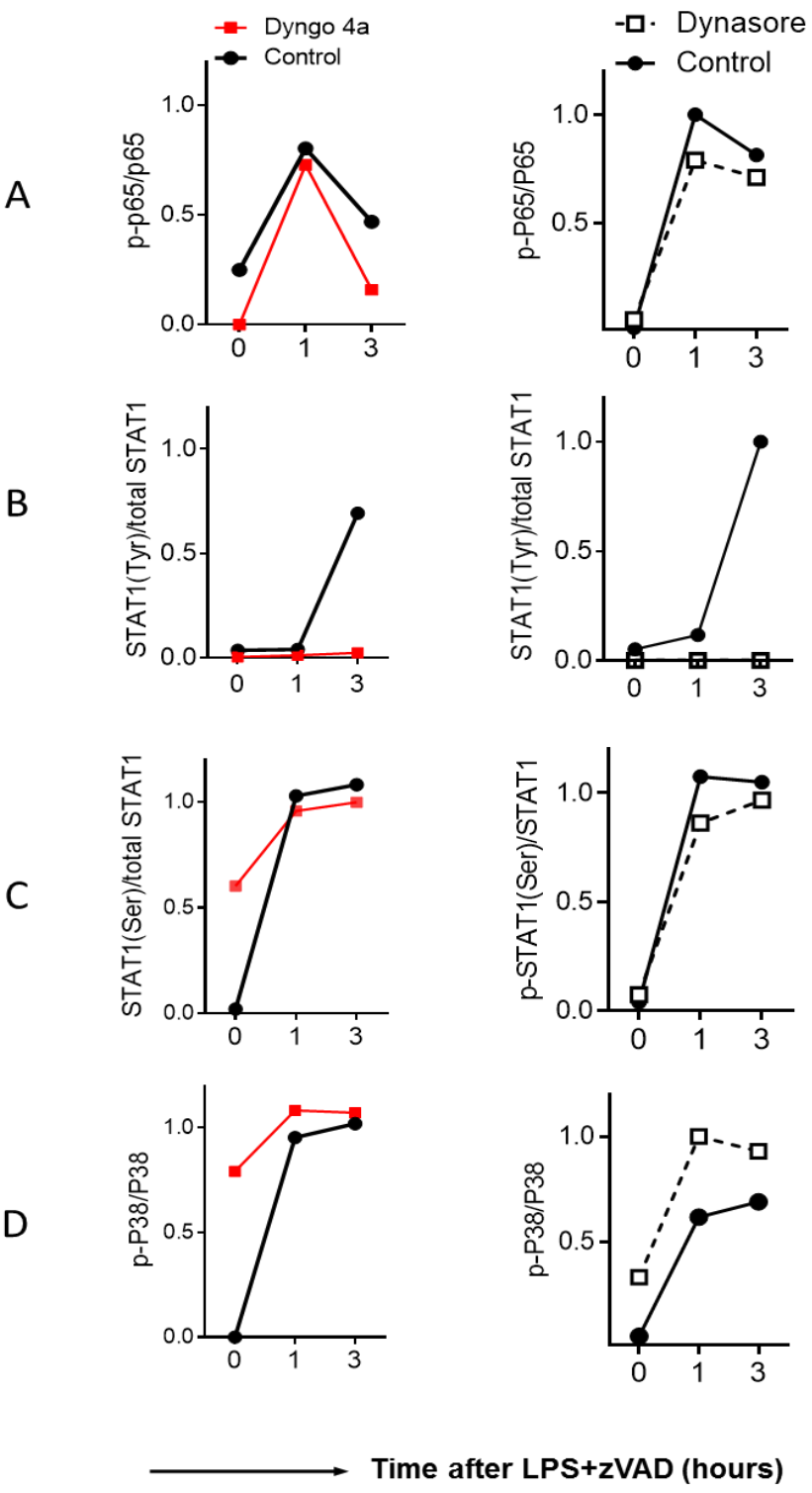
A
B
C
D
Dyngo 4a
Control
Dynasore
Control
p-p65/p65
p-P65/P65
STAT1(Tyr)/total STAT1
STAT1(Tyr)/total STAT1
STAT1(Ser)/total STAT1
p-STAT1(Ser)/STAT1
p-P38/P38
p-P38/P38
1.0
0.5
0.0
0
1
3
Time after LPS+zVAD (hours)

Figure 24. Densitometric analysis of necrosome-associated proteins modulated by Dyngo 4a and Dynasore following TLR4-driven necroptosis. The densitometry analysis on the western blots (Fig. 23 A-D) was done by ImageJ software to quantitate the average ratio of proteins (i.e. p-P65/total P65) over at least three separate experiments performed as described before. Densitometric analysis of each protein is shown only for the first three-hour post activation. The data are representative of three independent experiments

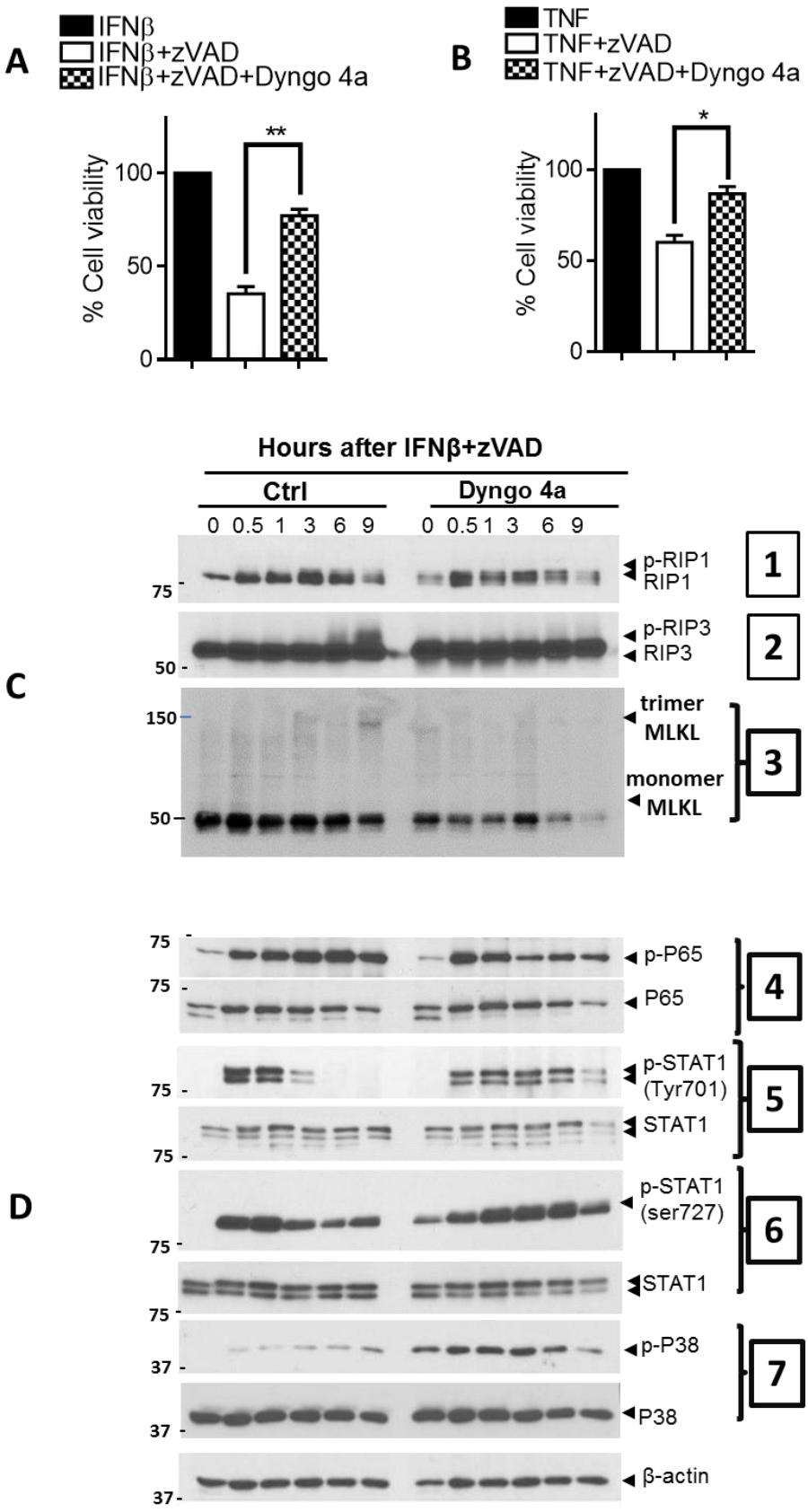
A
IFNβ
IFNβ+zVAD
IFNβ+zVAD+Dyngo 4a
% Cell viability
100
50
0
**
B
TNF
TNF+zVAD
TNF+zVAD+Dyngo 4a
% Cell viability
100
50
0
*
C
Hours after IFNβ+zVAD
Ctrl
Dyngo 4a
0 0.5 1 3 6 9
0 0.5 1 3 6 9
75
p-RIP1
RIP1
1
50
p-RIP3
RIP3
2
150
50
trimer
MLKL
monomer
MLKL
3
D
75
p-P65
75
P65
4
75
p-STAT1
(Tyr701)
STAT1
5
75
p-STAT1
(ser727)
6
75
STAT1
75
p-P38
37
37
P38
7
37
β-actin

Figure 25. Dyngo 4a inhibits necroptosis of macrophages induced by cytokines (IFN-β and TNF). BMDMs from WT mice (C57BL/6) were pretreated with Dyngo 4a (50μM) or left without pre-treatment. After 30min, the cells were treated with IFN-β (1000U/mL) or TNF (50 ng/mL), with or without zVAD (50 μM), as a pan-caspase inhibitor in 96-well plates. After 24 hours, the cell viability was measured by MTT assay (A-B). Graphs show the percentage of viable cells ± SEM relative to control (black bars). All experiments were done at least in triplicates. *P < 0.05; **P < 0.01; ***P < 0.001.

Immunoblot analysis of proteins modulated by Dyngo 4a following IFN-β-driven necroptosis (C-D). The cells were treated with IFN-β (1000U/mL) + zVAD (50uM) ± Dyngo 4a (50μM) in 24-well plates for various time intervals (hour) as indicated. Samples were lysed with SDS buffer and the cell lysates were then examined for the key proteins involved in necrosome, such as RIPK1, RIPK3, and MLKL (C1-C3) or necroptosis-associated signaling pathways such as p65 NF-kB (D 4), STAT1 (D5-D6), and p38 MAPK (D7) using western blotting. Western blot data are representative of three independent experiments

4. 2. 6. Impact of Dyngo 4a on the assembly of Complex II and necrosome

Necrosome signaling is triggered when RIPK1 is segregated from the Complex I, which then results in the interaction of RIPK1 with FADD, caspase-8, and RIPK3. Although our experiments revealed that Dyngo 4a enhanced the phosphorylation of RIPK1, there was potent inhibition of phosphorylation of RIPK3 and MLKL (Fig. 22 B-C). We, therefore, evaluated whether treatment of the cells with Dyngo 4a during necrosome signaling impacted the interaction of RIPK1 with other proteins involved in necrosome signaling. We immuno-precipitated RIPK3 with an anti-RIPK3 antibody coupled to magnetic beads at three hours post-LPS+zVAD treatment of macrophages in the presence or absence of Dyngo 4a. RIPK3 immuno-precipitates were then subjected to western blotting against RIPK1, FADD, caspase-8, and MLKL. Western blotting was also performed against actin, which should not be present in the immuno-precipitate. As is shown in Fig. 26, treatment of the cells with Dyngo 4a resulted in reduced interaction between various necrosome members with RIPK3. Interestingly, there was a reduction in RIPK1-RIPK3's interaction with Dyngo 4a treatment, which correlated with reduced RIPK3, but not RIPK1, phosphorylation. The results suggest that the interaction of RIPK1 with RIPK3 is critically dependent on the phosphorylation of RIPK3, but not RIPK1. Reduction in RIPK3-MLKL interaction in Dyngo 4a treated cells provides a mechanistic basis for the inhibitory impact of Dyngo 4a on the necroptosis of mouse macrophages.

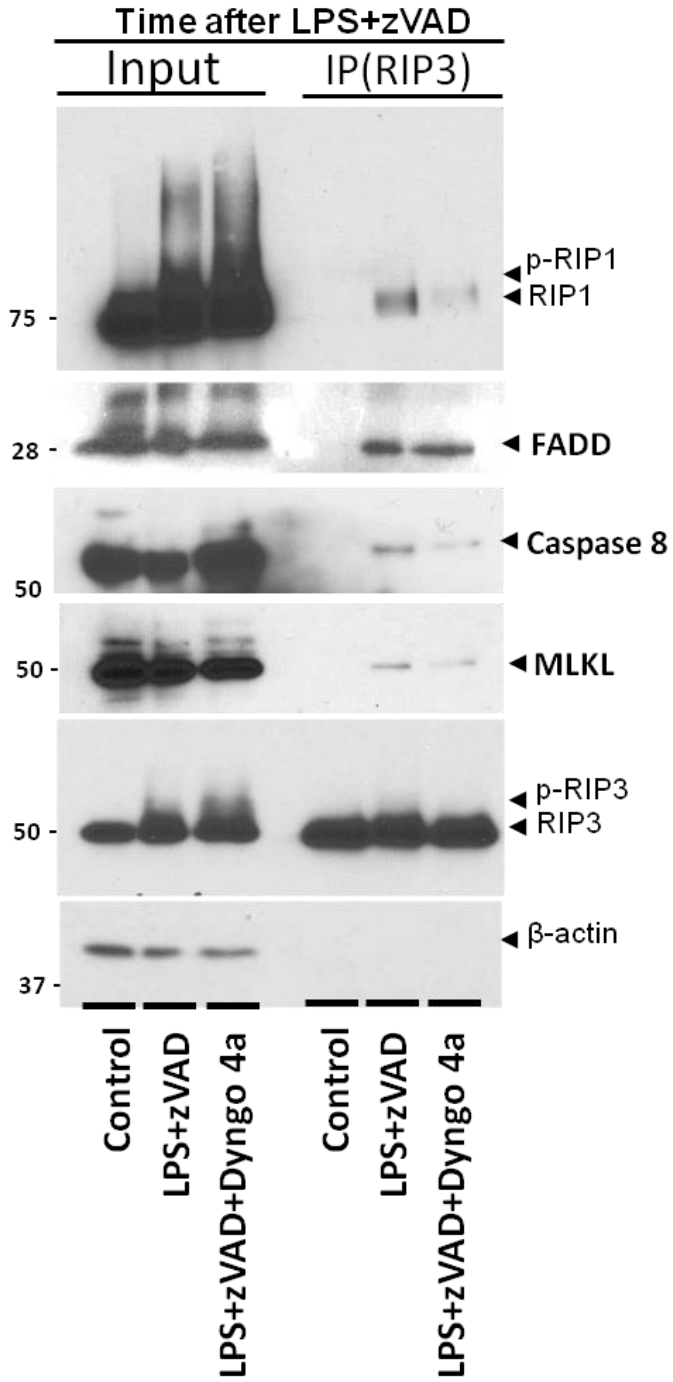
Time after LPS+zVAD
Input
IP(RIP3)
p-RIP1
RIP1
75
28
FADD
Caspase 8
50
50
MLKL
p-RIP3
RIP3
50
β-actin
37
Control
LPS+zVAD
LPS+zVAD+Dyngo 4a
Control
LPS+zVAD
LPS+zVAD+Dyngo 4a

Figure 26. Dyngo 4a impaired the assembly of various necrosome members with RIPK3. BMDMs from WT mice were pre-treated with Dyngo 4a for 30 minutes or left without pre-treatment and treated with LPS (100 mg/mL) + zVAD (50 μM) in 24-well plate for 3 hours. Cells were lysed and RIPK3 was immuno-precipitated with an anti-RIPK3 antibody coupled to magnetic beads and then subjected to western blotting against RIPK1, FADD, caspase-8, and MLKL. β-actin, which should not be detected in the immuno-precipitate, was used as a control.

4. 3. Dyngo 4a rescues macrophages from necroptosis by activating the p38 MAPK pathway

4. 3. 1. Dyngo 4a is a potent activator of p38 MAPK

After observing a significant inhibition of LPS- or cytokine-induced necroptosis of macrophages pretreated with Dyngo 4a, we were interested in further exploring the underlying mechanisms. We evaluated the impact of Dyngo 4a on the activation of p38 MAPK in macrophages at various time intervals in the absence of necrosome signaling. As shown in Fig. 27 (A-C), Dyngo 4a by itself induced rapid and potent activation of the p38 MAPK in macrophages, compared to Dynasore that had very less impact (27 A-B). We then tested the impact of other dynamin inhibitors (such as Dynole and MiTMab) and observed that Dyngo 4a had the strongest impact on phosphorylation of p38 MAPK. Furthermore, the activation of p38 MAPK by Dyngo 4a resulted in the subsequent activation (phosphorylation) of the downstream kinase MK2 (Fig. 27 C). Thus, these results indicate that in addition to inhibition of receptor endocytosis and cytokine expression, Dyngo 4a induces potent activation of the p38 MAPK signaling.

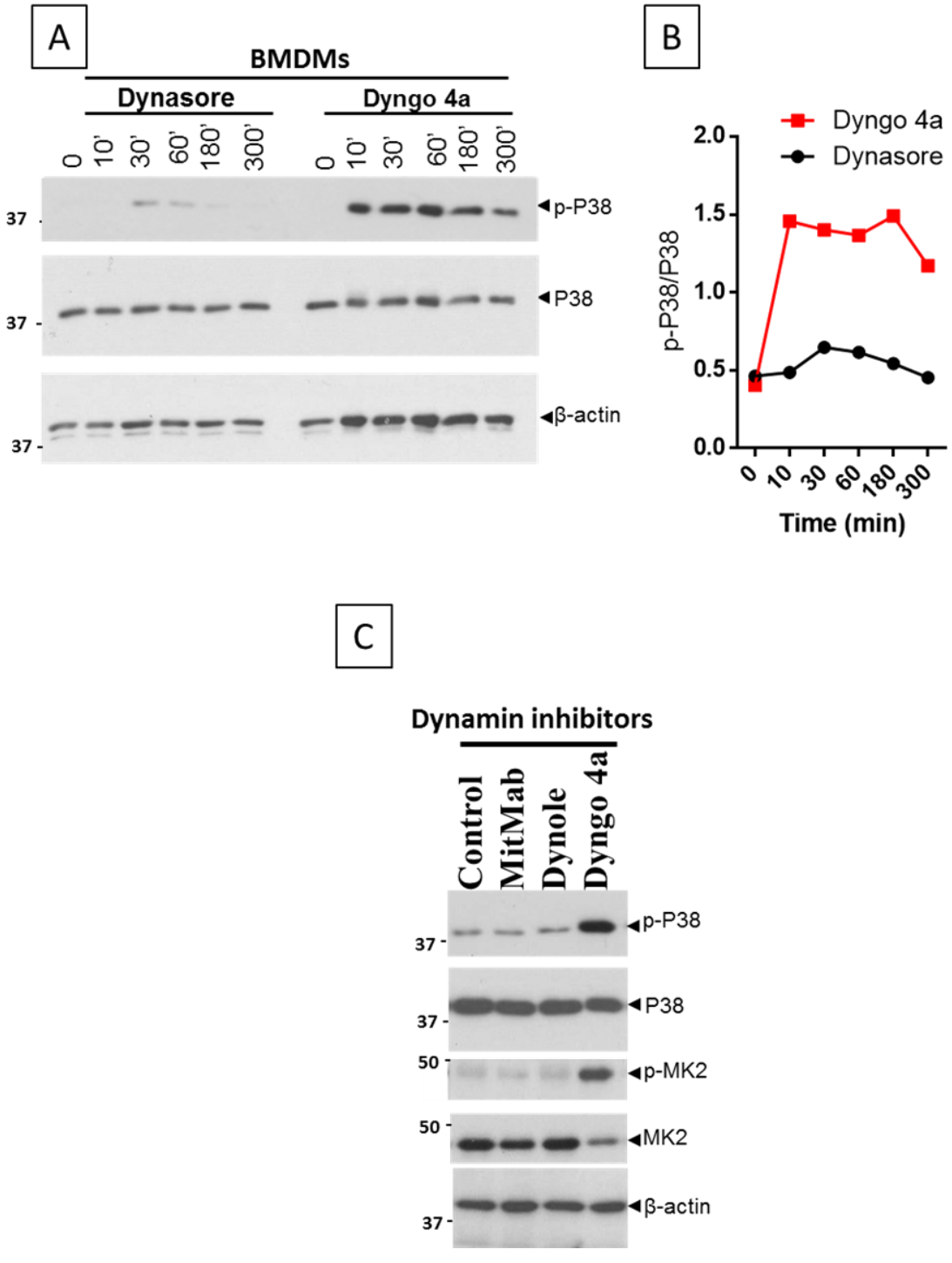
A
BMDMs
Dynasore
Dyngo 4a
0
10'
30'
60'
180'
300'
37
p-P38
P38
β-actin
B
Dyngo 4a
Dynasore
p-P38/P38
2.0
1.5
1.0
0.5
0.0
0
10
30
60
180
300
Time (min)
C
Dynamin inhibitors
Control
MitMab
Dynole
Dyngo 4a
p-P38
P38
50
p-MK2
MK2
β-actin

Figure 27. Dyngo 4a can strongly activate p38 MAPK and MK2. BMDMs from WT mice were pre-treated with various dynamin inhibitors for various time intervals (0-300 minutes) as indicated. Immunoblot comparison of the total and phosphorylated p38 MAPK in BMDMs treated with Dynasore (80µM) or Dyngo 4a (50µM) in 24-well plates (A) and its densitometric analysis (B); Immunoblot comparison of the total and phosphorylated p38 MAPK and MK2 in the BMDMs treated with Dyngo 4a (50µM), Dynole (10µM), and MiTMAB (10µM) in 24-well plates after one hour (C). Samples were lysed with SDS buffer and the cell lysates were then examined for p38 MAPK and downstream MK2. Western blot data are representative of three independent experiments

4. 3. 2. Inhibition of p38 MAPK promotes the induction of necroptosis

Since Dyngo 4a induced more potent activation of p38 MAPK than other dynamin inhibitors, and it was the only inhibitor that inhibited necroptosis of the cells, we evaluated if Dyngo 4a's ability to inhibit necroptosis was due to its ability to induce activation of p38 MAPK. Inhibition of p38 MAPK with LY2228820 or SB 203580 resulted in augmentation of necroptosis following necrosome signaling induced by LPS+zVAD (Fig. 28A).

To test whether the inhibition of p38 MAPK could also sensitize macrophages to necroptosis induced by other pathways, the same experiment was performed using IFN-β+zVAD (28 B). While these experiments indicated that the concurrent inhibition of p38 MAPK and caspases amplifies necroptosis in macrophages, the full impact of p38 MAPK could not be discerned. Potent necroptosis was induced by 50 μM of zVAD, even in the absence of p38 MAPK inhibition. Thus, to fully evaluate the impact of p38 MAPK, we decided to use a reduced concentration of zVAD. Previous results had indicated that macrophages undergo little necroptosis at 10μM of zVAD (see 4.1.1, Fig. 9 B). We treated WT BMDMs with a combination of LPS and zVAD (10 μM) in the presence or absence of LY2228820 and evaluated cell death at 24 hours. Interestingly, the combination of LY2228820 and 10μM of zVAD stimulated potent induction of necroptosis (Fig. 29 A). In contrast, no cell death was observed when LY2228820 (the p38 MAPK inhibitor) was absence. Thus, these results indicate that p38 MAPK signaling is an efficient regulator of necroptosis.

To investigate the mechanisms behind the impact of p38 MAPK on necroptosis, we performed western blotting of cell extracts at various time intervals post cell stimulation. The inhibition of p38 MAPK resulted in the complete inhibition of RIPK1 phosphorylation (Fig.

29 B, the first gel from top and Fig. 29 C). Furthermore, the phosphorylation of RIPK3 was undetectable at the lower concentration of zVAD, and the addition of the p38 MAPK inhibitor resulted in a slight induction of RIPK3 phosphorylation (Fig. 29 B, the second gel from top and Fig. 29 D). Intriguingly, despite little phosphorylation of RIPK1 and RIPK3 in cells treated with the p38 MAPK inhibitor, the phosphorylation of MLKL was induced as early as three hours post-treatment of cells (Fig. 29 E). It is worth mentioning that the phosphorylation of RIPK1 is induced by LPS, which could be independent of zVAD concentration (McComb et al., 2012). Surprisingly, our experiments showed that the p38 MAPK inhibitor suppressed the phosphorylation of RIPK1. This might indicate that p38 MAPK promotes RIPK1 phosphorylation. When macrophages were pretreated with Dyngo 4a, a potent p38 MAPK activator, an increase in RIPK1 phosphorylation is detected (see 4.3.1, Fig. 27). This result provided more support for the importance of p38 MAPK in the phosphorylation of RIPK1 (Fig. 22 A). Taken together, our findings demonstrate the critical role of p38 MAPK in suppressing necroptosis signaling in mouse BMDMs.

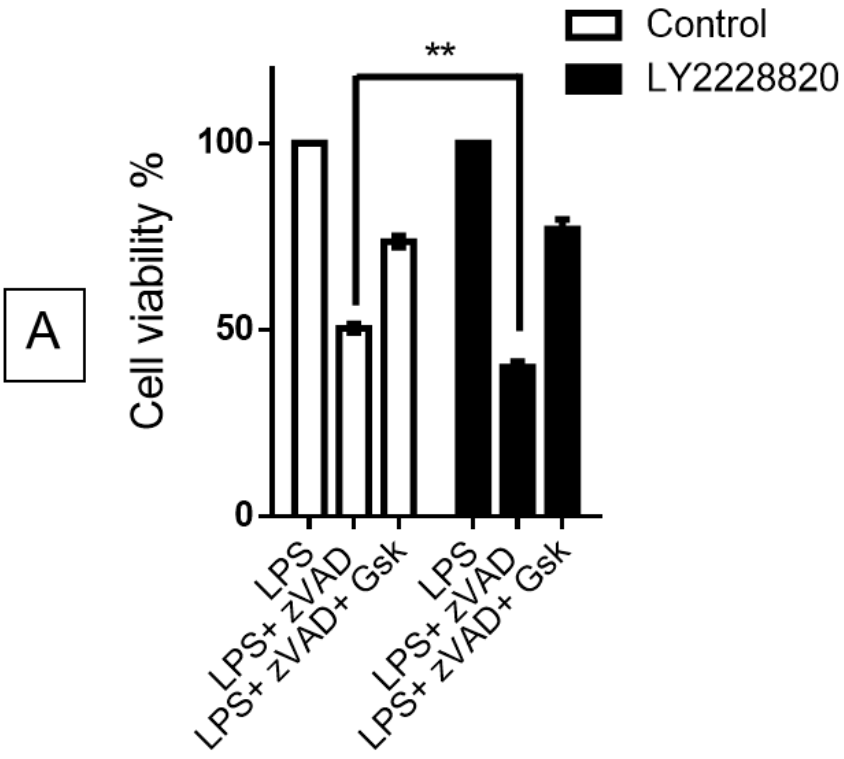
A
Control
LY2228820
**
Cell viability %
100
50
0
LPS
LPS+ zVAD
LPS+ zVAD+ Gsk
LPS
LPS+ zVAD
LPS+ zVAD+ Gsk

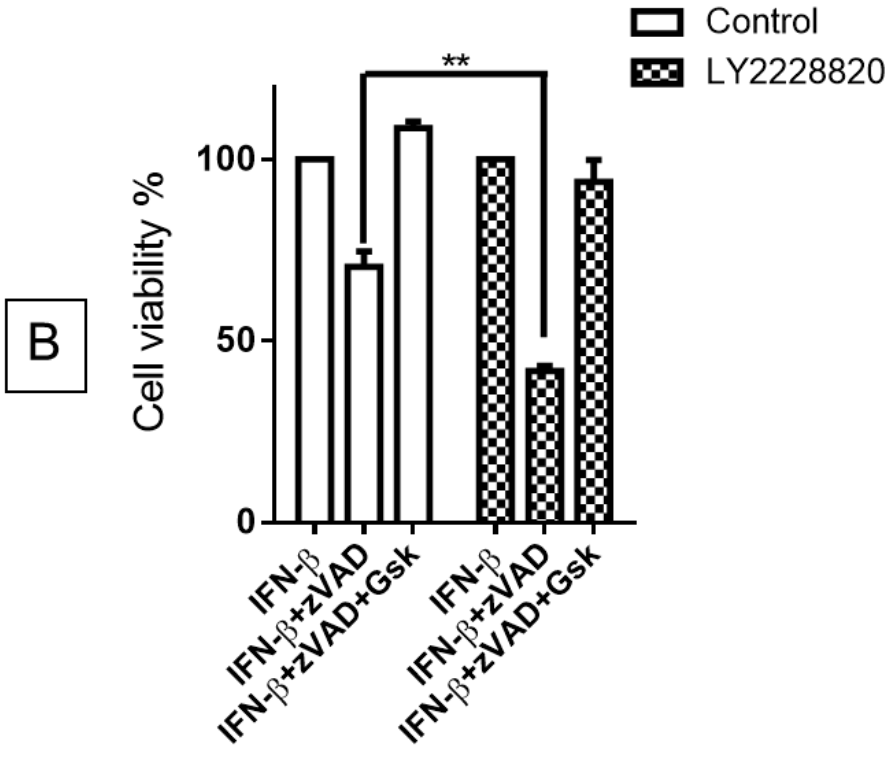
B
Control
LY2228820
**
Cell viability %
100
50
0
IFN-β
IFN-β+zVAD
IFN-β+zVAD+Gsk
IFN-β
IFN-β+zVAD
IFN-β+zVAD+Gsk

Figure 28. Inhibition of p38 MAPK facilitates the induction of necroptosis. BMDMs from WT mice (C57BL/6) were pretreated with or without LY2228820 (4μM), a p38 MAPK inhibitor, and post-treated with LPS (100ng/mL) ± zVAD (50μM) ± Gsk (5μM) (A), or IFN-β (1000U/mL) ± zVAD (50μM) ± Gsk (5μM) in 96-well plates (B). Graphs show the percentage of viable cells ± SEM relative to control (treated with LPS or IFN-β alone). All experiments were done at least in triplicates. $^{**}P < 0.01$.

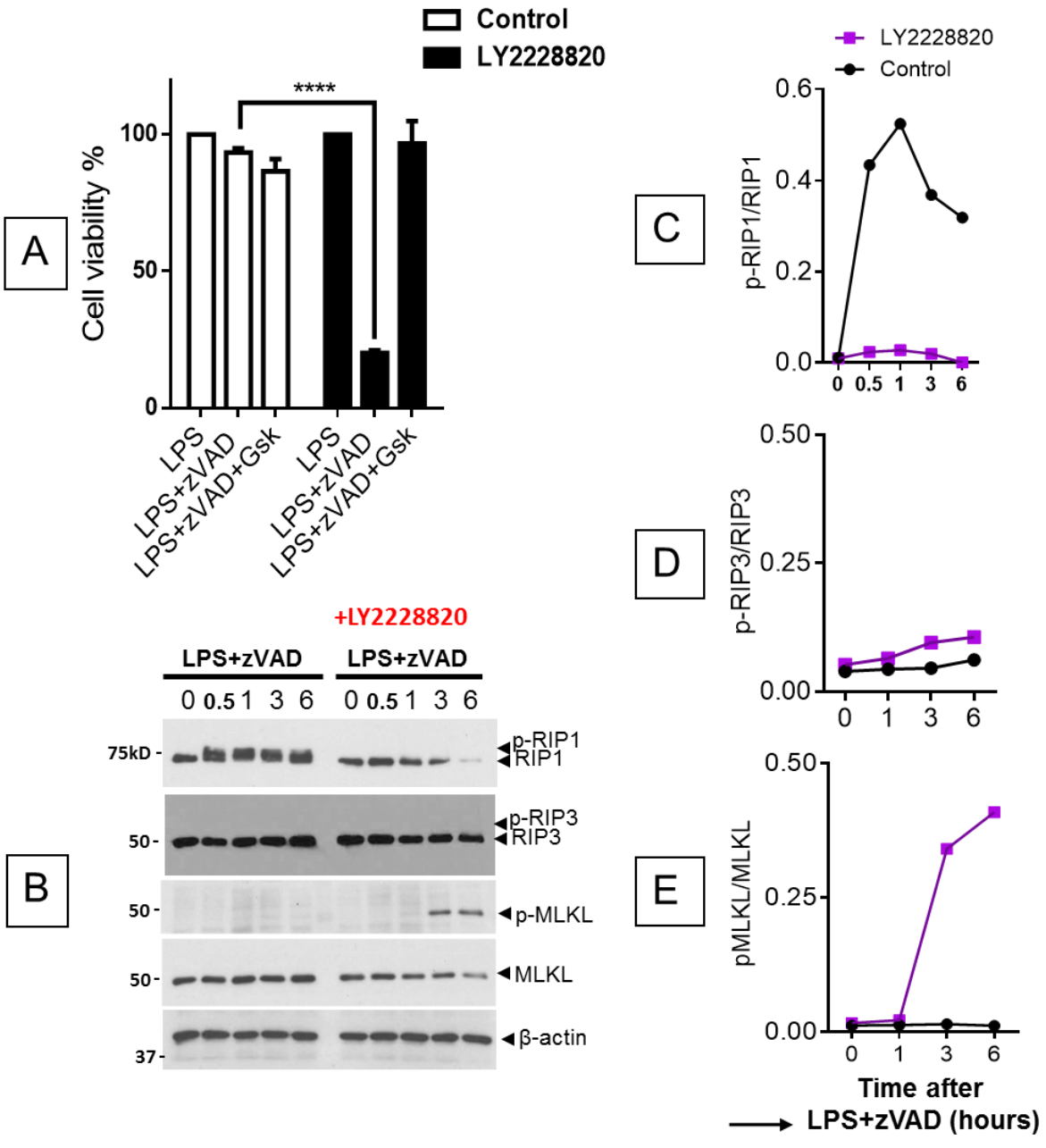
A
Control
LY2228820
Cell viability %
****
100
50
0
LPS
LPS+zVAD
LPS+zVAD+Gsk
LPS
LPS+zVAD
LPS+zVAD+Gsk
B
+LY2228820
LPS+zVAD
LPS+zVAD
0 0.5 1 3 6
0 0.5 1 3 6
75kD
p-RIP1
RIP1
p-RIP3
RIP3
50
p-MLKL
MLKL
β-actin
37
C
LY2228820
Control
p-RIP1/RIP1
0.6
0.4
0.2
0.0
0 0.5 1 3 6
D
p-RIP3/RIP3
0.50
0.25
0.00
0 1 3 6
E
pMLKL/MLKL
0.50
0.25
0.00
0 1 3 6
Time after
LPS+zVAD (hours)

Figure 29. Inhibition of p38 MAPK drastically increased the sensitivity of macrophages to normally non-necroptotic concentration of zVAD, a pan-caspase inhibitor. BMDMs from WT mice (C57BL/6) were pretreated with or without LY2228820 (4µM), a p38 MAPK inhibitor, before treating the cells with LPS (100ng/mL) ± zVAD 10µM ± Gsk (5µM) in 96-well plates and cell death was measured by MTT assay (A). Graphs show the percentage of viable cells ± SEM relative to control (treated with LPS alone). All experiments were done at least in triplicates. ****P < 0.0001; The Immunoblot comparison of key proteins of necrosome (RIPK1, RIPK3, and MLKL) for the cells pre-treated with or without LY2228820 (4µM) and post-treatment with LPS (100ng/mL) +zVAD (10µM) (B) in 24-well plates for varying time intervals (hour) as indicated. Samples were lysed with SDS buffer and the cell lysates were examined. The densitometry analysis on the western blots was done by ImageJ software to quantitate the average ratio of necroptotic proteins (i.e. pRIPK1/total RIPK1) over at least three separate experiments (C-E). Western blot data are representative of three independent experiments

4. 3. 3. Inhibition of p38 MAPK drastically increased necroptosis of BMDMs exposed to non-necroptotic concentrations of caspase-8 inhibitor

Since zVAD inhibits various caspases, we decided to test the impact of p38 MAPK inhibition using a specific caspase-8 inhibitor, Z-IETD. It has been suggested that zVAD treatment induces necroptosis through inhibition of caspase-8 (Fricker et al., 2013; Wu et al., 2011). We considered the possibility that p38 MAPK represses the necroptotic effects of caspase-8 inhibition. Accordingly, we first pre-treated macrophages with a dose of Z-IETD-FMK, a specific caspase-8 inhibitor that does not induce necroptosis in mouse macrophages. The inhibition of p38 MAPK in the pretreated macrophages showed a dramatic induction of necroptosis in these cells, confirming the repressive role of p38 MAPK on necroptosis in the cells (Fig. 30 A). To investigate p 38 MAPK's impact on the molecular signaling responsible for the induction of necroptosis in macrophages, western blotting was performed on cell lysates collected at various time intervals. As was observed with zVAD treatment, cells treated with the caspase-8 inhibitor and the p38 MAPK inhibitor displayed no RIPK1 or RIPK3 phosphorylation, but rather a potent activation of MLKL phosphorylation (Fig. 30 B). Since the phosphorylation of MLKL is the terminal step in necroptosis, these results corroborate the cell death data (Fig. 30 A). This data validates the results of previous experiments with low concentration of zVAD and shows that p38 MAPK plays a pivotal role in protecting mouse macrophages against TLR4-induced necroptosis.

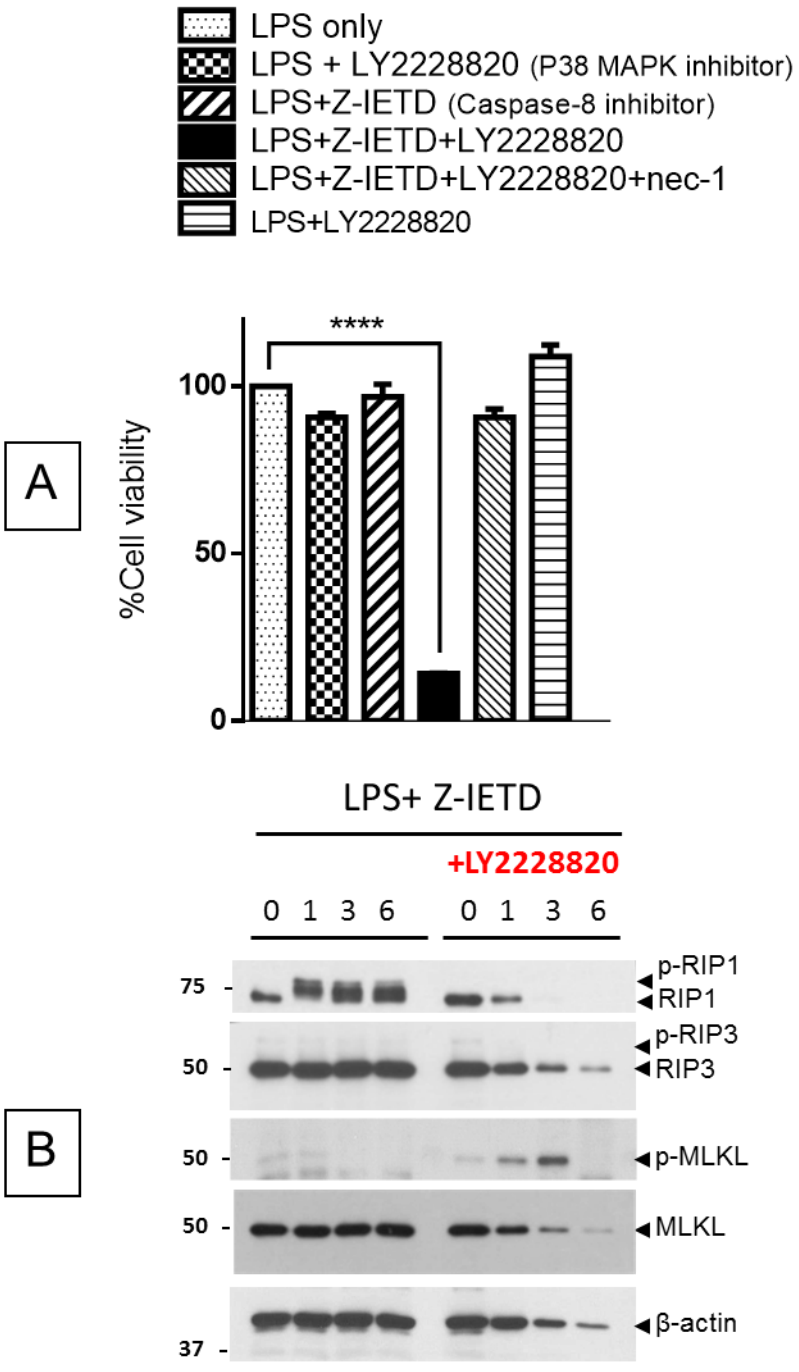
LPS only
LPS + LY2228820 (P38 MAPK inhibitor)
LPS+Z-IETD (Caspase-8 inhibitor)
LPS+Z-IETD+LY2228820
LPS+Z-IETD+LY2228820+nec-1
LPS+LY2228820
A
%Cell viability
****
100
50
0
LPS+ Z-IETD
+LY2228820
0 1 3 6 0 1 3 6
B
75
50
50
50
37
p-RIP1
RIP1
p-RIP3
RIP3
p-MLKL
MLKL
β-actin

Figure 30. Inhibition of p38 MAPK significantly enhanced the sensitivity of macrophages to normally non-necroptotic concentration of Z-IETD, a specific caspase-8 inhibitor. BMDMs from WT mice (C57BL/6) were pretreated with or without LY2228820 (4μM), a p38 MAPK inhibitor, before treating the cells with LPS (100ng/mL) ± Z-IEDT (40μM) ± nec-1 (30μM) in 96-well plates and cell death was measured by MTT assay (A). Graphs show the percentage of viable cells ± SEM relative to control (treated with LPS alone). All experiments were done at least in triplicates. ****P < 0.0001; The Immunoblot comparison of key proteins of necrosome (RIPK1, RIPK3, and MLKL) for the cells pre-treated with or without LY2228820 (4μM) and post-treated with LPS (100ng/mL) + Z-IEDT (40μM) (B) in 24-well plates for varying time intervals (0-6 hours) as indicated. Samples were lysed with SDS buffer and the cell lysates were examined. Western blot data are representative of three independent experiments

.

4. 3. 4. Inhibition of p38 MAPK strongly overcomes Dyngo 4a mediated rescue of macrophages from necroptosis

Having observed that Dyngo 4a is a potent activator of p38 MAPK and that the inhibition of p38 MAPK enhances necroptosis of macrophages, we wanted to evaluate whether the necroptosis of macrophages prevented by treatment with Dyngo 4a would be reversed by inhibition of p38 MAPK. We pretreated WT BMDMs with Dyngo 4a, LY2228820 (p38 MAPK inhibitor), or both Dyngo 4a and LY2228820. Cells were then treated with LPS+zVAD to induce necroptosis, and cell viability was evaluated by measuring the incorporation of MTT. As shown in Fig. 31 A, treatment of cells with Dyngo 4a resulted in the rescue of cells from necroptosis, which was then overcome and this rescuing impact was then overcome by treatment of cells with p38 MAPK inhibitor.

To confirm that the concurrent treatment of cells with both Dyngo 4a and p38 MAPK inhibitor resulted in necroptosis, we performed western blotting on cell extracts at various intervals (Fig. 30 and 31). As was shown in the previous experiment (Fig. 22 A), the pre-treatment of cells with Dyngo 4a did not inhibit the phosphorylation of RIPK1 (Fig. 31 B-1, Fig. 32 A), but it did inhibit the phosphorylation of RIPK3 (Fig. 31 B-2, Fig. 32 B) and the phosphorylation of MLKL was prevented during the critical first five hours post treatment (Fig. 31 B-3, Fig. 32 C). Treatment of cells with the p38 MAPK inhibitor resulted in potent inhibition of RIPK1 phosphorylation (Fig. 31 C-1, Fig. 32 A), and a slight inhibition of RIPK3 phosphorylation (Fig. 31 C-1, Fig. 32 B). At one-hour post treatment with LPS+zVAD, the phosphorylation of MLKL was only detectable when cells were also treated with the p38 MAPK inhibitor (Fig. 31 C-3, Fig. 32 C). Interestingly, when cells were treated

with both Dyngo 4a and LY2228820, the phosphorylation of RIPK1 was not restored (Fig. 31 C-1, Fig. 32 A), suggesting that the inhibition of p38 MAPK had a dominant impact on reducing the phosphorylation of RIPK1. The combination of Dyngo 4a and the p38 MAPK inhibitor resulted in the complete inhibition of the phosphorylation of RIPK3 (Fig. 31 C-2, Fig. 32 B). Surprisingly, despite the inhibition of both RIPK1 and RIPK3 phosphorylation by the Dyngo 4a and LY2228820 (p38 MAPK inhibitor) combination, phosphorylation of MLKL was induced early, after three hours (Fig. 31 C- 3, Fig. 32 C), which could be sufficient to induce necroptosis. Taken together, these results indicate that the treatment of cells with the dynamin inhibitor Dyngo 4a inhibits necroptosis; however, this appears to be due to the activation of p38 MAPK pathway by Dyngo 4a.

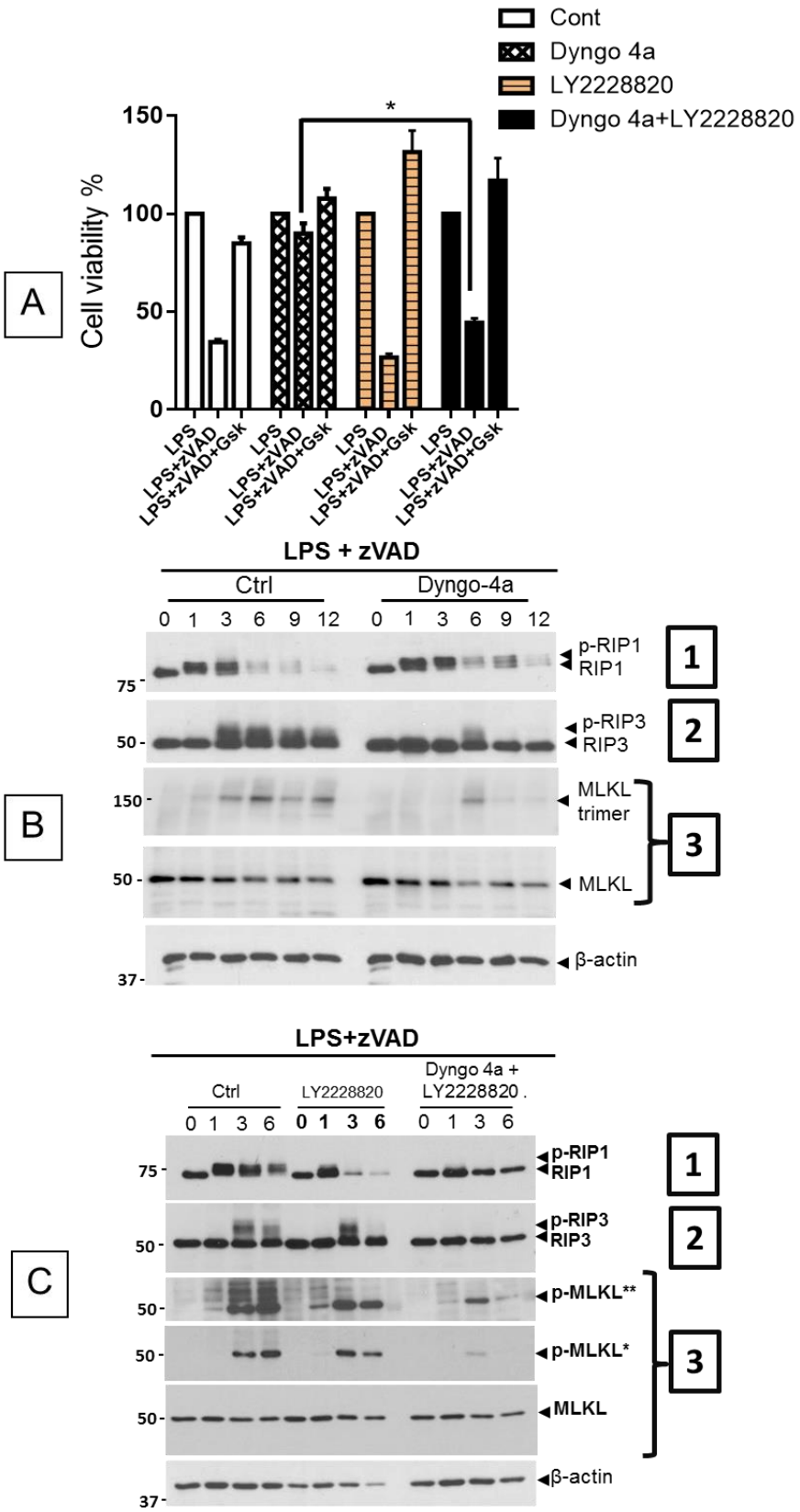
A
Cont
Dyngo 4a
LY2228820
Dyngo 4a+LY2228820
Cell viability %
150
100
50
0
*
LPS
LPS+zVAD
LPS+zVAD+Gsk
B
LPS + zVAD
Ctrl
Dyngo-4a
0 1 3 6 9 12 0 1 3 6 9 12
75
50
150
50
37
p-RIP1
RIP1
p-RIP3
RIP3
MLKL
trimer
MLKL
β-actin
1
2
3
C
LPS+zVAD
Ctrl
LY2228820
Dyngo 4a +
LY2228820
0 1 3 6 0 1 3 6 0 1 3 6
75
50
50
50
50
37
p-RIP1
RIP1
p-RIP3
RIP3
p-MLKL**
p-MLKL*
MLKL
β-actin
1
2
3

Figure 31. Inhibition of p38 MAPK results in abrogation of the Dyngo-4a-induced rescue of macrophages from necroptosis. BMDMs from WT mice (C57BL/6) were pretreated with or without LY2228820 (4μM), a p38 MAPK inhibitor, or Dyngo 4a (50μM) + LY2228820 (4μM) before treating with LPS (100ng/mL) ± zVAD (50μM) ± Gsk (4μM) in 96-well plates (A); Immunoblot comparison of the key proteins of necrosome (RIP1, RIP3, and MLKL) after treating the BMDMs with LPS (100ng/mL) + zVAD (50μM) ± Dyngo 4a (50μM) in 24-well plates for various time intervals (0-6 hours) as indicated (B); Immunoblot comparison of the key proteins of necrosome (RIP1, RIP3, and MLKL) after treating the BMDMs with LPS (100ng/mL) + zVAD (50μM) ± LY2228820 (4μM) ± Dyngo 4a (50μM) in 24-well plates (C). * = lower exposure time; ** = higher exposure time. Western blot data are representative of three independent experiments.

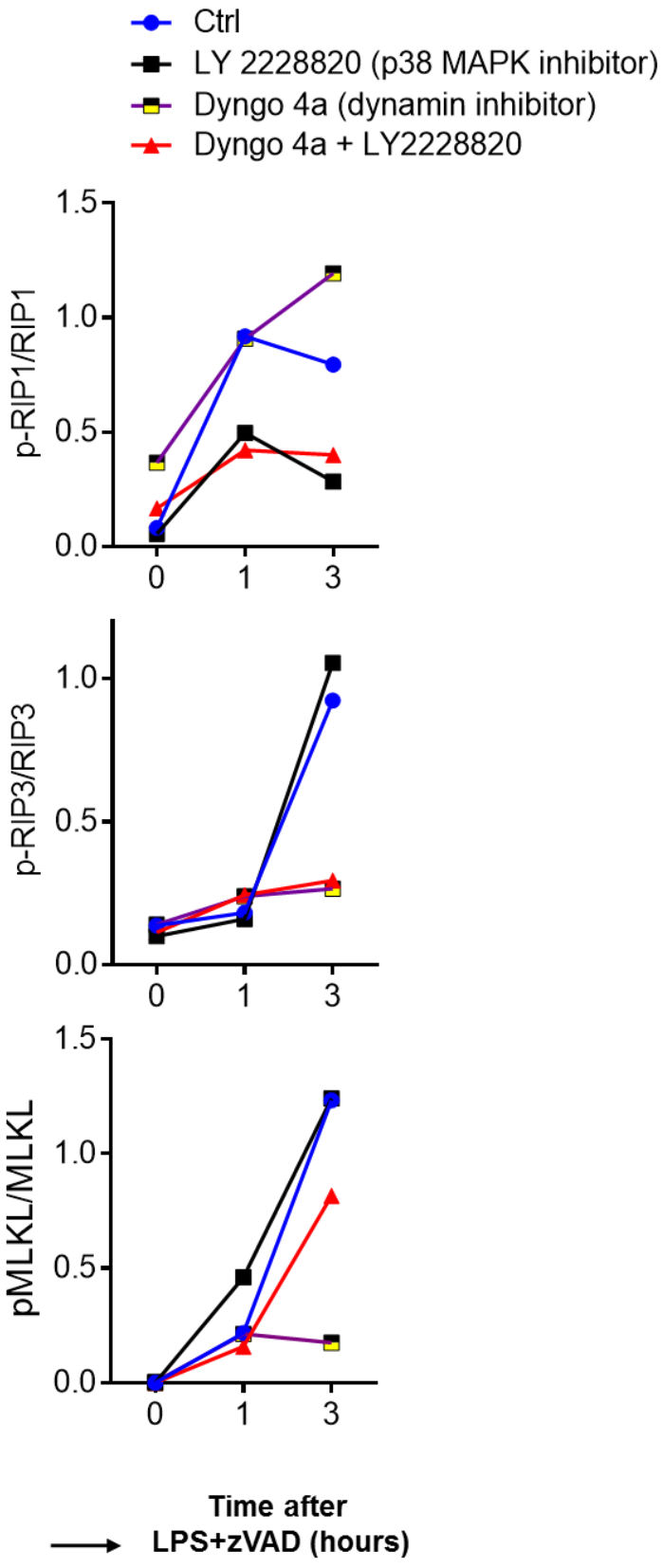
Ctrl
LY 2228820 (p38 MAPK inhibitor)
Dyngo 4a (dynamin inhibitor)
Dyngo 4a + LY2228820
p-RIP1/RIP1
p-RIP3/RIP3
pMLKL/MLKL
1.5
1.0
0.5
0.0
0
1
3
Time after
LPS+zVAD (hours)

Figure 32. **Densitometric analysis of proteins modulated by LY2228820, Dyngo 4a, and the combination of Dyngo 4a and LY2228820 during TLR4-driven necroptosis.** The densitometry analysis on the western blots (Fig. 31 B & C) was done by ImageJ software to quantitate the average ratio of necroptotic proteins (i.e. p-RIP1/total RIP1) over at least three separate experiments performed as described before (Fig. 31). The data are representative of three independent experiments.

4. 3. 5. Inhibition of MK2 promotes necroptosis

Since the inhibition of p38 MAPK enhanced necroptosis of macrophages, we speculated that the same effect would be induced through inhibiting of the key downstream kinase, MAPKAPK2 (MK2). To confirm this, we pretreated WT BMDMs with DMSO or p38 MAPK inhibitor (LY2228820) and stimulated them with LPS+zVAD. The western blotting performed on cell extracts at various time intervals revealed that the inhibition of p38 MAPK results in complete blockage of MK2 phosphorylation (Fig. 33 A).

Having confirmed the impact of p38 MAPK inhibition on the phosphorylation of MK2, we wanted to investigate whether the inhibition of MK2 could also promote necroptosis of macrophages treated with LPS+zVAD. After pre-treating the WT BMDMs with either the DMSO or MK2 inhibitors (PF 3644022), we stimulated the cells with LPS and a low concentration (10μM) of zVAD. Previous results had indicated that this reduced concentration of zVAD does not result in necroptosis of macrophages (see 4.3.2). However, the low concentration of zVAD, when used in conjunction with the p38 MAPK inhibitor, made cells vulnerable to necroptosis. Results indicated that the inhibition of MK2 resulted in increased necroptosis of macrophages following treatment with LPS+zVAD (Fig 33 B).

To investigate the mechanisms further, we performed western blotting of cell extracts at various time intervals post stimulation of the cells. MK2 inhibitor completely inhibited the phosphorylation of RIPK (Fig. 33 C, the first gel from the top, Fig. 34 A), like what was observed with the p38 MAPK inhibitor. Furthermore, the addition of PF 3644022 caused a slight induction of RIPK3 phosphorylation (Fig. 33 C, the second gel from the top, Fig. 34 B). Since the cells were stimulated with LPS and the low concentration of zVAD, RIPK3

phosphorylation and necroptosis were not detectable in control cells. Inhibition of MK2 resulted in early phosphorylation of MLKL (Fig. 33 and 34 C), similar to what was observed with the p38 MAPK inhibitor. Collectively, these results demonstrate that MK2 signaling plays a protective role during necroptosis signaling of macrophages.

4. 3. 6. Inhibition of MK2 has no effect on Dyngo 4a-mediated rescue of macrophages from necroptosis

After confirming that the inhibition of MK2, like the inhibition of p38 MAPK, enhances necroptosis of macrophages induced by LPS+zVAD, we wanted to determine whether Dyngo 4a induced rescue of macrophages from necroptosis was mediated by activation of MK2. Previous results revealed that the inhibition of p38 MAPK can significantly reverse the Dyngo 4a- induced rescue of macrophages (See 4.3.4, Fig. 31). Thus, we speculated that the inhibition of MK2 would have a promoting impact on necroptosis of macrophages. WT BMDMs were pretreated with different inhibitors, including Dyngo 4a, p38 MAPK inhibitor and MK2 inhibitor. Some cells were treated with combinations of Dyngo 4a and p38 MAPK inhibitor, or Dyngo 4a and MK2 inhibitor. Necroptosis was induced by treating cells with LPS+zVAD, and the RIPK3 inhibitor GSK was used as a control to confirm the mechanism of cell death. While the inhibition of p38 MAPK reversed the rescue of cells from necroptosis caused by Dyngo 4a, the inhibition of MK2 did not have a statistically significant impact (Fig. 35). Thus, it is conceivable that Dyngo 4a promotes the rescue of cells from necroptosis through p38 MAPK signaling which does not involve MK2.

A

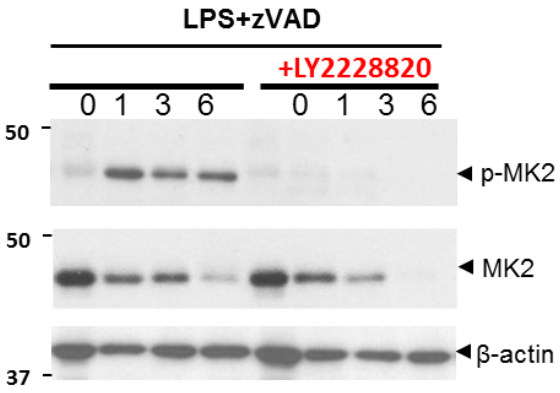
LPS+zVAD
+LY2228820
0 1 3 6 0 1 3 6
50
p-MK2
50
MK2
37
β-actin

B

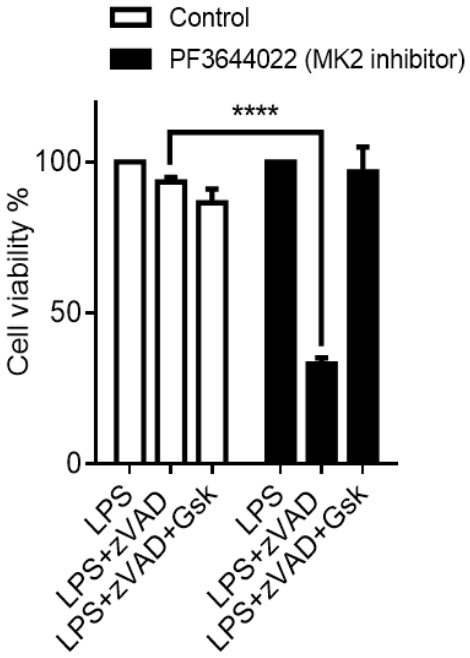
Control
PF3644022 (MK2 inhibitor)
****
Cell viability %
100
50
0
LPS
LPS+zVAD
LPS+zVAD+Gsk
LPS
LPS+zVAD
LPS+zVAD+Gsk

C

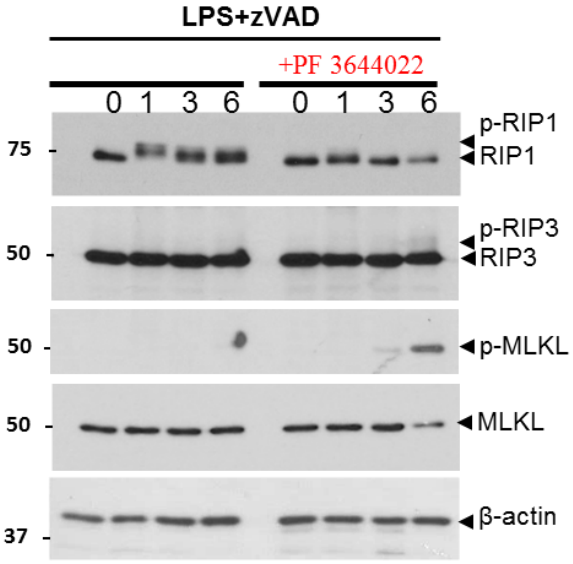
LPS+zVAD
+PF 3644022
0 1 3 6 0 1 3 6
75
p-RIP1
RIP1
50
p-RIP3
RIP3
50
p-MLKL
50
MLKL
37
β-actin

Figure 33. Inhibition of MK2, like inhibition of p38 MAPK, promotes necroptosis. BMDMs from WT mice (C57BL/6) were pretreated with or without LY2228820 (4μM), a p38 MAPK inhibitor, and post-treated with LPS (100ng/mL) + zVAD (10μM) in 24-well plates for varying time intervals (0-6 hours) as indicated. Samples were lysed with SDS buffer and the cell lysates were examined for phosphorylated and un-phosphorylated MK2 by western blotting (A); BMDMs were pretreated with or without PF3644022 (5μM), an MK2 inhibitor, in 96-well plates for 30 minutes and post-treated with LPS (100ng/mL) ± zVAD 10μM ± Gsk (5μM) and cell death was measured by MTT assay. All experiments were done at least in triplicates. ****P < 0.0001; Immunoblot comparison of the key proteins of necrosome (RIP1, RIP3, and MLKL) after pre-treating the cells with PF3644022 (5μM) in 96-well plates for 30 minutes and post-treating with LPS (100ng/mL) + zVAD (10μM) (C). The data are representative of three independent experiments.

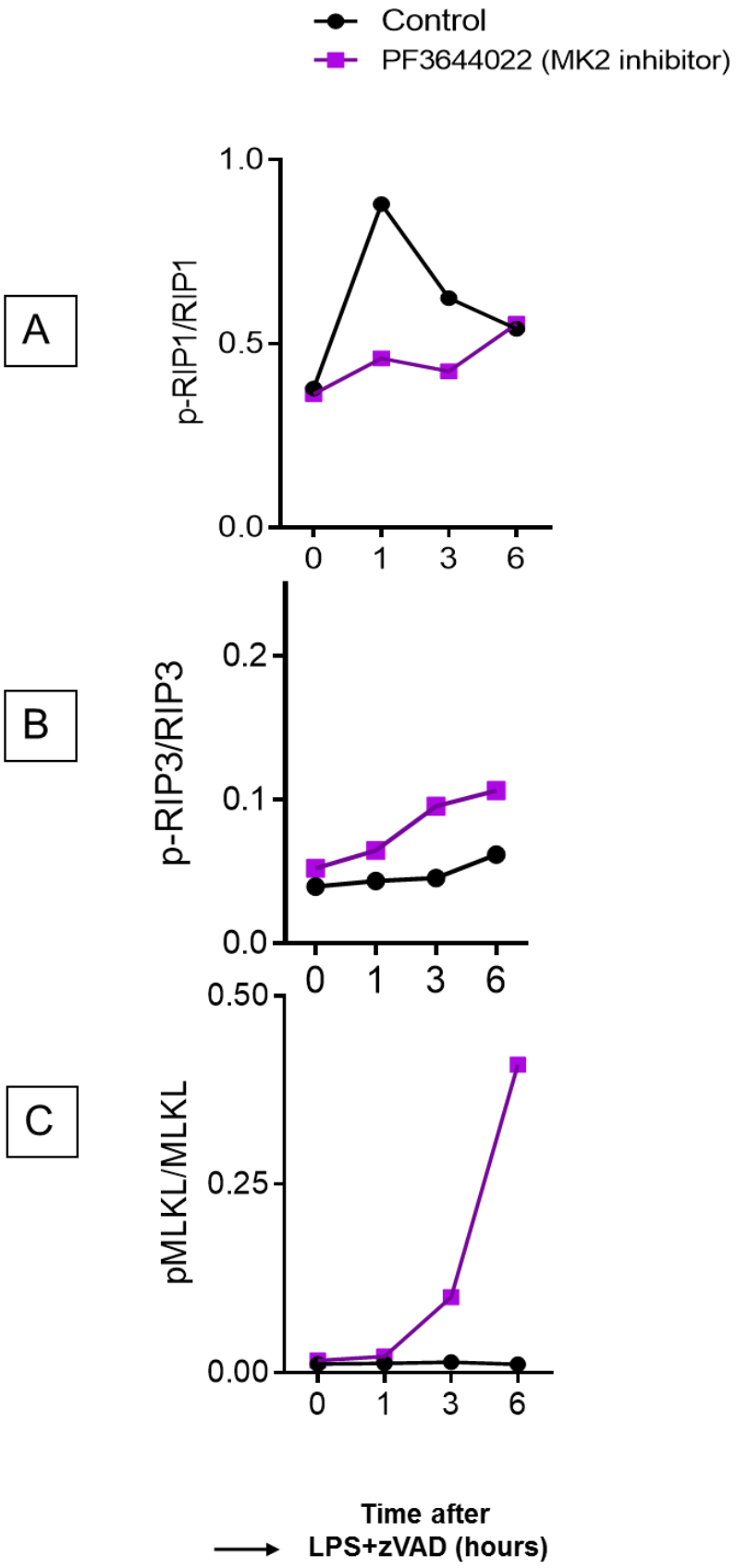
Control
PF3644022 (MK2 inhibitor)
A
p-RIP1/RIP1
1.0
0.5
0.0
0
1
3
6
B
p-RIP3/RIP3
0.2
0.1
0.0
0
1
3
6
C
pMLKL/MLKL
0.50
0.25
0.00
0
1
3
6
Time after
LPS+zVAD (hours)

Figure 34. **Densitometric analysis of proteins modulated by MK2 inhibitor during TLR4-driven necroptosis.** The densitometry analysis on the western blots (Fig. 33 C) was done by ImageJ software to quantitate the average ratio of necroptotic proteins (i.e. p-RIP1/RIP1) over at least three separate experiments performed as described before (Fig. 33). Densitometric analysis of each protein is shown for six-hour post activation (A-B). Data are representative of at least two independent experiments.

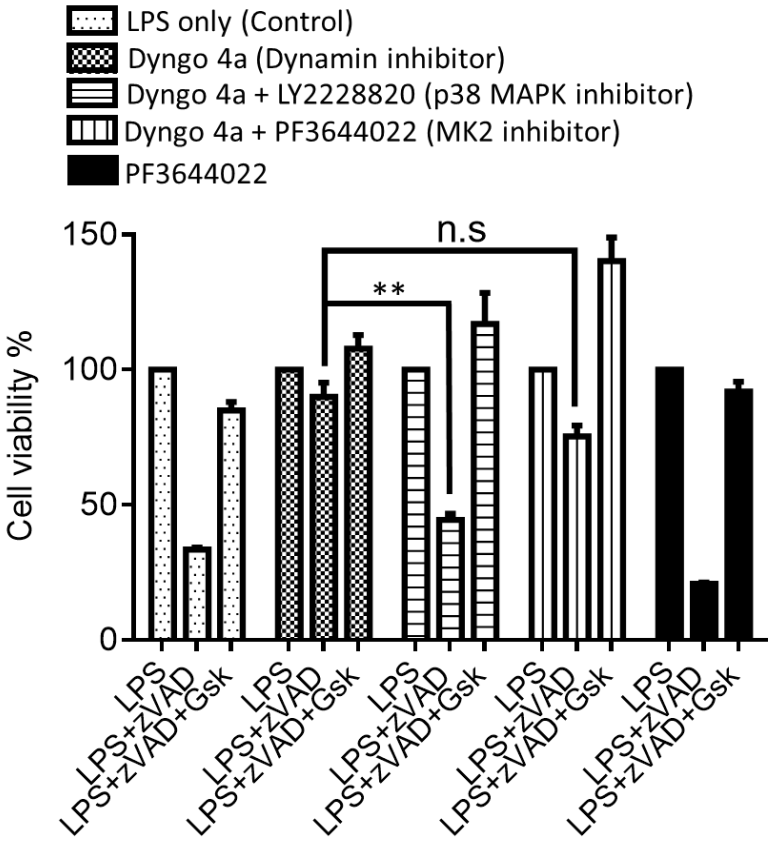
LPS only (Control)
Dyngo 4a (Dynamin inhibitor)
Dyngo 4a + LY2228820 (p38 MAPK inhibitor)
Dyngo 4a + PF3644022 (MK2 inhibitor)
PF3644022
Cell viability %
150
100
50
0
n.s
**
LPS
LPS+zVAD
LPS+zVAD+Gsk

Figure 35. Inhibition of MK2 had no significant impact on Dyngo 4a- induced rescue of macrophages from necroptosis. BMDMs from WT mice (C57BL/6) were pretreated with or without Dyngo 4a (50μM), a dynamin inhibitor, LY2228820 (4μM), a p38 MAPK inhibitor, PF3644022 (5μM), an MK2 inhibitor, and combination of Dyngo 4a (50μM) and LY2228820 (4μM) or PF3644022 (5μM) in 96-well plates for 30 minutes and post-treating with LPS (100ng/mL) ± zVAD (50μM) ± Gsk (4μM). Cell death was measured by MTT assay. All experiments were done at least in triplicates. Data are representative of at least three independent experiments. Data were normalized based on the LPS data (Control).
** $P < 0.01$.

5.0 DISCUSSION

While necroptosis appears to play an important role during infection, the activation of necroptosis has also been shown to play a deleterious role in various chronic inflammatory diseases that are induced by sterile triggers (Pierdomenico, 2014; Weinlich et al., 2017). Since macrophages and macrophage-like cells (such as kupfer cells and microglia) pervade various non-lymphoid organs, deciphering the mechanisms that induce and regulate the necroptosis of macrophages is currently receiving a lot of attention (Karunakaran, 2016). On the other hand, necroptotic macrophages can be potentially strong effector cells of the innate immune system to eradicate many viral or bacterial diseases. Therefore, while our knowledge about the mechanisms of necroptosis signaling has significantly increased, the precise molecular mechanisms are far from clear.

5.1 IFNAR1 and TNFR1/2 crosstalk during TLR4-induced necroptosis of macrophages depends on LPS concentration

While it was previously reported that TNF-R signaling is required for the necroptosis of fibroblasts, it was unclear whether this operates through the TNF-R1 or TNF-R2. Since TNF-R1 signaling is required for ripoptosome induced cell death (Dondelinger et al., 2016), it was assumed that TNF-R1 signaling mediates necroptosis. Recently, it was reported that TLR4-induced necroptosis requires TNF-R2 signaling, but not TNF-R1 signaling (Legarda, 2016), and LPS-induced necroptosis was abrogated in TNF $^{-/-}$ macrophages (Legarda, 2016). It was further shown that IFNAR1 engagement was required to induce the expression of TNFR2 during necroptosis signaling by LPS+zVAD. Legarda et al., (2016) confirmed our previous lab results showing the critical role of IFNAR1 engagement in the induction of

necroptosis in macrophages (McComb, 2014). However, previous results from our lab did not observe any impact of TNF-R1/R2 signaling in the necroptosis of macrophages following LPS+zVAD treatment (McComb, 2014). The differences in the requirement of TNF-R signaling in necroptosis obtained by McComb et al. (2014) and Legarda et al. (2016) could be explained by the amounts of LPS used in the two studies. While McComb et al. have performed their experiments with 100 ng/ml of LPS, Legarda et al. performed their experiments using 1 ng/ml of LPS. Using 100ng/mL of LPS in our experiments, we showed that TNFR1/2 is dispensable for LPS-induced necroptosis of macrophages (Fig. 12). Further mechanistic studies, with both low and high concentrations of LPS, would be needed to decipher the role of TNFR1/2 engagement in the TLR4-driven necroptosis of primary macrophages.

5. 2 LPS-induced necroptosis requires IFNAR1 signaling, but not secretion of IFN-I

Our lab had previously reported that IFNAR1-signaling through the trimeric transcriptional complex ISGF3 promotes necroptosis of macrophages (McComb, 2014). Using a neutralizing antibody against IFNAR1, our studies indicated that blocking IFNAR1 signaling does not rescue macrophages from necroptosis (Fig. 14). Although IFNAR1 signaling is required for LPS-induced necroptosis, since IFNAR1 cells are highly resistant to necroptosis, we suggest that this occurs through a mechanism that does not require secretion of IFN-I. Legarda et al. (2016) reported similar results using a neutralizing antibody against TNF-R. They found LPS-induced necroptosis was abrogated in $Tnf^{-/-}$ macrophages, however, a soluble TNF antagonist could not induce death in $Tnf^{+/+}$ macrophages, indicating that necroptosis happens in a cell-autonomous manner.

5. 3. MLKL, is a hallmark of TLR4-induced necroptosis of macrophages

MLKL has been shown to be a key effector molecule in necroptosis, as it trimerizes after phosphorylation, relocates to the cell membrane, where it induces pore formation in the membrane (Cai et al., 2014; Dondelinger et al., 2014; Wang et al., 2014). The results of our experiments indicate that MLKL gets phosphorylated during the necroptosis signaling of macrophages (Fig. 22 C). While the phosphorylation of RIPK3 has been considered essential for subsequent downstream phosphorylation of MLKL (Cai, 2014; Murphy 2015; Rodriguez et al, 2016), we were able to observe a key new insight. We observed that when cells are treated with a p38 MAPK inhibitor during necrosome signaling, MLKL gets phosphorylated (Fig. 31 C-3) even when no RIPK3 phosphorylation is detectable (Fig. 31 C-2). This shows that phosphorylation of RIPK3 is not a pre-requisite for phosphorylation of MLKL. Further studies will be required to decipher the mechanism.

5. 4. The role of the endocytosis of TLR4 in macrophage necroptosis

Various dynamin inhibitors that were used in our study inhibited the internalization of TLR4 (Fig. 15, 16) and activation of the TRIF/IRF3 pathway (Fig. 17). These findings were verified by flow cytometry, confocal microscopy, and western blotting. Similar results were reported by Kegan et al. (2008), Czerkies et al. (2013), and Płóciennikowska et al. (2015), where inhibitors of dynamin were shown to block the endocytosis of TLR4 in murine macrophages. Wang et. al. (2012) indicated that the internalization of TLR4 is clathrin/dynamin dependent and is required for activation of the TRAM–TRIF-dependent signaling pathway. In another study, Rajaiah et al. (2015) demonstrated the inhibitory impact of Dynasore on IRF3 activation, which is dependent on TLR4 internalization. Ultimately, it

appears that dynamin-dependent endocytosis is the predominant pathway for TLR4/TRIF signaling.

Using ELISA or CBA to measure the impact on cytokine expression following TLR4-engagement, we also observed that the expression of various cytokines after TLR4-activation was significantly reduced by dynamin inhibitors (Fig. 21). These results are in agreement with a previous study which reported that the treatment of macrophages with Dynasore results in the inhibition of cytokine production (Kagan et al., 2008). Latvala et al. (2014) indicated that the inhibition of dynamin-dependent endocytosis in human macrophages can attenuate the induction of IL-1β, TNF, IFN-β and CXCL-10 mRNAs (Latvala et al., 2014).

Taken together, our findings are consistent with other studies which showed that different dynamin inhibitors can inhibit internalization of TLR4 and TRIF-dependent IRF3 signaling (Fig. 17).

It is important to mention that we used only small molecule inhibitors in our study because they offer many distinct advantages over other means of dynamin inhibition. While the knock-down of dynamin by siRNA can be an alternative approach, this technique is very difficult for proteins that are highly expressed in cells, such as dynamin (data not shown). Zhang et al. (2009) have previously reported the difficulties of introducing exogenous nucleotides, such as siRNA, into certain primary cells, especially primary macrophages. There are several reasons for this, which are associated with the phagocytotic function of macrophages. As a front line of the innate immune system, macrophages actively detect pathogens and danger signals, responding with phagocytosis and the digestion of pathogens. In this regard, they express many potent enzymes to degrade nucleotides and are ready to react rapidly and vigorously to the presence of any foreign particle. We speculate that this approach would be more tedious for proteins, such as dynamin, that are needed for

endocytosis. Uptake of dynamin siRNA in intracellular vesicles requires endocytosis, and a knock down of dynamin would, in turn, result in sequestration of the system. Escape from these vesicles may represent a major barrier to triggering RNA interference (RNAi) and thereby affect the efficacy of siRNA. As our experiments revealed (data not shown), siRNA failed to knockdown dynamin II, a highly expressed protein in macrophages. Therefore, we preferred to use small molecule inhibitors against dynamin, as they are able to rapidly block endocytosis and the receptor does not have a chance to switch from the dynamin-dependent pathway to another endocytosis pathway.

Although Dyngo 4a had previously been shown to be a more potent inhibitor of dynamin in comparison to other inhibitors (Harper et al., 2013; Mccluskey et al., 2013), we observed that the endocytosis of TLR4 was blocked by various dynamin inhibitors (Dynasore, Dynole, and Dyngo 4a) to the same degree. Similarly, both Dyngo 4a and Dynasore inhibited cytokine production by macrophages to the same degree (Fig. 21). Surprisingly, despite the inhibition of TLR4 internalization by various dynamin inhibitors, only Dyngo 4a was able to inhibit TLR4-induced necroptosis in macrophages (Fig. 18, 19, and 20). Thus, these results indicate that dynamin-dependent endocytosis of TLR4 does not affect necroptosis of macrophages, and point to a unique impact of Dyngo 4a on mechanisms other than receptor endocytosis.

A key question that arises out of this I s why the treatment of cells with Dynasore fails to inhibit necroptosis when it appears to substantially block the production of TNF following the treatment of cells with LPS+zVAD (Fig. 21). One answer could be that the impact of dynamin inhibitors on TLR internalization block the transcription of cytokines or exocytosis of cytokines following translation, and it is not clear which of those two events are impacted by dynamin inhibitors. Our results (Fig. 14) and those of others (Legarda et al., 2016) have

shown that cytokines can induce necroptosis without being secreted. If dynamin inhibitors only impact the exocytosis of cytokines and not gene translation, then this explains the differential results that we obtained with Dynasore treatment on cytokine expression and necroptosis.

5. 5. The Impact of Dyngo 4a on MAPK signaling

Since we were surprised by the observation that the only dynamin inhibitor that can rescue macrophages from TLR4-induced necroptosis is Dyngo 4a, the evaluation of the mechanisms involved by western blotting unveiled that Dyngo 4a is also a potent activator of the p38 MAPK pathway. What we have uncovered, the rapid and significant activation of p38 MAPK by Dyngo 4a, is an intriguing new finding. Eichel et al. (2016) had previously shown that blocking dynamin activity by Dyngo 4a, can effectively stall clathrin-coated structures (CCSs) on the plasma membrane. The blockage of these endocytotic bodies would increase the cell surface maintenance of recruited β-arrestin-2, which acts as a scaffold protein and a regulator of signal transduction of G-protein-coupled receptors (GPCRs). This raises the possibility that CCSs not only serve as sites of ERK1/2 (MAPK) activation by β-arrestin-2, but also shape the kinetics of β1AR-induced ERK1/2 signaling according to CCS surface lifetime, thereby enhancing MAPK (ERK1/2) activation. Also, Li et al. (2014) reported that β-arrestin-2 can form complexes with p38 MAPK and this interaction then facilitates p38 MAPK activation after LPS stimulation in mouse peritoneal macrophages. Similarly, Sun et al. (2002) suggested an ASK1-mediated mechanism of enhancement of p38 MAPK activation. Using these studies, taken together with our findings, we can, therefore, speculate that Dyngo 4a may act in a similar fashion to enhance the activation of p38 MAPK.

Further studies are necessary, however, to determine the precise mechanism by which Dyngo 4a enhances phosphorylation of p38 MAPK.

5. 6. Impact of various p38 MAPK isoforms on the rescue of macrophages from necroptosis

The inhibitory impact of Dyngo 4a on necroptosis is efficient and correlates with its inhibitory impact on endocytosis and its ability to activate the p38 MAPK. By revealing the mechanism through which Dyngo 4a inhibits necroptosis, we uncovered a major inhibitory role of p38 MAPK signaling in necroptosis. Several lines of evidence have shown that p38 MAPK can prevent apoptosis in various cell types. Alvarado-Kristensson et al. (2004) showed that p38 MAPK can phosphorylate caspase-8 at Ser364 thereby leading to inhibition of caspase-8, which in turn, protects neutrophils from Fas-induced cell death. It has been also demonstrated that p38α MAPK is required to suppress ER stress-induced macrophage apoptosis in vitro and macrophage-driven advanced atherosclerotic lesions in mice (Seimon et al., 2009). While there are some reports on the impact of p38 MAPK on apoptosis, to the best of our knowledge, the inhibitory mechanism of p38 MAPK on macrophage necroptosis is still unknown. Thus, clarification of the mechanism behind the inhibitory role of p38 MAPK on necroptosis can shed light on the mechanism that has so far been unknown in this context.

Two subsets of p38 MAPK, p38α/p38β, and p38γ/p38δ can activate different downstream kinases following TLR engagement (Escós et al., 2016; Risco and Cuenda, 2012). While p38α/p38β are major activators of MAPKAPK2 (MK2) and MAPKAPK3 (MK3), these kinases are not activated by p38γ/p38δ. Interestingly, MK2 has been shown to inactivate heat shock transcription factor-1 (HSF1) by promoting Ser 121

phosphorylation (Jacobsen AV, et al. 2016). This phosphorylation results in the inhibition of HSF1's ability to bind to heat shock elements (HSEs) in the promoter region of heat shock proteins including HSP90 (Wang X, et al. 2006). Phosphorylation of HSF1 by MK2 also results in an inactive HSF1-HSP90 cytosolic complex. HSP90 has recently been shown to be required for the oligomerization and membrane translocation of MLKL, the final step in necroptosis (Jacobsen AV, et al. 2016). On the other hand, in the absence of active MK2, p38γ/p38δ can phosphorylate HSF1 at other sites such as Ser 326 (Fig. 36), resulting in the activation of HSF1 and forming a trimeric structure and the release of HSP90 in the cytosol. Following the oligomerization of HSF1, it would be translocated into the nucleus to express various genes such as HSP90 and histone deacetylase 1 (HDAC1)(Leach et al., 2016; Fritah et al., 2009). HDAC1, like HSP90, is considered as an important up-regulator of necroptosis (Wang et al., 2013; Zhao et al., 2016). Collectively, we speculate that the activation of MK2 by p38α/p38β may be an alternative mechanism through which MK2 regulates necrosome signaling (Fig. 36). It is not clear whether the protection afforded by p38α/β MAPK is unique to MK2/MK3, or is common to all p38 MAPK down-stream signaling molecules.

5. 7. ARF6 inhibition could rescue macrophages from TLR4-induced necroptosis

Several recent studies have shown the contribution of small GTPase ARF6 in both TRIF and MyD88- dependent signaling (Van Acker et al., 2014). This protein, the ore, appears to be a good target for controlling TLR4-driven necroptosis as well. Van Acker et al. (2014) demonstrated the crucial role ARF6 has in regulating the TRAM/TRIF-dependent pathway in TLR4 signaling. As discussed before, the TRIF-dependent pathway plays an important role in TLR4-mediated necroptosis. Moreover, Zhu et al. (2012) revealed that the ARF6 nucleotide binding site opener (ARNO), as an activator of ARF6, can bind directly to

the adaptor protein MyD88. Interestingly, Davis et al. (2014) have shown that the MyD88-ARNO-ARF6-signaling axis can promote LPS-induced endothelial permeability and is responsible for a vascular leak caused by endotoxemia. Thus, we speculate that targeting ARF6 could be an alternative way to block macrophage necroptosis. Further studies with ARF6 inhibitors are required to decipher how ARF6 signaling following TLR4-engagement leads to the necroptosis of macrophages.

6.0 CONCLUSION

In this study, we have revealed some novel insights into the mechanisms that regulate necroptosis of mouse macrophages. We have uncovered that the inhibition of necroptosis of macrophages with the dynamin inhibitor Dyngo 4a is due to the activation of the p38 MAPK pathway. Observation of the induction of necroptosis in mouse macrophages via inhibition of p38 MAPK and the downstream MK2 has unveiled an important role for MAPK signaling. Furthermore, having shown that Dyngo 4a can promote the rescue of macrophages from necroptosis through p38 MAPK signaling, which is not dependent on MK2, we can conclude that there could be more than one downstream targets of p38 MAPK that regulates necroptosis of macrophages. Trempolec et al., (2013) have reported a wide variety of substrates of p38 MAPK including Ser/Thr kinases (GSK3β, MK5, MNKs, MSK1, and PKCε), various transcription factors (ATF2, USF1), DNA binding (H2AX, Rb1), and regulatory proteins (BCL2L11, caspase-3, caspase-8, TAB1). Further investigations are needed, however, to reveal the impact of various p38 MAPK isoforms and downstream substrates on the regulation of necroptosis in macrophages. While the cytokines secreted in response to necroptotic stimuli were significantly decreased in the presence of inhibitors of

dynamin-mediated endocytosis, there was no impact on necroptosis. These results suggest that receptor internalization by endocytosis is important in cytokine secretion, but not in cell death by necroptosis. Furthermore, we have revealed a new mechanism through which cytokines influence the necroptosis of cells as they can induce necroptosis without being secreted by the cell.

Lastly, our study also showed that the phosphorylation of upstream kinase RIPK1 involved in necroptosis signaling is not dependent on endocytosis of TLR4. On the other hand, phosphorylation of the downstream kinase, RIPK3 is dependent on endocytosis of TLR4.

In conclusion, the results of this thesis have unveiled novel mechanisms of regulation of macrophage necroptosis (Fig. 37). Necroptosis has been shown to promote numerous inflammatory conditions such as ischemia-reperfusion injury, sepsis, inflammatory bowel disease, amyotrophic lateral sclerosis, lethal dermatitis, liver injury (Saeed and Jun, 2014; Kaczmarek et al., 2013). We hope that the findings of our research can help future researchers in developing therapies against various inflammatory pathologies.

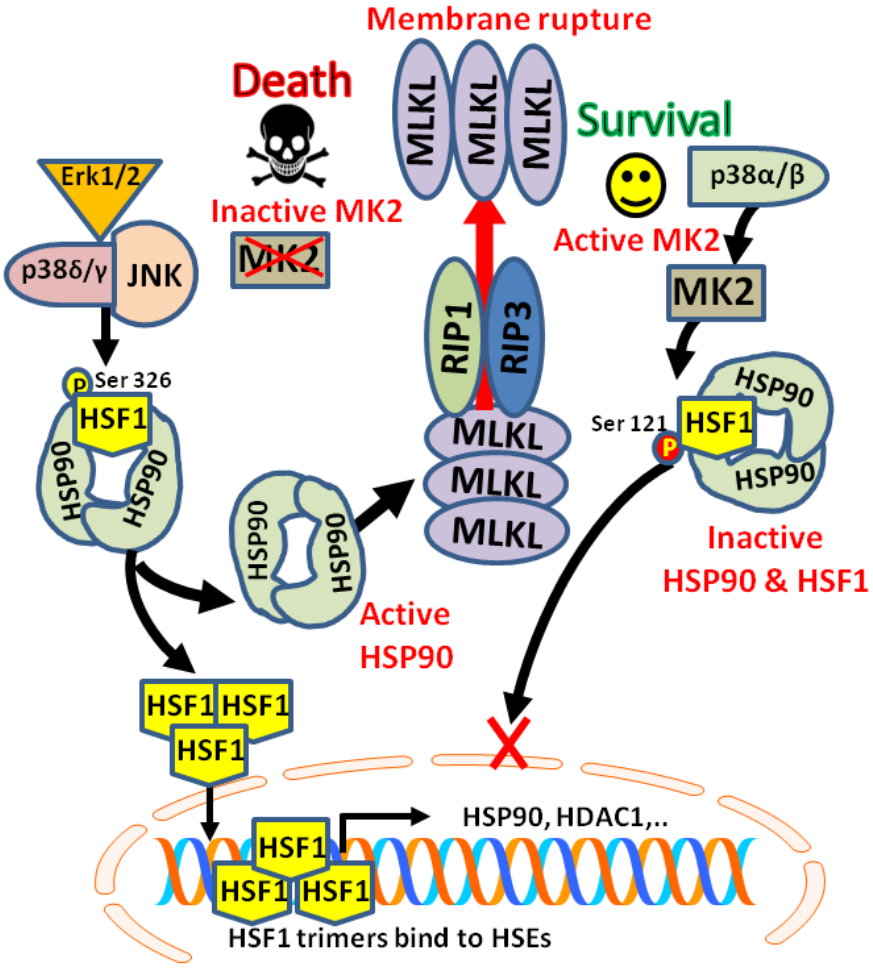
Membrane rupture
Death
MLKL
MLKL
MLKL
Survival
Erk1/2
Inactive MK2
p38α/β
Active MK2
p38δ/γ
JNK
MK2
RIP1
RIP3
MK2
P Ser 326
HSF1
HSP90
HSP90
MLKL
MLKL
MLKL
HSP90
HSP90
Ser 121
HSF1
HSP90
HSP90
Inactive
HSP90 & HSF1
Active
HSP90
HSF1 HSF1
HSF1
HSP90, HDAC1,..
HSF1
HSF1 HSF1
HSF1 trimers bind to HSEs

Figure 36. A schematic model of the regulation of necroptosis by various MAPkinases through activation /inactivation of MK2 in mammalian cells. Phosphorylation of HSF1 at Serin 121, intensifies HSF1-HSP90 binding which results in blockage of HSF1 trimerization as well as inactivation of HSP90 dimers required for oligomerizing and translocating of MLKL to the cell membrane to induce necroptosis. whereas, in the absence of active MK2, phosphorylation of HSF1 can happen at the other sites such as Ser 326, which is required for activating of HSF1 and triggering its trimmer structure as well as releasing HSP90.

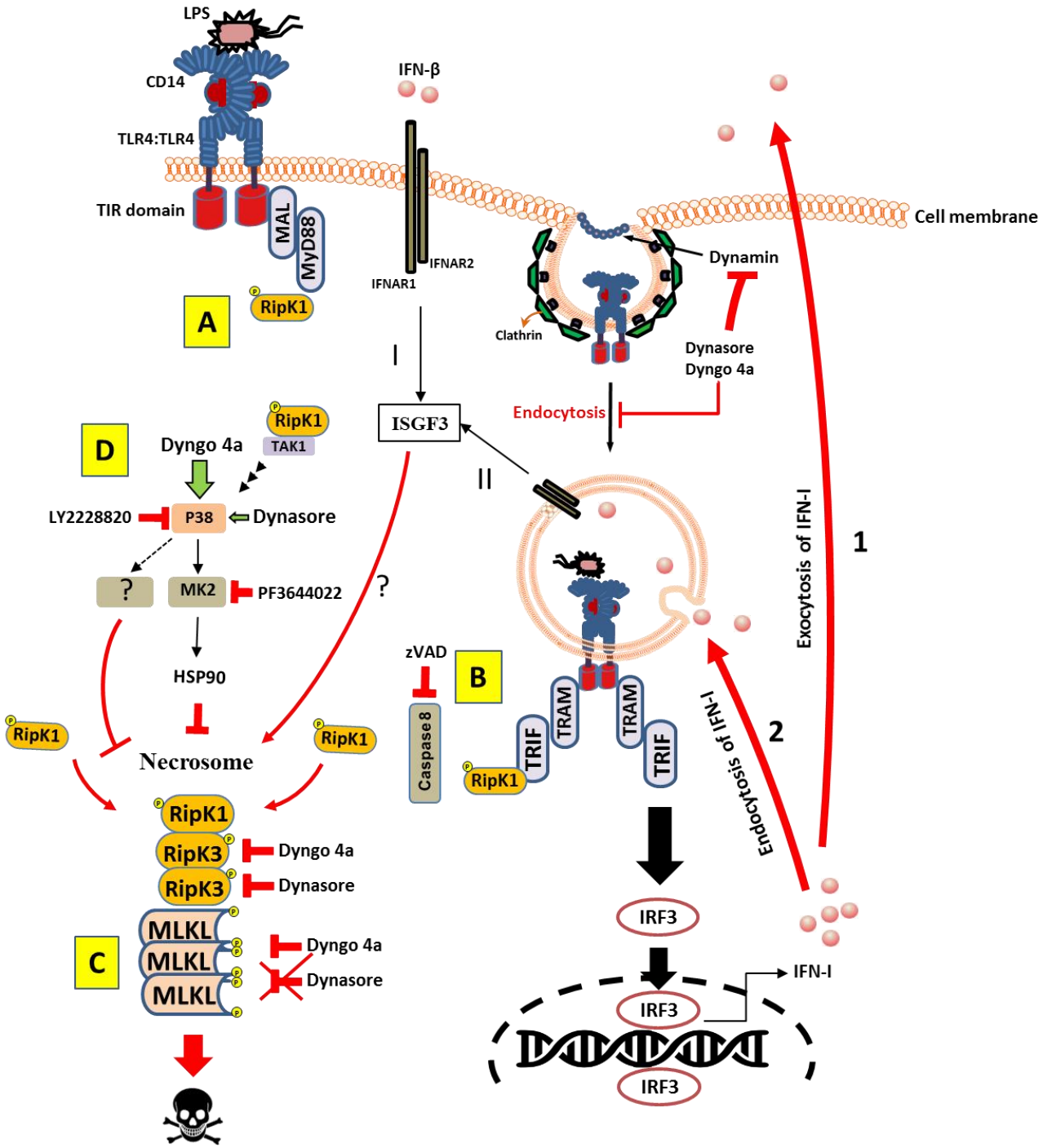
LPS
CD14
TLR4:TLR4
TIR domain
MAL
MyD88
RipK1
A
IFN-β
IFNAR1
IFNAR2
I
ISGF3
Cell membrane
Dynamin
Clathrin
Dynasore
Dyngo 4a
Endocytosis
II
Exocytosis of IFN-I
1
2
Endocytosis of IFN-I
D
Dyngo 4a
RipK1
TAK1
LY2228820
P38
Dynasore
?
MK2
PF3644022
HSP90
?
RipK1
RipK1
Necrosome
RipK1
RipK3
RipK3
Dyngo 4a
Dynasore
C
MLKL
MLKL
MLKL
Dyngo 4a
Dynasore
zVAD
B
Caspase8
RipK1
TRIF
TRAM
TRAM
TRIF
IRF3
IRF3
IRF3
IFN-I

Figure 37. Thesis model of TLR4-driven necroptosis. Rapidly after TLR4 stimulation with corresponding ligands (such as LPS), Rip1 is phosphorylated at the cell surface in an endocytosis-independent manner (A). Upon engagement of TLR4 receptor, necroptosis would be induced in the absence of caspase activity (B). Importantly, stimulation of TLR4 promotes type I IFN (IFN-I) production through the activation of various IRFs such as IRF3 which is an endocytosis-dependent event (B). Internalization of TLR4 is significantly depends on dynamin. Once produced, IFN-I is able to induce an autocrine signal through the IFNAR1 signaling pathway (see I & II). Signaling through the ISGF3 complex is required via an unknown mechanism for necroptosis in macrophages. Although IFNAR1 signaling is needed, secretion (exocytosis) of IFN-I (see arrow #1) is not required to trigger this event, suggesting that this can occur through an intracellular mechanism which does not require the secretion of IFN-I (see arrow #2). Furthermore, dynamin-mediated endocytosis promotes RIPK3 phosphorylation. For TLR4-induced necroptosis to occur, MLKL phosphorylation is essential (C). Formation of the necrosome can be inhibited by p38 MAPK, likely via an unknown indirect kinase activity and its downstream kinase MK2 (see Fig. 36). Inhibition of p38 MAPK and MK2 promotes necroptosis. LY2228820 is a p38 MAPK inhibitor; PF3644022 is an MK2 inhibitor; Dyngo 4a and Dynasore, are dynamin inhibitors, however, only Dyngo 4a is able to inhibit phosphorylation of MLKL and necroptosis. In addition, Dyngo 4a activates p38 MAPK significantly more than Dynasore (see green arrows) (D).

7.0 REFERENCES

1. Adhikari, A., Xu, M., and Chen, Z. J. (2007). Ubiquitin-mediated activation of TAK1 and IKK. Oncogene *26*, 3214–3226.
2. Alvarado-Kristensson, M., Melander, F., Leandersson, K., Rönnstrand, L., Wernstedt, C., and Andersson, T. (2004). p38-MAPK signals survival by phosphorylation of caspase-8 and caspase-3 in human neutrophils. J. Exp. Med. *199*, 449–458.
3. Almagro, M.C., and Vucic, D. (2015). Necroptosis: Pathway diversity and characteristics. Semin. Cell Dev. Biol. *39*, 56–62.
4. Barbieri, E., Di Fiore, P.P., and Sigismund, S. (2016). Endocytic control of signaling at the plasma membrane. Curr. Opin. Cell Biol. *39*, 21–27.
5. Blouin, C.M., and Lamaze, C. (2013). Interferon gamma receptor: The beginning of the journey. Front. Immunol. *4*. *276*, 1–10.
6. Bratton, S.B., and Salvesen, G.S. (2010). Regulation of the Apaf-1–caspase-9 apoptosome. J. Cell Science *123*, 3209–3214.
7. Brault, M., Stetson, D.B., and Oberst, A. (2016). Type I interferon and TNF signaling plays key synergistic role in programmed necrosis. J. Immunol. *196*, 202–17.
8. Brenner, D., Blaser, H., and Mak, T.W. (2015). Regulation of tumour necrosis factor signalling: live or let die. Nat. Rev. Immunol. 15, 362–374.
9. Cai, Z., Jitkaew, S., Zhao, J., Chiang, H. C., Choksi, S., Liu, J., Ward, Y., Wu, L.G., and Liu, Z. G. (2014). Plasma membrane translocation of trimerized MLKL protein is required for TNF-induced necroptosis. Nat. Cell Biol. *16*, 55–65.
10. Chan, F. K., Luz, N. F., and Moriwaki, K. (2015). Programmed Necrosis in the cross talk of cell death and inflammation. Annu. Rev. Immunol. *33*, 79–106.
11. Chen, W., Wu, J., Li, L., Zhang, Z., Ren, J., Liang, Y., Chen, F., Yang, C., Zhou, Z., Su, S.S., et al. (2015). Ppm1b negatively regulates necroptosis through dephosphorylating Rip3. Nat. Cell Biol. *17*, 434–444.
12. Christofferson, D.E., and Yuan, J. (2010). Necroptosis as an alternative form of programmed cell death. Curr. Opin. Cell Biol. *22*, 263–268.
13. Claudinon, J., Gonnord, P., Beslard, E., Marchetti, M., Mitchell, K., Boularan, C., Johannes, L., Eid, P., and Lamaze, C. (2009). Palmitoylation of interferon-α (IFN-α) receptor subunit IFNAR1 is required for the activation of Stat1 and Stat2 by IFN-α. J. Biol. Chem. *284*, 24328–24340.
14. Cobos-Jiménez, V., Booiman, T., Hamann, J., and Kootstra, N.A. (2011). Macrophages and HIV-1. Curr. Opin. HIV AIDS *6*, 385–390.
15. Conrad, M., Angeli, J.P.F., Vandenabeele, P., and Stockwell, B.R. (2016). Regulated necrosis: disease relevance and therapeutic opportunities. Nat. Rev. Drug Discov. *15*, 348–366.
16. Cuenda, A., and Rousseau, S. (2007). p38 MAP-kinases pathway regulation, function and role in human diseases. Biochim. Biophys. Acta *1773*, 1358–1375.
17. Dannappel, M., Vlantis, K., Kumari, S., Polykratis, A., Kim, C., Wachsmuth, L., Eftychi, C., Lin, J., Corona, T., Hermance, N., et al. (2014). RIPK1 maintains epithelial homeostasis by inhibiting apoptosis and necroptosis. Nature *513*, 90–94.

18. Davis, C.T., Zhu, W., Gibson, C.C., Bowman-Kirigin, J., Sorensen, L., Ling, J., Sun, H., Navankasattusas, S., and Li, D.Y. (2014). ARF6 Inhibition Stabilizes the Vasculature and Enhances Survival during Endotoxic Shock. J. Immunol. *192*, 6045–6052.
19. Doherty, G.J., and McMahon, H.T. (2009). Mechanisms of endocytosis. Annu. Rev. Biochem. *78*, 857–902.
20. Dondelinger, Y., Darding, M., Bertrand, M.J.M., and Walczak, H. (2016). Poly-ubiquitination in TNFR1-mediated necroptosis. Cell. Mol. Life Sci. *73*, 2165–2176.
21. Doyle, S.L., and O'Neill, L.A.J. (2006). Toll-like receptors: From the discovery of NFKB to new insights into transcriptional regulations in innate immunity. Biochem. Pharmacol. *72*, 1102–1113.
22. Elmore, S. (2007). Apoptosis: A review of programmed cell death. Toxicologic Pathology *35*, 495–516.
23. Eichel, K., Jullié, D., and von Zastrow, M. (2016). β-Arrestin drives MAP kinase signalling from clathrin-coated structures after GPCR dissociation. Nat. Cell Biol. *18*, 303–310.
24. Escós, A., Risco, A., Alsina-Beauchamp, D., and Cuenda, A. (2016). p38γ and p38δ Mitogen Activated Protein Kinases (MAPKs), New Stars in the MAPK Galaxy. Front. Cell Dev. Biol. *4*, 31.
25. Ferguson, S., and De Camilli, P. (2012). Dynamin, a membrane remodelling GTPase. Nat Rev Mol Cell Biol *13*, 75–88.
26. Fricker, M., Vilalta, A., Tolkovsky, A.M., and Brown, G.C. (2013). Caspase inhibitors protect neurons by enabling selective necroptosis of inflamed microglia. J. Biol. Chem. *288*, 9145–9152.
27. Fritah, S., Col, E., Boyault, C., Govin, J., Sadoul, K., Chiocca, S., Christians, E., Khochbin, S., Jolly, C., and Vourc'h, C. (2009). Heat-shock factor 1 controls genome-wide acetylation in heat-shocked cells. Mol. Biol. Cell *20*, 4976–4984.
28. Fuchs, Y., and Steller, H. (2011). Programmed cell death in animal development and disease. Cell *147*, 742–758.
29. Fulda, S., Gorman, A.M., Hori, O., and Samali, A. (2010). Cellular stress responses: Cell survival and cell death. Int. J. Cell Biol. *2010,* 1-23.
30. Galluzzi, L., and Kroemer, G. (2008). Necroptosis: A Specialized Pathway of Programmed Necrosis. Cell *135*, 1161–1163.
31. Galluzzi, L., Kepp, O., and Kroemer, G. (2014). MLKL regulates necrotic plasma membrane permeabilization. Cell Res. *24*, 139–140.
32. Gao, D., Yang, J., Wu, Y., Wang, Q., Wang, Q., Lai, E.Y., and Zhu, J. (2016). Targeting dynamin 2 as a novel pathway to inhibit cardiomyocyte apoptosis following oxidative stress. Cell. Physiol. Biochem. *39*, 2121–2134.
33. Goh, L.K., and Sorkin, A. (2013). Endocytosis of receptor tyrosine kinases. Cold Spring Harb. Perspect. Biol. *5*, a017459.
34. Hanyaloglu, A.C. and von Zastrow, M. (2008). Regulation of GPCRs by Endocytic Membrane Trafficking and Its Potential Implications. Annu. Rev. Pharmacol. Toxicol. 48, 537–568.
35. Harper, C.B., Popoff, M.R., McCluskey, A., Robinson, P.J., and Meunier, F.A. (2013). Targeting membrane trafficking in infection prophylaxis: Dynamin inhibitors. Trends Cell Biol. *23*, 90–101.
36. He, M.X., and He, Y.W. (2013). A role for c-FLIP(L) in the regulation of apoptosis,

autophagy, and necroptosis in T lymphocytes. Cell Death Differ. *20*, 188–197.
37. He, S., Liang, Y., Shao, F., and Wang, X. (2011). Toll-like receptors activate programmed necrosis in macrophages through a receptor-interacting kinase-3-mediated pathway. Proc. Natl. Acad. Sci. *108*, 20054–20059.
38. Hill, T.A., Odell, L.R., Quan, A., Abagyan, R., Ferguson, G., Robinson, P.J., and McCluskey, A. (2004). Long chain amines and long chain ammonium salts as novel inhibitors of dynamin GTPase activity. Bioorganic Med. Chem. Lett. *14*, 3275–3278.
39. Hill, T.A., Gordon, C.P., McGeachie, A.B., Venn-Brown, B., Odell, L.R., Chau, N., Quan, A., Mariana, A., Sakoff, J.A., Chircop, M., et al. (2009). Inhibition of dynamin mediated endocytosis by the Dynoles-Synthesis and functional activity of a family of indoles. J. Med. Chem. *52*, 3762–3773.
40. Irannejad, R., Tsvetanova, N.G., Lobingier, B.T., and von Zastrow, M. (2015). Effects of endocytosis on receptor-mediated signaling. Curr. Opin. Cell Biol. *35*, 137–143.
41. Jacobsen AV, Lowes, K. N., Tanzer, M. C., Lucet, I. S., Hildebrand, J. M., Petrie, E. J., … Murphy, J. M. (2016) HSP90 activity is required for MLKL oligomerisation and membrane translocation and the induction of necroptotic cell death. Cell Death Dis. *7*, e2051.
42. Jouan-Lanhouet, S., Riquet, F., Duprez, L., Vanden Berghe, T., Takahashi, N., and Vandenabeele, P. (2014). Necroptosis, in vivo detection in experimental disease models. Semin. Cell Dev. Biol. *35*, 2–13.
43. Kaczmarek, A., Vandenabeele, P., and Krysko, D. V. (2013). Necroptosis: The Release of damage-associated molecular patterns and its physiological relevance. Immunity *38*, 209–223.
44. Kagan, J.C., Su, T., Horng, T., Chow, A., Akira, S., and Medzhitov, R. (2008). TRAM couples endocytosis of Toll-like receptor 4 to the induction of interferon-beta. Nat. Immunol. *9*, 361–368.
45. Karunakaran, D., Geoffrion, M., Wei, L., Gan, W., Richards, L., Shangari, P., DeKemp, E.M., Beanlands, R.A., Perisic, L., Maegdefessel, L., et al. (2016). Targeting macrophage necroptosis for therapeutic and diagnostic interventions in atherosclerosis. Sci. Adv. *2*, e1600224.
46. Khan, S., Lopez-Dee, Z., Kumar, R., and Ling, J. (2013). Activation of NFkB is a novel mechanism of pro-survival activity of glucocorticoids in breast cancer cells. Cancer Lett. *337*, 90–95.
47. Latvala, S., Mäkelä, S.M., Miettinen, M., Charpentier, E., and Julkunen, I. (2014). Dynamin inhibition interferes with inflammasome activation and cytokine gene expression in Streptococcus pyogenes-infected human macrophages. Clin. Exp. Immunol. *178*, 320–333.
48. Leach, M.D., Farrer, R.A., Tan, K., Miao, Z., Walker, L.A., Cuomo, C.A., Wheeler, R.T., Brown, A.J.P., Wong, K.H., and Cowen, L.E. (2016). Hsf1 and Hsp90 orchestrate temperature-dependent global transcriptional remodelling and chromatin architecture in Candida albicans. Nat. Commun. *7*, 11704.
49. Legarda, D., Justus, S.J., Ang, R.L., Rikhi, N., Li, W., Moran, T.M., Zhang, J., Mizoguchi, E., Zelic, M., Kelliher, M.A., et al. (2016). CYLD Proteolysis Protects Macrophages from TNF-Mediated Auto-necroptosis Induced by LPS and Licensed by Type I IFN. Cell Rep. *15*, 2449–2461.
50. Legler, D.F., Micheau, O., Doucey, M.A., Tschopp, J., and Bron, C. (2003). Recruitment of TNF receptor 1 to lipid rafts is essential for TNFα-mediated NF-κB activation. Immunity *18*, 655–664.

51. Li, H., Hu, D., Fan, H., Zhang, Y., LeSage, G.D., Caudle, Y., Stuart, C., Liu, Z., and Yin, D. (2014). β-Arrestin 2 negatively regulates Toll-like receptor 4 (TLR4)-triggered inflammatory signaling via targeting p38 MAPK and interleukin 10. J. Biol. Chem. *289*, 23075–23085.
52. Linkermann, A., and Green, D.R. (2014). Necroptosis. N. Engl. J. Med. *370*, 455–465.
53. Lu, G., Young, J.K., Han, J., Herschman, H.R., Stefani, E., and Wang, Y. (2006). TAB-1 modulates intracellular localization of p38 MAP kinase and downstream signaling. J. Biol. Chem. *281*, 6087–6095.
54. Lundmark, R., Doherty, G.J., Howes, M.T., Cortese, K., Vallis, Y., Parton, R.G., and McMahon, H.T. (2008). The GTPase-activating protein GRAF1 regulates the CLIC/GEEC endocytic pathway. Curr. Biol. *18*, 1802–1808.
55. Macia, E., Ehrlich, M., Massol, R., Boucrot, E., Brunner, C., and Kirchhausen, T. (2006). Dynasore, a cell-permeable inhibitor of dynamin. Dev. Cell *10*, 839–850.
56. Marchetti, M., Monier, M.-N., Fradagrada, A., Mitchell, K., Baychelier, F., Eid, P., Johannes, L., and Lamaze, C. (2006). Stat-mediated signaling induced by type I and type II Interferons (IFNs) is differentially controlled through lipid microdomain association and clathrin-dependent endocytosis of IFN receptors. Mol. Biol. Cell *17*, 2896–2909.
57. Mccluskey, A., Daniel, J.A., Hadzic, G., Chau, N., Clayton, E.L., Mariana, A., Whiting, A., Gorgani, N.N., Lloyd, J., Quan, A., et al. (2013). Building a better dynasore: The dyngo compounds potently inhibit dynamin and endocytosis. Traffic. *14*, 1272–1289.
58. McComb, S., Cheung, H.H., Korneluk, R.G., Wang, S., Krishnan, L., and Sad, S. (2012). cIAP1 and cIAP2 limit macrophage necroptosis by inhibiting Rip1 and Rip3 activation. Cell Death Differ. *19*, 1791–1801.
59. McComb, S., Cessford, E., Alturki, N. a., Joseph, J., Shutinoski, B., Startek, J.B., Gamero, a. M., Mossman, K.L., and Sad, S. (2014). Type-I interferon signaling through ISGF3 complex is required for sustained Rip3 activation and necroptosis in macrophages. Proc Natl Acad Sci U S A. *111*, E3206–E3213.
60. McKay, M.M., and Morrison, D.K. (2007). Integrating signals from RTKs to ERK/MAPK. Oncogene *26*, 3113–3121.
61. Miaczynska, M., and Stenmark, H. (2008). Mechanisms and functions of endocytosis. J. Cell Biol. *180*, 7–11.
62. Moore, K.J., Sheedy, F.J., and Fisher, E.A. (2013). Macrophages in atherosclerosis: a dynamic balance. Nat. Rev. Immunol. *13*, 709–721.
63. Morioka, S., Broglie, P., Omori, E., Ikeda, Y., Takaesu, G., Matsumoto, K., and Ninomiya-Tsuji, J. (2014). TAK1 kinase switches cell fate from apoptosis to necrosis following TNF stimulation. J. Cell Biol. *204*, 607–623.
64. Murphy, J.M., Czabotar, P.E., Hildebrand, J.M., Lucet, I.S., Zhang, J.G., Alvarez-Diaz, S., Lewis, R., Lalaoui, N., Metcalf, D., Webb, A.I., et al. (2013). The pseudokinase MLKL mediates necroptosis via a molecular switch mechanism. Immunity *39*, 443–453.
65. Neal, M.D., Sodhi, C.P., Jia, H., Dyer, M., Egan, C., Yazji, I., Good, M., Afrazi, A., Marino, R., Slagle, D., et al. (2012). Toll-like receptor 4 is expressed on intestinal stem cells and regulates their proliferation and apoptosis via the p53-upregulated modulator of apoptosis. J. Biol. Chem. *287*, 37296–37308.
66. Nikoletopoulou, V., Markaki, M., Palikaras, K., and Tavernarakis, N. (2013). Crosstalk between apoptosis, necrosis and autophagy. Biochim. Biophys. Acta. Mol. Cell Res. *1833*, 3448–3459.

67. O'Donnell, M.A., and Ting, A.T. (2012). NF-κB and ubiquitination: Partners in disarming RIPK1-mediated cell death. Immunol. Res. *54*, 214–226.
68. O'Donnell, M.A., Legarda-Addison, D., Skountzos, P., Yeh, W.C., and Ting, A.T. (2007). Ubiquitination of RIP1 regulates an NF-κB-independent cell-death switch in TNF signaling. Curr. Biol. *17*, 418–424.
69. Oeckinghaus, A., Hayden, M.S., and Ghosh, S. (2011). Crosstalk in NF-κB signaling pathways. Nat. Immunol. *12*, 695–708.
70. Ofengeim, D., Ito, Y., Najafov, A., Zhang, Y., Shan, B., DeWitt, J. P., Ye, J., Zhang, X., Chang, A., Vakifahmetoglu-Norberg, H., et al. (2015). Activation of necroptosis in multiple sclerosis. Cell Rep. *10*, 1836–1849.
71. Okada, R., Yamauchi, Y., Hongu, T., Funakoshi, Y., Ohbayashi, N., Hasegawa, H., and Kanaho, Y. (2015). Activation of the small G protein Arf6 by dynamin2 through guanine nucleotide exchange factors in endocytosis. Sci. Rep. *5*, 14919.
72. Pasparakis, M., and Vandenabeele, P. (2015). Necroptosis and its role in inflammation. Nature *517*, 311–320.
73. Pierdomenico, M., Negroni, A., Stronati, L., Vitali, R., Prete, E., Bertin, J., Gough, P.J., Aloi, M., and Cucchiara, S. (2014). Necroptosis is active in children with inflammatory bowel disease and contributes to heighten intestinal inflammation. Am. J. Gastroenterol. *109*, 279–287.
74. Quan, A., McGeachie, A.B., Keating, D.J., van Dam, E.M., Rusak, J., Chau, N., Malladi, C.S., Chen, C., McCluskey, A., Cousin, M. a, et al. (2007). Myristyl trimethyl ammonium bromide and octadecyl trimethyl ammonium bromide are surface-active small molecule dynamin inhibitors that block endocytosis mediated by dynamin I or dynamin II. Mol. Pharmacol. *72*, 1425–1439.
75. Rajaiah, R., Perkins, D.J., Ireland, D.D.C., and Vogel, S.N. (2015). CD14 dependence of TLR4 endocytosis and TRIF signaling displays ligand specificity and is dissociable in endotoxin tolerance. Proc. Natl. Acad. Sci. U. S. A. *112*, 8391–8396.
76. Reems, J.A., Wang, W., Tsubata, K., Abdurrahman, N., Sundell, B., Tijssen, M.R., van der Schoot, E., Summa, F. Di, Patel-Hett, S., Italiano, J., et al. (2008). Dynamin 3 participates in the growth and development of megakaryocytes. Exp. Hematol. *36*, 1714–1727.
77. Risco, A., and Cuenda, A. (2012). New Insights into the p38γ and p38δ MAPK Pathways. J. Signal Transduct. *2012*, 1–8.
78. Robinson, N., McComb, S., Mulligan, R., Dudani, R., Krishnan, L., and Sad, S. (2012). Type I interferon induces necroptosis in macrophages during infection with *Salmonella enterica* serovar Typhimurium TL-13. Nat. Immunol. *13*, 954–962.
79. Rodriguez, D. A, Weinlich, R., Brown, S., Guy, C., Fitzgerald, P., Dillon, C.P., Oberst, a, Quarato, G., Low, J., Cripps, J.G., et al. (2016). Characterization of RIPK3-mediated phosphorylation of the activation loop of MLKL during necroptosis. Cell Death Differ. *23*, 76–88.
80. Ruckdeschel, K., Pfaffinger, G., Haase, R., Sing, A., Weighardt, H., Häcker, G., Holzmann, B., and Heesemann, J. (2004). Signaling of apoptosis through TLRs critically involves toll/IL-1 receptor domain-containing adapter inducing IFN-beta, but not MyD88, in bacteria-infected murine macrophages. J. Immunol. *173*, 3320–3328.
81. Saeed, W. K., and Jun, D.W. (2014). Necroptosis: An emerging type of cell death in liver diseases. World J. Gastroenterol. *20*, 12526–12532.
82. Samaj, J., Baluska, F., Voigt, B., Schlicht, M., Volkmann, D., and Menzel, D. (2004).

Endocytosis, actin cytoskeleton, and signaling. Plant Physiol. *135*, 1150–1161.
83. Scheidereit, C. (2006). IkB kinase complexes: gateways to NF-kB activation and transcription. Oncogene *25*, 6685–6705.
84. Schilling, R., Geserick, P., and Leverkus, M. (2014). Characterization of the ripoptosome and its components: Implications for anti-inflammatory and cancer therapy. Methods Enzymol. *545*, 83–102.
85. Schneider-Brachert, W., Tchikov, V., Neumeyer, J., Jakob, M., Winoto-Morbach, S., Held-Feindt, J., Heinrich, M., Merkel, O., Ehrenschwender, M., Adam, D., et al. (2004). Compartmentalization of TNF Receptor 1 Signaling. Immunity *21*, 415–428.
86. Schütze, S., and Schneider-Brachert, W. (2009). Impact of TNF-R1 and CD95 internalization on apoptotic and antiapoptotic signaling. Results Probl. Cell Differ. *49*, 63–85.
87. Schütze, S., Tchikov, V., and Schneider-Brachert, W. (2008). Regulation of TNFR1 and CD95 signalling by receptor compartmentalization. Nat. Rev. Mol. Cell Biol. *9*, 655–662.
88. Schworer, S.A., Smirnova, I.I., Kurbatova, I., Bagina, U., Churova, M., Fowler, T., Roy, A.L., Degterev, A., and Poltorak, A. (2014). Toll-like receptor-mediated down-regulation of the deubiquitinase cylindromatosis (CYLD) protects macrophages from necroptosis in wild-derived mice. J. Biol. Chem. *289*, 14422–14433.
89. Scita, G., and Di Fiore, P.P. (2010). The endocytic matrix. Nature *463*, 464–473.
90. Seimon, T.A., Wang, Y., Han, S., Senokuchi, T., Schrijvers, D.M., Kuriakose, G., Tall, A.R., and Tabas, I.A. (2009). Macrophage deficiency of p38-MAPK promotes apoptosis and plaque necrosis in advanced atherosclerotic lesions in mice. J. Clin. Invest. *119*, 886–898.
91. Sigismund, S., Confalonieri, S., Ciliberto, A., Polo, S., Scita, G., and Di Fiore, P.P. (2012). Endocytosis and signaling: cell logistics shape the eukaryotic cell plan. Physiol. Rev. *92*, 273–366.
92. Sun, S.C. (2010). Non-canonical NF-κB signaling pathway. Nat. Publ. Gr. 21, 71–8571.
93. Sun, Y., Cheng, Z., Ma, L., and Pei, G. (2002). β-arrestin2 is critically involved in CXCR4-mediated chemotaxis, and this is mediated by its enhancement of p38 MAPK activation. J. Biol. Chem. *277*, 49212–49219.
94. Takaesu, G., Surabhi, R.M., Park, K.J., Ninomiya-Tsuji, J., Matsumoto, K., and Gaynor, R.B. (2003). TAK1 is critical for IkB kinase-mediated activation of the NF-κB pathway. J. Mol. Biol. *326*, 105–115.
95. Tang, S.C., Lathia, J.D., Selvaraj, P.K., Jo, D.G., Mughal, M.R., Cheng, A., Siler, D.A., Markesbery, W.R., Arumugam, T. V., and Mattson, M.P. (2008). Toll-like receptor-4 mediates neuronal apoptosis induced by amyloid β-peptide and the membrane lipid peroxidation product 4-hydroxynonenal. Exp. Neurol. *213*, 114–121.
96. Tsai, S., Bose, J., Defrêne, N., Pagé, A., Cesaro, P.A., Shil, S.M., Pokharel, T.R., Kannan, J.B., Baseman, S. Y., Tsai, J.A., et al. (2015). Regulation of TLR3 Activation by S100A9. J Immunol Mater. Suppl. *195*, 4426–4437.
97. Trempolec, N., Dave-Coll, N., and Nebreda, A.R. (2013). SnapShot: p38 MAPK Substrates. Cell *152*, 924–924.
98. Van Acker, T., Eyckerman, S., Vande Walle, L., Gerlo, S., Goethals, M., Lamkanfi, M., Bovijn, C., Tavernier, J., and Peelman, F. (2014). The small GTPase Arf6 is essential for the Tram/Trif pathway in TLR4 signaling. J. Biol. Chem. *289*, 1364–1376.
99. Vandenabeele, P., Galluzzi, L., Vanden Berghe, T., and Kroemer, G. (2010). Molecular

mechanisms of necroptosis: an ordered cellular explosion. Nat. Rev. Mol. Cell Biol. *11*, 700–714.

100. Vanden Berghe, T. Vanden, Linkermann, A., Jouan-Lanhouet, S., Walczak, H., and Vandenabeele, P. (2014). Regulated necrosis: the expanding network of non-apoptotic cell death pathways. Nat. Rev. Mol. Cell Biol. *15*, 135–147.
101. Vanden Berghe, T., Kaiser, W.J., Bertrand, M.J., and Vandenabeele, P. (2015). Molecular crosstalk between apoptosis, necroptosis, and survival signaling. Mol. Cell. Oncol. *2*, e975093.
102. Wagner, E.F., and Nebreda, A.R. (2009). Signal integration by JNK and p38 MAPK pathways in cancer development. Nat. Rev. Cancer *9*, 537–549.
103. Wan, T., Liu, T., Zhang, H., Tang, S., and Min, W. (2010). AIP1 functions as Arf6-GAP to negatively regulate TLR4 signaling. J. Biol. Chem. *285*, 3750–3757.
104. Wang, D., Zhao, M., Chen, G., Cheng, X., Han, X., Lin, S., Zhang, X., and Yu, X. (2013). The histone deacetylase inhibitor vorinostat prevents TNFα-induced necroptosis by regulating multiple signaling pathways. Apoptosis. *18*, 1348–1362.
105. Wang, H., Chen, Y., Han, J., Meng, Q., Xi, Q., Wu, G., and Zhang, B. (2016a). DCAF4L2 promotes colorectal cancer invasion and metastasis via mediating degradation of NF-κb negative regulator PPM1B. Am. J. Transl. Res. *8*, 405–418.
106. Wang X, Khaleque MA., Zhao M.J., Zhong R., Gaestel M., Calderwood S.K. (2006) Phosphorylation of HSF1 by MAPK-activated protein kinase 2 on serine 121, inhibits transcriptional activity and promotes HSP90 binding. J. biol. Chem. *281*,782–791.
107. Wang, Z., Ji, J., Peng, D., Ma, F., Cheng, G., and Qin, F.X.F. (2016b). Complex regulation pattern of IRF3 activation revealed by a novel dimerization reporter system. J. Immunol. *196*, 4322–4330.
108. Watanabe, S., Trimbuch, T., Camacho-Pérez, M., Rost, B.R., Brokowski, B., Söhl-Kielczynski, B., Felies, A., Davis, M.W., Rosenmund, C., and Jorgensen, E.M. (2014).Clathrin regenerates synaptic vesicles from endosomes. Nature *515*, 228–233.
109. Wei, S., Moon, H.G., Zheng, Y., Liang, X., An, C.H., and Jin, Y. (2013). Flotillin-2 modulates Fas signaling mediated apoptosis after hyperoxia in lung epithelial cells. PLoS One. *8*, e77519.
110. Weinlich, R., Oberst, A., Beere, H.M., and Green, D.R. (2017). Necroptosis in development, inflammation and disease. Nat. Rev. Mol. Cell Biol. *18*, 127–136.
111. Wertz, I.E., and Dixit, V.M. (2010). Signaling to NF-kappaB: regulation by ubiquitination. Cold Spring Harb. Perspect. Biol. *2*, 1-19.
112. Wu, Y. T., Tan, H. L., Huang, Q., Sun, X. J., Zhu, X., and Shen, H. M. (2011). zVAD-induced necroptosis in L929 cells depends on autocrine production of TNFα mediated by the PKC-MAPKs-AP-1 pathway. Cell Death Differ. *18*, 26–37.
113. Wynn, T.A., and Vannella, K.M. (2016). Macrophages in tissue repair, Regeneration, and Fibrosis. Immunity *44*, 450–462.
114. Wynn, T.A., Chawla, A., and Pollard, J.W. (2013). Macrophage biology in development, homeostasis and disease. Nature *496*, 445–455.
115. Ye, Y. C., Yu, L., Wang, H. J., Tashiro, S., Onodera, S., and Ikejima, T. (2011). TNFα-Induced Necroptosis and Autophagy via Supression of the p38–NF-κB Survival Pathway in L929 Cells. J. Pharmacol. Sci. *117*, 160–169.
116. Zhang, X., Edwards, J.P., and Mosser, D.M. (2009). The expression of exogenous genes in macrophages: Obstacles and opportunities. Methods Mol. Biol. *531*, 123–143.

117. Zhao, F., Zhang, J., Liu, Y.S., Li, L., and He, Y.L. (2011). Research advances on flotillins. Virol. J. *8*, 479.
118. Zhao, X.M., Chen, Z., Zhao, J.B., Zhang, P.P., Pu, Y.F., Jiang, S.H., Hou, J.J., Cui, Y.M., Jia, X.L., and Zhang, S.Q. (2016). Hsp90 modulates the stability of MLKL and is required for TNF-induced necroptosis. Cell Death Dis. *7*, e2089.
119. Zhou, W., and Yuan, J. (2014). Necroptosis in health and diseases. Semin. Cell Dev. Biol. *35*, 14–23.